

NISTIR 88-3899



Elevated Temperature Deformation of Structural Steel

B. A. Fields
R. J. Fields

U.S. DEPARTMENT OF COMMERCE
National Institute of Standards and Technology
(Formerly National Bureau of Standards)
Metallurgy Division
Gaithersburg, MD 20899

December 1988
Issued March 1989

Prepared for
American Iron and Steel Institute
Washington, DC

NISTIR 88-3899

Elevated Temperature Deformation of Structural Steel

B. A. Fields
R. J. Fields

U.S. DEPARTMENT OF COMMERCE
National Institute of Standards and Technology
(Formerly National Bureau of Standards)
Metallurgy Division
Gaithersburg, MD 20899

December 1988

Issued March 1989



National Bureau of Standards became the National Institute of Standards and Technology on August 23, 1988, when the Omnibus Trade and Competitiveness Act was signed. NIST retains all NBS functions. Its new programs will encourage improved use of technology by U.S. industry.

Prepared for
American Iron and Steel Institute
Washington, DC

**U.S. DEPARTMENT OF COMMERCE
Robert A. Mosbacher, Secretary
Ernest Ambler, Acting Under Secretary
for Technology
NATIONAL INSTITUTE OF STANDARDS
AND TECHNOLOGY
Raymond G. Kammer, Acting Director**

Abstract

The results of tensile and creep tests on steels close to the American specification for ASTM A36 have been used to formulate an equation from which elastic, plastic, creep and total strains can be calculated. Correlations between measured and predicted strains for Australian AS A149 and Japanese SS41 steels, both close to the A36 specification, are shown and good agreement is found.

The above mentioned equation is also used to construct deformation mechanism (i.e., elastic, plastic, or creep) maps for times of 2 minutes to 4 hours at temperature. From these maps the deformation mechanisms operating at a given temperature and stress can be seen. The dominant mechanism for each set of conditions is given. In addition the maps show contours of total strain values of 1, 2, and 5%.

TABLE OF CONTENTS

Abstract

1. Introduction
2. Specimen Material
3. Calculation of Elastic Strain
4. Calculation of Plastic Strain
5. Calculation of Creep Strain
6. Calculation of Total Strain
7. Correlation of Measured and Calculated Plastic Strains
8. Correlation of Measured and Calculated Creep Strains
9. Correlation of Measured and Calculated Total Strains
10. Correlation of Measured and Calculated Strains for SS41
 - 10.1. Plastic Strains
 - 10.2. Creep Strains
11. Deformation Mechanism Maps
12. Construction of the Deformation Mechanism Maps
 - 12.1. The Boundary At Which Fracture Occurs
 - 12.2. The Boundary between ELASTIC and Elastic PLASTIC
 - 12.3. The Boundary between Elastic CREEP and Elastic Plastic CREEP
 - 12.4. The Boundary between ELASTIC and Elastic CREEP
 - 12.5. The Boundary between Elastic PLASTIC and Elastic PLASTIC Creep
 - 12.6. The Boundary between Elastic PLASTIC Creep and Elastic Plastic CREEP
 - 12.7. Total Strain Contours of 1%, 2%, and 5%
13. Conclusions

TABLES

- Table 1. Compositions and Tensile Properties for A36, AS A149, and SS41 Steels
- Table 2. Values of Plastic Strain for AS A149 from Knight⁽¹⁾
- Table 3. Values of Plastic Strain for AS A149 from Skinner⁽⁵⁾
- Table 4. Values of $\log F(t)$ and $G(t)$ Where $\epsilon_p = F\sigma^G$
- Table 5. Values of $A(t)$, $B(t)$ and $C(t)$ Where $\epsilon_c = At^B\sigma^C$
- Table 6a. Measured and Calculated Strains during Loading at 350°C
- Table 6b. Measured and Calculated Strains during Loading at 400°C
- Table 6c. Measured and Calculated Strains during Loading at 450°C
- Table 6d. Measured and Calculated Strains during Loading at 500°C
- Table 6e. Measured and Calculated Strains during Loading at 550°C
- Table 6f. Measured and Calculated Strains during Loading at 600°C
- Table 6g. Measured and Calculated Strains during Loading at 650°C
- Table 7. Calculated Values of Plastic Strains
- Table 8. Measured and Calculated Plastic and Total Strains for SS41 Steel
- Table 9a. Measured and Calculated Creep Strains for SS41 during Loading at 350°C
- Table 9b. Measured and Calculated Creep Strains for SS41 during Loading at 450°C
- Table 9c. Measured and Calculated Creep Strains for SS41 during Loading at 550°C
- Table 9d. Measured and Calculated Creep Strains for SS41 during Loading at 600°C
- Table 10. Construction of a Deformation Mechanism Map for a Loading Time of 60 mins.

- Table 10a. The Boundary At Which Fracture Occurs
- Table 10b. The Boundary Between ELASTIC and Elastic PLASTIC
- Table 10c. The Boundary Between Elastic CREEP and Elastic Plastic CREEP
- Table 10d. The Boundary Between ELASTIC and Elastic CREEP
- Table 10e. The Boundary Between Elastic PLASTIC and Elastic PLASTIC Creep
- Table 10f. The Boundary Between Elastic Plastic CREEP and Elastic PLASTIC
Creep
- Table 10g. Total Strain Contours of 1%, 2%, and 5%

FIGURES

- Figure 1. Normalized yield stress versus temperature for A36 and similar steels.
- Figure 2. The effect of temperature on the proof and flow stress of AS A149 steel at a strain rate of $2 \times 10^{-3} \text{ min}^{-1}$.
- Figure 3a. Plastic strain versus stress at 350°C.
- Figure 3b. Plastic strain versus stress at 400°C.
- Figure 3c. Plastic strain versus stress at 450°C.
- Figure 3d. Plastic strain versus stress at 500°C.
- Figure 3e. Plastic strain versus stress at 550°C.
- Figure 3f. Plastic strain versus stress at 600°C.
- Figure 3g. Plastic strain versus stress at 650°C.
- Figure 4. Log F versus temperature.
- Figure 5. Constant G versus temperature.
- Figure 6a. Creep strain versus time at 350°C.
- Figure 6b. Creep strain versus time at 400°C.
- Figure 6c. Creep strain versus time at 450°C.
- Figure 6d. Creep strain versus time at 500°C.
- Figure 6e. Creep strain versus time at 550°C.
- Figure 6f. Creep strain versus time at 600°C.
- Figure 6g. Creep strain versus time at 650°C.
- Figure 7. Parameter B versus temperature.
- Figure 8a. Creep strain versus stress at 350°C.
- Figure 8b. Creep strain versus stress at 400°C.
- Figure 8c. Creep strain versus stress at 450°C.
- Figure 8d. Creep strain versus stress at 500°C.

Figure 8e. Creep strain versus stress at 550°C.
Figure 8f. Creep strain versus stress at 600°C.
Figure 8g. Creep strain versus stress at 650°C.
Figure 9. Parameter C versus temperature.
Figure 10. Parameter A versus temperature.
Figure 11a. Correlation of measured and calculated plastic strain at 350°C.
Figure 11b. Correlation of measured and calculated plastic strain at 400°C.
Figure 11c. Correlation of measured and calculated plastic strain at 450°C.
Figure 11d. Correlation of measured and calculated plastic strain at 500°C.
Figure 11e. Correlation of measured and calculated plastic strain at 550°C.
Figure 11f. Correlation of measured and calculated plastic strain at 600°C.
Figure 12a. Correlation of measured and calculated creep strain at 350°C.
Figure 12b. Correlation of measured and calculated creep strain at 400°C.
Figure 12c. Correlation of measured and calculated creep strain at 450°C.
Figure 12d. Correlation of measured and calculated creep strain at 500°C.
Figure 12e. Correlation of measured and calculated creep strain at 550°C.
Figure 12f. Correlation of measured and calculated creep strain at 600°C.
Figure 12g. Correlation of measured and calculated creep strain at 650°C.
Figure 13a. Correlation of measured and calculated total strain at 350°C.
Figure 13b. Correlation of measured and calculated total strain at 400°C.
Figure 13c. Correlation of measured and calculated total strain at 450°C.
Figure 13d. Correlation of measured and calculated total strain at 500°C.
Figure 13e. Correlation of measured and calculated total strain at 550°C.
Figure 13f. Correlation of measured and calculated total strain at 600°C.
Figure 13g. Correlation of measured and calculated total strain at 650°C.

Figure 14a. SS41 Steel - Correlation of measured and calculated creep strain at 350°C.

Figure 14b. SS41 Steel - Correlation of measured and calculated creep strain at 450°C.

Figure 14c. SS41 Steel - Correlation of measured and calculated creep strain at 550°C.

Figure 14d. SS41 Steel - Correlation of measured and calculated creep strain at 600°C.

Figure 15. Deformation modes for 2 minutes at temperature.

Figure 16a. Deformation modes for 15 minutes at temperature.

Figure 16b. Deformation modes for 15 minutes at temperature.

Figure 17a. Deformation modes for 30 minutes at temperature.

Figure 17b. Deformation modes for 30 minutes at temperature.

Figure 18a. Deformation modes for 1 hour at temperature.

Figure 18b. Deformation modes for 1 hour at temperature.

Figure 19a. Deformation modes for 4 hours at temperature.

Figure 19b. Deformation modes for 4 hours at temperature.

SYMBOLS

ϵ_e - elastic strain, %

ϵ_p - plastic strain, %

ϵ_c - creep strain, %

ϵ_t - total strain, %

T - temperature, C

σ - stress, ksi

σ_y - yield stress, ksi

σ_{YRT} - room temperature yield stress, ksi

σ_T - tensile strength, ksi

E - Young's modulus, ksi

A - function of temperature

B - function of temperature

C - function of temperature

D - function of temperature

F - function of temperature

G - function of temperature

In this report the units used for temperature and stress are degrees C and ksi, respectively. This was done to be consistent with the report⁽¹⁾ from which the original data was taken. To convert stresses from ksi to MPa the value of stress in ksi should be multiplied by 6.89.

1. Introduction

With the increase of steel skeleton high rise buildings, it is becoming more important to be able to assess the damage sustained by such a building during and after a fire. An analysis of the problem needs to be based on a knowledge of certain basic facts. These include the determination of the stresses and temperatures involved and the calculation of the resulting strains. These strains can be subdivided into elastic, recoverable strain, ϵ_e ; plastic, time independent strain, ϵ_p ; and creep, time dependent strain, ϵ_c .

It is the purpose of the present study to develop an equation predicting the values of ϵ_e , ϵ_p and ϵ_c under conditions of constant stress and temperature, over a temperature range of 350 to 650°C, for periods of up to 4 hours. The empirical equation will have the form of

$$\epsilon_T = \epsilon_e + \epsilon_p + \epsilon_c \quad (1)$$

or

$$\epsilon_T = D\sigma + F\sigma^G + At^B\sigma^C \quad (2)$$

where ϵ_T is total strain and A, B, C, D, F, and G are all functions of temperature. This equation will be used to construct deformation mechanism maps showing the dominant mode of deformation for given conditions of temperature stress and time.

Given the importance of the subject, it would be expected that there would be a large body of data on which to base such a project. However, this is apparently not the case. To the writers' knowledge there are only two significant studies^(1,2) available in the literature. The work reported by Knight et al.⁽¹⁾ is particularly helpful as all their experimental data is tabulated for temperature, time, stress and resulting strain. Using this data

a set of equations has been developed and used to construct deformation mechanism maps. The work of Fujimoto et al.⁽²⁾ has been used to test the correlation between these predictions and separately obtained experimental results.

A future study might address the effect on the resulting strain, of varying the temperature with time, i.e. increasing the temperature to a maximum. The present assumption of constant temperature would certainly predict conservative behavior for the same duration as compared to the heating ramp that would occur in a fire.

2. Specimen Material

The original purpose of this study was to develop deformation mechanism maps for the American steel, ASTM A36. As stated in the introduction, only two significant sets of data were available in the literature, neither of these being obtained for A36 steel. The steel used by Knight et al.⁽¹⁾ was an Australian steel, AS A149, while Fujimoto et al.⁽²⁾ used a Japanese steel, SS41. The chemical compositions, yield strengths and tensile strengths for A36, AS A149 and SS41 are given in Table 1. It can be seen that for all three steels these values are not greatly different. There is, however, some difference in the variation of yield stress with increasing temperature. This can be seen in Figure 1 which includes results for A36^(3,4), AS A149⁽⁵⁾, SS41⁽²⁾ and for BS4360⁽⁶⁾, a British steel which falls within the specifications for A36. The yield stresses have been normalized with respect to the room temperature yield stress for each steel tested.

Considering the similarity between the Australian AS A149 and the ASTM A36 specifications and the completeness of the Australian data, the object of this project was pursued using the Australian data for creep and plasticity of

AS A149. Elastic behavior, which is rather insensitive to precise material specification, was obtained from a variety of sources as noted in the report.

3. Calculation of Elastic Strain

Since $E = \sigma/\epsilon$ for elastic behavior, where E is Young's Modulus, σ is stress and ϵ is strain, the elastic component of strain, ϵ_e , can be calculated as follows

$$\epsilon_e = \frac{\sigma}{E} \times 10^2 \% \quad (3)$$

In order to calculate ϵ_e at various temperatures, T , it is necessary to find E as a function of T . The following empirical expression was obtained⁽⁷⁾ using data for α -iron given by Dever⁽⁸⁾ over a temperature range of 0 to 650°C:

$$E = 29.3 \times 10^3 - 12.6T \quad (4)$$

Values of E versus T are given by several authors for steels close to A36^(2,3,9), but the results are not always consistent with each other. It was found that the variations in ϵ_e caused by using these different values was relatively small compared to the values of ϵ_T obtained at the same stress and temperature. For example consider conditions at 600°C, where the values of E show the biggest variation (21.7×10^3 ksi and 16.9×10^3 ksi, given by Dever and De Falco, respectively). For a stress of 17.6 ksi the value of ϵ_e calculated using equation 4 was 0.081%, while that obtained using De Falco's value of E was 0.104%. Compared to the total strain observed after 2 minutes, at this stress and temperature, $\epsilon_T = 0.41\%$, the variation in ϵ_e was considered relatively insignificant. Thus all values of ϵ_e were calculated using the equation

$$\epsilon_e = \frac{\sigma \times 10^2}{(29.3 \times 10^3 - 12.6T)} \% \quad (5)$$

4. Calculation of Plastic Strain

The data given by Knight et al. are for various loads at temperatures between 350 and 650°C for times of 2 to 960 minutes. An assumption was made, by the present authors, that at 2 minutes any creep strain, ϵ_c , was negligible and that the strain observed at that time, ϵ_{2min} , was due to elastic, ϵ_e , and plastic, ϵ_p , components only. Obtaining ϵ_e by using equation (5), one may calculate ϵ_p as follows:

$$\epsilon_p = \epsilon_{2min} - \epsilon_e \quad (6)$$

Resulting values of ϵ_e and ϵ_p are given in Table 2. Since ϵ_p is time independent, it is only necessary to find an equation linking ϵ_p with the stress, σ , for a given temperature, T, i.e.,

$$\epsilon_p = F\sigma^G \quad (7)$$

where F and G are functions of temperature. Data for ϵ_p and σ were taken from two reports, one by Knight, Skinner and Lay⁽¹⁾ and the other by Skinner⁽⁵⁾, and are listed in Tables 2 and 3, respectively. Using the second reference, data was obtained from a graph reproduced here as Figure 2. This figure shows the contours of strains from 0.01 to 5% during tensile testing at a strain rate of $2 \times 10^{-3} \text{ min}^{-1}$ over a temperature range of 0 to 650°C.

Figures 3a to 3g show values of ϵ_p plotted against σ on a log-log scale. It can be seen that for all temperatures the results are well represented by straight lines, enabling calculation of the constants log F and G from equation (7) at each temperature. The values of log F and G obtained in this manner are given in Table 4 and are plotted against temperature in Figures 4 and 5. Least squares fitting of the results gave

$$\log F = -0.00041 * T^{1.647} \quad (8)$$

and

$$G = T/(147 - 0.161 * T) \quad (9)$$

Therefore,

$$\epsilon_p = 10^{-(0.00041 * T^{1.647})} * \sigma^{T/(147 - 0.161 * T)} \quad (10)$$

5. Calculation of Creep Strain

Because creep strain is time dependent it is necessary to find an equation of the form:

$$\epsilon_c = At^B \sigma^C \quad (11)$$

where ϵ_c is creep strain, t is time and A , B , and C are functions of temperature. Values of ϵ_c were found using equation (1).

Figures 6a to 6g show log-log plots of ϵ_c versus t for different values of σ . The results are well represented by straight lines as shown. For each temperature an average value of B was found (Table 5) and these were then plotted linearly against temperature as shown in Figure 7. Least squares fitting gave the equation

$$B = -1.1 + 0.0035 * T \quad (12)$$

The same procedure was repeated for log-log plots of ϵ_c versus σ for different values of t as seen in Figures 8a to 8g. Average values of C (Table 5) were plotted linearly against temperature in Figure 9, but this time the results were very scattered. In spite of this, least squares fitting was used to obtain a straight line resulting in the relationship

$$C = 2.1 + 0.0064 * T \quad (13)$$

Values of the constant A in equation (11) were found by calculating $\log \epsilon_c / t^B \sigma^C$ for each stress and time at a given temperature (Table 5). The results were averaged and plotted against temperature in Figure 10.

This time the points can be represented by two straight lines intersecting at 500°C. The equations for the two lines in Figure 10 are:

for $T < 500^\circ\text{C}$

$$A = 10^{-(6.10 + 0.573 * T)} \quad (14)$$

for $T > 500^\circ\text{C}$

$$A = 10^{-(13.25 - 0.00851 * T)} \quad (15)$$

Calculation of values of A at $T = 500^\circ\text{C}$ can be made using either of equations (14) or (15). Having obtained values for constants A, B, and C equation (9), $\epsilon_c = At^B\sigma^C$ can now be evaluated.

6. Calculation of Total Strain

The total strain, ϵ_T , is the sum of the elastic, plastic and creep strains:

$$\epsilon_T = \epsilon_e + \epsilon_p + \epsilon_c \quad (1)$$

where

$$\epsilon_e = 10^2 * \sigma / (29300 - 12.6 * T) \quad (5)$$

$$\epsilon_p = 10^{-(0.00041 * T^{1.647})} * \sigma^T / (147 - 0.016 * T) \quad (10)$$

and for $T < 500^\circ\text{C}$

$$\epsilon_c = 10^{-(6.10 + 0.00573 * T)} * t^{(-1.1 + 0.0035 * T)} * \sigma^{(2.1 + 0.0064 * T)} \quad (16)$$

or for $T \geq 500^\circ\text{C}$

$$\epsilon_c = 10^{-(13.25 - 0.00851 * T)} * t^{(-1.1 + 0.0035 * T)} * \sigma^{(2.1 + 0.0064 * T)} \quad (17)$$

where T is in degrees C, σ is in ksi and ϵ is in %.

Using these equations values of ϵ_e , ϵ_p , ϵ_c and ϵ_T were calculated for each temperature, stress and time reported by Knight et al.⁽¹⁾ The resulting values are listed in Table 6 along with the data measured by Knight et al.

7. Correlation of Measured and Calculated Plastic Strains

Values of plastic strain calculated using equation (10) are given in Table 7. Figures 11a to 11f show plots of measured and calculated plastic strains versus stress for temperatures ranging from 350 to 600°C. The measured values include results from both the creep studies of Knight et al.⁽¹⁾ and the tensile testing work of Skinner⁽⁵⁾. As can be seen, the correlation between results at all temperatures is good.

8. Correlation of Measured and Calculated Creep Strains

Figures 12a to 12g show plots of measured and calculated creep strains for temperatures of 350 to 650°C. The correlation of many of the results is excellent while for some the agreement is not so good. Two things should be noted: (1) Except in one case, the calculated values of creep strain are higher than those measured, thus overestimating the strain achieved and giving a conservative prediction. (2) During work at 550°C Knight et al.⁽¹⁾ carried out two tests at the same stress of 23.4 ksi. As these gave different values of creep strain both sets of results are included in Figure 12e. It can be seen that one set is in better agreement with the calculated value than is the other. A similar situation occurs at 350°C where two strains of 47.9 and 48.0 ksi were used. It can be seen in Figure 12a that there was apparently higher creep strain resulting from the lower stress. These two cases are the only indications of possible experimental error in the work of Knight et al.

9. Correlation of Measured and Calculated Total Strains

Figures 13a to 13g show plots of measured and calculated total strains for three different stress levels at temperatures between 350°C and 650°C for times of up to 8 hours. Once again, in general the agreement is very good. As

for creep strain, where there are discrepancies the calculated result always overestimates the total strain thus giving conservative values for any given condition. As also noted in the last section, two sets of results for the same stress were given by Knight et al.⁽¹⁾ at 550°C. Both are included in Figure 13e, thus giving an indication of possible experimental variations.

10. Correlation of Measured and Calculated Strains for SS41

As stated in the introduction, creep testing on SS41, a steel close to A36 specifications, was carried out by Fujimoto et al.⁽²⁾ This work can be used to test the correlation between values predicted by equations (16) and (17) and separately obtained experimental results. Values of plastic, creep and total strains measured by Fujimoto et al. were obtained from the figures included in reference 2. These values are shown in Tables 8 and 9. It will be shown that the agreement for creep strains is remarkably good, while this is not so true for plastic strains.

10.1 Plastic Strains

It was noted in Section 2 that the temperature dependences of the yield stresses are different for the various steels considered, as shown in Figure 1. These differences are very marked for the two steels relevant to the discussion here, i.e., AS A149 and SS41. For example, at 400°C the values of σ_Y/σ_{YRT} are 0.81 and 0.63, respectively. Thus at a given temperature and load a specimen made of SS41 steel will show a considerably larger plastic strain than will one made of AS A149 steel. A comparison of results predicted by equations (16) and (17) and those measured by Fujimoto is given in Table 8.

10.2 Creep Strain

Values of creep strain for SS41 are shown in Tables 9a to 9d. These include results measured by Fujimoto et al.⁽²⁾ and values predicted both by

Fujimoto and the present investigation. One point should be noted: The value of t is the time during which creep occurred and does not include the time of two minutes assumed by the present authors to involve only elastic and plastic strains, see Section 4. Thus, before using equations (16) and (17) to predict creep strains, two minutes needs to be added to each value of the time t as given by Fujimoto.

Figures 14a to 14d show the correlation between the measurements and both predictions for ϵ_c during loading at temperatures of 350, 450, 550, and 600°C. Figure 14a shows the results for the highest stress level used at 350°C. In Figures 14a and 14b the correlations can be seen to be good. In Figure 14c, at a temperature of 550°C and a stress of 17.8 ksi, it can be seen that while the agreement between the present prediction and the measurements of Fujimoto is not so good, it is considerably better than that for the prediction of Fujimoto et al. themselves. In Figure 14d, at a temperature of 600°C and a stress of 10.7 ksi, the prediction of Fujimoto is too low while that of the present investigation is too high. For a stress of 14.2 ksi both predictions are low but that from equation (17) is closer to the measured values.

It should also be noted that for each temperature, stress and time only one specimen was tested. No indication is given of possible experimental variation, such as that found in the two cases carried out by Knight et al.⁽¹⁾ and mentioned previously.

11. Deformation Mechanism Maps

A deformation mechanism map is a map that shows the deformation modes operating under known conditions of time, temperature and stress. In the present case the deformation consists of elastic, plastic, and creep modes. Equations (16) and (17) and data from the tensile tests of Skinner⁽⁵⁾ have been

used to construct such maps for times of 2, 15, 30, 60, and 240 minutes at temperature, see Figures 15-19b.

Figure 15 shows a map for conditions after two minutes at temperature. As was stated in Section 4, it was assumed that at 2 minutes only the elastic and plastic modes were operating and that creep was negligible. Thus this map consists of only three areas, one of which is dominated by elasticity, one by plasticity and one in which fracture has occurred. Also shown are the contours of total strain values of 1, 2, and 5%. Figure 16a shows deformation modes after 15 minutes at temperature and includes creep as a deformation mechanism. Figure 16b shows the same map as 16a but includes total strain value contours of 1, 2, and 5%. Figures 17a to 19b show maps obtained after 30, 60, and 240 minutes at temperature, respectively. In all the maps the dominant deformation mode existing in each area is shown underlined. In the following section the construction of a Deformation Mechanism Map for a loading time of 60 minutes is considered.

12. Construction of the Deformation Mechanism Maps

Many pieces of information have to be considered in order to construct a deformation mechanism map. These include:

12.1 The Boundary at which Fracture Occurs

This boundary was deduced from the tensile test results of Skinner⁽⁵⁾ as shown in Figure 2. Values of σ_T , the U.T.S. are given in Table 10a. For temperatures of 500°C and above values were taken directly from Figure 2. Between 350 and 500°C the curve was extrapolated by eye.

12.2 The Boundary between ELASTIC and Elastic PLASTIC

This boundary, seen in Figure 15, is also present in all the other maps. The critical condition was considered to be a plastic strain, ϵ_p , of 0.1%.

When $\epsilon_p \geq 0.1\%$ plasticity dominated while when $\epsilon_p \leq 0.1\%$ elasticity was the dominant mode. The boundary had to be obtained for two ranges of temperatures - above and below 350°C. Above 350°C, equations (15) and (16) were used to calculate the stress causing $\epsilon_p = 0.1\%$ for each temperature. Since the equations were not valid for temperatures below 350°C the boundary in this range was constructed using the contour of 0.1% proof stress taken from Figure 2⁽⁵⁾. The results are shown in Table 10b. As would be desired both methods gave close to the same value of stress at 350°C, so that the elastic/plastic boundary was continuous across this temperature.

12.3 The Boundary between Elastic CREEP and Elastic Plastic CREEP

For conditions such that creep occurs this boundary will be a continuation of the previous one between elastic and elastic plastic. See Figure 16. The critical value of plastic strain was taken to be 0.1%.

12.4 The Boundary between ELASTIC and Elastic CREEP

Equations (16) and (17) were used to calculate conditions at which $\epsilon_c = 0.1\%$. The results are shown in Table 10d. Above this boundary creep was considered to be dominant.

12.5 The Boundary between Elastic PLASTIC and Elastic PLASTIC Creep

Once again it was necessary to calculate conditions at which $\epsilon_c = 0.1\%$. For temperatures above 350°C equation (16) was used. Below 350°C the curve was extrapolated backwards by eye. The results are given in Table 10e. Above this boundary, although there is some creep, plasticity remains the dominant mode.

12.6 The Boundary between Elastic PLASTIC Creep and Elastic Plastic CREEP

For this boundary equation (16) were used to find the conditions at which $\epsilon_p = \epsilon_c$. The results are given in Table 10f. Above the boundary

plasticity is dominant while below it creep dominates.

12.7 Total Strain Contours of 1%, 2%, and 5%

On Figures 16b, 17b, 18b, and 19b total strain contours of 1, 2, and 5% are shown. At 350°C and above these were calculated from equations (16) and (17). Below 350°C these contours were taken from those shown in Figure 2. The values of stress for these total strains are given in Table 10g.

13. Conclusions

1. Using data for Australian steel A149 an equation has been developed that enables calculation of elastic, plastic, creep and total strains for given conditions of stress and time, and for temperatures between 350 and 650°C.

2. Correlation between the measured and predicted strains is good.

3. The prediction for values of creep strain was tested against separately obtained results for the Japanese steel, SS41. The agreement is good.

4. Deformation mechanism maps were constructed using the above equation, for times of 2 to 240 minutes and temperatures of 350 to 650°C. The dominant mechanism for any given condition of temperature, stress and time is shown on the maps.

Acknowledgements

We would like to thank the American Iron and Steel Institute (A.I.S.I.) for financial support and encouragement of the study reported here. In particular, the efforts of Mr. David Jeans and Mrs. Kathleen Almand of A.I.S.I. to collect data from American steel producers and to disseminate the early fruits of this work in order to stimulate industrial interaction is greatly appreciated.

References

1. Knight, D., Skinner, D. H., and Lay, M. G., "Prediction of Isothermal Creep," Broken Hill Proprietary Company, Clayton, Victoria, Australia. Melbourne Research Lab. Report 18/2, April 1971, pp. 1-14.
2. Fujimoto, M., Furumur, F., Ave, T., and Shinohara, Y., "Primary Creep of Structural Steel (SS41) at High Temperatures," Trans. A.I.J., No. 296, October 1980, pp. 145-157.
3. De Falco, F. D., "Investigation of the Compressive Response of Modern Structural Steels at Fire Load Temperatures," Doctoral Dissertation, University of Connecticut, 1974, pp. 1-50.
4. Holt, J. M., "Short-Time Elevated-Temperature Tensile Properties of USS COR-TEN and USS TRI-TEN High Strength Low-Alloy Steels, USS MAN-TEN (A440) High Strength Steel and ASTM A36 Steel," (57.19-901) (1) Progress Report (n-HS-2), United States Steel, Applied Research Lab., Monroeville, Pennsylvania, October 1964.
5. Skinner, D. H., "Determination of High Temperature Properties of Steel," Broken Hill Proprietary Company, Melbourne, Australia, Technical Bulletin, Vol. 16, No. 2, November 1972, pp. 10-21.
6. Jerath, V., Cole, K. J., and Smith, C. I., "Elevated Temperature Properties of Structural Steel Manufactured by the British Steel Corporation," Report T/RS/1189/11/80C, British Steel Corp., Teeside, England, July 1980.
7. Fields, R. J., "Fracture Mechanisms in Round Bars with a Detailed Study of Finger-Like Crack Growth," Ph.D Thesis, University of Cambridge, 1978, p. 208.

8. Dever, D. J., "Temperature Dependence of the Elastic Constants in α -Iron Single Crystals: Relationship to Spin Order and Diffusion Anomalies," J. Appl. Phys., Vol. 43, 1972, p. 3293.
9. Brockenbrough, R. L., "Investigation of Heat Curved Girders," Presented at the Annual Meeting of the American Assoc. of State Highway Officials, Minneapolis, Minnesota, December 1968.

Table 1. Compositions and Tensile Properties for
ASTM A36, AS A149, and SS41 Steels

	<u>A36</u>	<u>A149(1)</u>	<u>SS41(2)</u>
C		0.27	0.18
Si		0.128	0.24
Mn		0.65	0.73
P	max 0.04	0.033	0.016
S	max 0.05	0.041	0.017
Ni	--	0.086	--
Cr	--	0.16	--
Cu	--	0.01	--
σ_y psi	36,000	35,500	35,300
MPA	250	245	243
σ_T psi	58,000 to 80,000	70,500	62,400
MPA	400 to 550	487	431

Table 2. Values of Plastic Strain for AS A149 from Knight et al.⁽¹⁾

Temp. C	σ ksi	$E \times 10^3$ ksi	$\epsilon_{2min} \%$	$\epsilon_e = \frac{\sigma}{E_T} \%$	$\epsilon_p = \epsilon_{2min} - \epsilon_e \%$
350	32.1	24.9	.28	.13	.15
	40.2		.84	.16	.68
	47.9		1.90	.19	1.71
	48.0		1.68	.19	1.49
	52.3		2.35	.21	2.14
	56.2		3.30	.23	3.07
	60.1		3.70	.24	3.46
	61.0		3.68	.25	3.43
400	21.1	24.3	.13	.09	.04
	23.2		.18	.10	.08
	38.8		.95	.16	.79
	48.6		2.07	.20	1.87
	51.7		2.51	.21	2.30
	56.0		3.43	.23	3.20
	450		21.1	23.6	.10
23.2		.15	.10		.05
31.9		.44	.14		.30
41.8		1.20	.17		1.03
45.1		1.90	.19		1.71
46.7		2.31	.20		2.11
48.1		2.75	.20		2.55
500		21.0	23.0		.15
	23.4	.20		.10	.10
	28.1	.37		.12	.25
	31.1	.60		.14	.46
	32.2	.82		.14	.68
	34.0	1.04		.15	.89
	37.0	1.28		.16	1.12
	550	16.1		22.4	.09
18.5		.12	.08		.04
20.3		.24	.09		.15
23.4		.29	.10		.19
23.4		.35	.11		.24
25.0		.43	.11		.32
26.7		.70	.12		.58
600		9.7	21.7		.03
	12.0	.10		.06	.04
	12.8	.15		.06	.09
	16.5	.21		.08	.13
	17.6	.41		.08	.33

Table 2. (continued)
Values of Plastic Strain for AS A149 from Knight et al. (1)

Temp. C	σ ksi	$E \times 10^3$ ksi	$\epsilon_{2min} \%$	$\epsilon_e = \frac{\sigma}{E_T} \%$	$\epsilon_p = \epsilon_{2min} - \epsilon_e \%$
650	4.8	21.1	.06	.02	.04
	6.4		.07	.03	.04
	8.8		.07	.04	.03
	11.2		.20	.05	.15

Table 3. Values of Plastic Strain for AS A149 from Skinner⁽⁵⁾

Temp. C	σ ksi	$E_T \times 10^3$ ksi	$\epsilon_p + \epsilon_e$ %	$\epsilon_e = \frac{\sigma}{E_T}$ %	ϵ_p %
350	21.6	24.9	--	--	0.01
	24.8		--	--	0.05
	26.2		--	--	0.10
	27.2		0.25	0.11	0.14
	29.1		--	--	0.20
	32.4		0.5	0.13	0.37
	39.3		1.0	0.16	0.84
	44.5		1.5	0.18	1.32
	49.2		2.0	0.20	1.80
	53.4		2.5	0.21	2.29
	56.4		3.0	0.23	2.77
	58.8		3.5	0.24	3.26
	61.1		4.0	0.25	3.75
	62.7		4.5	0.25	4.25
	64.4		5.0	0.26	4.74
400	20.6	24.3	--	--	0.01
	23.1		--	--	0.05
	26.0		--	--	0.10
	27.2		0.25	0.11	0.14
	29.1		--	--	0.20
	32.1		0.5	0.13	0.37
	38.1		1.0	0.16	0.84
	43.3		1.5	0.18	1.22
	47.3		2.0	0.19	1.81
	51.1		2.5	0.21	2.24
	53.2		3.0	0.22	2.78
	55.1		3.5	0.23	3.27
	57.0		4.0	0.23	3.77
	58.3		4.5	0.24	4.26
	59.4		5.0	0.24	4.76
450	19.9	23.6	--	--	0.01
	23.2		--	--	0.05
	25.5		--	--	0.10
	26.8		0.25	0.11	0.16
	28.3		--	--	0.20
	31.1		0.5	0.13	0.37
	36.2		1.0	0.15	0.85
	40.3		1.5	0.17	1.33
	42.8		2.0	0.18	1.82
	45.2		2.5	0.18	2.32
	46.5		3.0	0.19	2.81
	47.3		3.5	0.19	3.31
	48.3		4.0	0.20	3.80
	49.1		4.5	0.20	4.30
	50.3		5.0	0.21	4.79

Table 3. (continued)
Values of Plastic Strain for AS A149 from Skinner⁽⁵⁾

Temp. C	σ ksi	$E_T \times 10^3$ ksi	$\epsilon_p + \epsilon_e$ %	$\epsilon_e = \frac{\sigma}{E_T}$ %	ϵ_p %
500	20.2	23.0	--	--	0.01
	22.2		--	--	0.05
	24.3		--	--	0.10
	26.1		0.25	0.11	0.14
	26.1		--	--	0.20
	29.0		0.5	0.13	0.37
	33.4		1.0	0.15	0.85
	35.3		1.5	0.15	1.35
	36.7		2.0	0.16	1.84
	36.9		2.5	0.16	2.34
	38.7		3.0	0.17	2.83
	38.7		3.5	0.17	3.33
	38.7		4.0	0.17	3.83
	40.5		4.5	0.18	4.32
	40.5		5.0	0.18	4.82
550	14.4	22.4	--	--	0.01
	17.6		--	--	0.05
	19.2		--	--	0.10
	20.0		0.25	0.09	0.16
	20.7		--	--	0.20
	21.7		0.5	0.10	0.40
	23.9		1.0	0.11	0.89
	24.8		1.5	0.11	1.39
	24.8		2.0	0.11	1.89
	25.5		2.5	0.11	2.39
	25.5		3.0	0.11	2.89
	25.5		3.5	0.11	3.39
	25.5		4.0	0.11	3.89
	26.0		4.5	0.12	4.38
	26.0		5.0	0.12	4.88
600	10.6	21.7	--	--	0.01
	12.9		--	--	0.05
	13.9		--	--	0.10
	13.9		0.25	0.06	0.19
	14.7		--	--	0.20
	15.5		0.5	0.07	0.43
	15.5		1.0	0.07	0.93
	16.3		1.5	0.08	1.42
	16.3		2.0	0.08	1.92
	16.8		2.5	0.08	2.42
	16.8		3.0	0.08	2.92
	16.8		3.5	0.08	3.42
	17.3		4.0	0.08	3.92
	17.3		4.5	0.08	4.42
	17.3		5.0	0.08	4.92

Table 3. (continued)
Values of Plastic Strain for AS A149 from Skinner⁽⁵⁾

Temp. C	σ ksi	$E_T \times 10^3$ ksi	$\epsilon_p + \epsilon_1$ %	$\epsilon_e = \frac{\sigma}{E_T}$ %	ϵ_p %
650	8.1	18.1	--	--	0.01
	9.7		--	--	0.05
	10.3		--	--	0.10
	10.3		0.25	0.06	0.19
	11.1		--	--	0.20
	11.1		0.5	0.06	0.44
	11.1		1.0	0.06	0.94
	11.1		1.5	0.06	1.44
	11.1		2.0	0.06	1.94
	11.1		2.5	0.06	2.44
	11.1		3.0	0.06	2.94
	11.1		3.5	0.06	3.44
	11.1		4.0	0.06	3.94
	11.1		4.5	0.06	4.44
	11.1		5.0	0.06	4.94

Table 4. Values of log F(T) and G(T) where $\epsilon_p = F\sigma^G$

Temp. C	log F	G
350	-6.406	3.918
400	-7.838	4.816
450	-9.657	6.062
500	-11.16	7.315
550	-13.44	9.703
600	-13.79	11.40
650	-17.68	17.00

Table 5. Values of A(T), B(T) and C(T) where $\epsilon_c = At^B \sigma^C$

Temp. C	A	B	C
350	8.04	0.15	3.8
400	8.48	0.31	3.9
450	8.74	0.45	4.9
500	8.9	0.58	7.2
550	8.61	0.71	5.9
600	8.2	1.00	6.5
650	7.6	1.24	4.7

Table 6a. Measured and Calculated Strains During Loading at 350C

Temp C	Ex10 ³ ksi	σ ksi	$\frac{\sigma}{\sigma_{yRT}}$	t mins	calculated strains %				measured strains %			
					ϵ_e	ϵ_p	ϵ_c	ϵ_T	ϵ_e	ϵ_p	ϵ_c	ϵ_T
350	24.9	32.1	.90	2	.13	.29	0	.42	.13	.15	0	.28
				4			.03	.45			.07	.35
				6			.03	.45			.07	.35
				10			.04	.46			.07	.35
				18			.04	.46			.07	.35
				30			.04	.46			.07	.35
				60			.04	.46			.08	.36
				120			.05	.47			.07	.35
				240			.05	.47			.07	.35
				480			.06	.48			.07	.35
				960			.06	.48			.12	.40
350	24.9	40.2	1.13	2	.16	.70	0	.86	.16	.68	0	.84
				4			.08	.94			.07	.91
				6			.08	.94			.08	.92
				10			.10	.95			.08	.92
				18			.10	.96			.08	.92
				30			.11	.97			.09	.93
				60			.12	.98			.10	.94
				120			.13	.99			.12	.96
				240			.14	1.00			.14	.98
				480			.15	1.01			.16	1.00
				960			.17	1.03			.18	1.02
350	24.9	47.9	1.35	2	.19	1.37	0	1.56	.19	1.71	0	1.90
				4			.17	1.73			.20	2.10
				6			.18	1.74			.21	2.11
				10			.20	1.76			.22	2.12
				18			.22	1.78			.23	2.13
				30			.23	1.79			.25	2.15
				60			.26	1.82			.27	2.17
				120			.28	1.84			.30	2.20
				240			.30	1.87			.34	2.24
				480			.33	1.89			.38	2.28
				960			.36	1.92			.44	2.34
350	24.9	48.0	1.35	2	.19	1.38	0	1.57	.19	1.49	0	1.68
				4			.17	1.74			.15	1.83
				6			.18	1.76			.16	1.84
				10			.2	1.77			.17	1.85
				18			.22	1.79			.18	1.87
				30			.24	1.81			.19	1.88
				60			.26	1.83			.21	1.89
				120			.28	1.85			.22	1.90
				240			.31	1.88			.25	1.93
				480			.34	1.91			.29	1.97
				960			.37	1.94			.32	2.00

Table 6a. Continued

Temp C	Ex10 ³ ksi	σ ksi	$\frac{\sigma}{\sigma_{yRT}}$	t mins	calculated strains %				measured strains %			
					ϵ_e	ϵ_p	ϵ_c	ϵ_T	ϵ_e	ϵ_p	ϵ_c	ϵ_T
350	24.9	52.3	1.47	2	.21	1.92	0	2.13	.21	2.14	0	2.35
				4			.25	2.38			.21	2.56
				6			.27	2.40			.22	2.57
				10			.29	2.42			.23	2.58
				18			.32	2.45			.24	2.59
				30			.34	2.47			.27	2.62
				60			.37	2.51			.29	2.64
				120			.41	2.54			.34	2.69
				240			.45	2.58			.39	2.74
				480			.49	2.62			.47	2.82
960			.53	2.66			.55	2.90				
350	24.9	56.2	1.58	2	.23	2.54	0	2.76	.23	3.07	0	3.30
				4			.34	3.10			.40	3.70
				6			.37	3.13			.43	3.73
				10			.40	3.16			.46	3.76
				18			.44	3.2			.48	3.78
				30			.47	3.23			.50	3.80
				60			.51	3.27			.55	3.85
				120			.56	3.32			.61	3.91
				240			.61	3.37			.69	3.99
				480			.67	3.43			.83	4.13
960			.73	3.49			1.00	4.30				
350	24.9	60.1	1.69	2	.24	3.29	0	3.53	.24	3.46	0	3.70
				4			.45	3.99			.48	4.18
				6			.49	4.02			.50	4.20
				10			.53	4.06			.53	4.23
				18			.58	4.11			.56	4.26
				30			.62	4.15			.60	4.30
				60			.68	4.21			.64	4.34
				120			.75	4.28			.74	4.44
				240			.82	4.35			.86	4.56
				480			.89	4.42			.99	4.69
960			.97	4.50			1.19	4.89				
350	24.9	61.0	1.72	2	.25	3.48	0	3.72	.25	3.43	0	3.68
				4			.48	4.20			.55	4.23
				6			.52	4.25			.58	4.26
				10			.57	4.29			.60	4.28
				18			.61	4.34			.64	4.32
				30			.66	4.39			.67	4.35
				60			.73	4.45			.70	4.38
				120			.79	4.51			.79	4.47
				240			.86	4.59			.89	4.57
				480			.94	4.67			1.04	4.72
960			1.03	4.76			1.27	4.95				

Table 6b. Measured and Calculated Strains During Loading at 400C

Temp C	Ex10 ³ ksi	σ ksi	$\frac{\sigma}{\sigma_{yRT}}$	t mins	calculated strains %				measured strains %			
					ϵ_e	ϵ_p	ϵ_c	ϵ_T	ϵ_e	ϵ_p	ϵ_c	ϵ_T
400	24.3	21.1	.59	2	.09	.03	0	.12	.09	.04	0	.13
				960			.05	.17		0	.13	
400	24.3	23.2	.65	2	.10	.05	0	.15	.10	.08	0	.18
				480			.07	.22		0	.18	
400	24.3	38.8	1.09	2	.16	.60	0	.76	.16	.79	0	.95
				4			.13	.89		.11	1.06	
				6			.15	.91		.13	1.08	
				10			.19	.95		.15	1.10	
				18			.23	1.00		.18	1.13	
				30			.28	1.04		.20	1.15	
				60			.35	1.11		.29	1.24	
				120			.35	1.19		.31	1.26	
				240			.53	1.29		.37	1.32	
				480			.64	1.41		.48	1.43	
400	24.3	48.6	1.37	2	.20	1.80	0	2.00	.20	1.87	0	2.07
				4			.44	2.44		.23	2.30	
				6			.50	2.50		.27	2.34	
				10			.58	2.58		.32	2.39	
				18			.70	2.70		.38	2.45	
				30			.81	2.81		.47	2.54	
				60			1.00	3.00		.57	2.64	
				120			1.23	3.23		.68	2.75	
				240			1.52	3.52		.89	2.96	
				480			1.87	3.87		1.17	3.24	
400	24.3	51.7	1.46	2	.21	2.42	0	2.63	.21	2.30	0	2.51
				4			.48	3.12		.29	2.80	
				6			.59	3.22		.34	2.85	
				10			.73	3.37		.41	2.92	
				18			.90	3.53		.49	3.00	
				30			1.06	3.70		.58	3.09	
				60			1.32	3.96		.72	3.23	
				120			1.64	4.27		.89	3.40	
				240			2.02	4.66		1.09	3.60	
				480			2.49	5.13		1.37	3.88	
400	24.3	56.0	1.58	2	.23	3.57	0	3.80	.23	3.20	0	3.43
				4			.69	4.50		.53	3.96	
				6			.86	4.66		.62	4.05	
				10			1.06	4.86		.72	4.15	
				18			1.30	5.10		.88	4.31	
				30			1.53	5.34		1.03	4.46	
				60			1.92	5.72		1.29	4.7	

Table 6c. Measured and Calculated Strains During Loading at 450C

Temp C	Ex10 ³ ksi	σ ksi	$\frac{\sigma}{\sigma_{yRT}}$	t mins	calculated strains %				measured strains %			
					ϵ_s	ϵ_p	ϵ_c	ϵ_T	ϵ_s	ϵ_p	ϵ_c	ϵ_T
450	23.6	21.1	.59	2	.09	.02	0	.11	.09	.01	0	.10
				4			.01	.12		.01	.11	
				6			.02	.13		.01	.11	
				10			.02	.13		.02	.12	
				18			.03	.14		.03	.13	
				30			.04	.15		.03	.13	
				60			.06	.17		.05	.15	
				120			.08	.19		.05	.15	
				240			.11	.22		.05	.15	
				480			.15	.27		.10	.20	
450	23.6	23.2	.65	2	.10	.04	0	.14	.10	.05	0	.15
				4			.02	.16		.01	.16	
				6			.03	.17		.01	.16	
				10			.04	.18		.02	.17	
				18			.05	.19		.02	.17	
				30			.06	.21		.05	.20	
				60			.09	.23		.07	.22	
				120			.13	.27		.10	.25	
				240			.18	.32		.13	.28	
				480			.25	.39		.16	.32	
450	23.6	31.9	.90	2	.13	.29	0	.43	.14	.30	0	.44
				4			.09	.52		.13	.57	
				6			.12	.55		.16	.60	
				10			.17	.60		.18	.62	
				18			.24	.67		.21	.65	
				30			.31	.75		.24	.68	
				60			.44	.87		.30	.74	
				120			.62	1.05		.37	.81	
				240			.87	1.30		.45	.89	
				480			1.21	1.64		.56	1.00	
450	23.6	41.8	1.18	2	.18	1.51	0	1.68	.18	1.02	0	1.20
				4			.35	2.03		.48	1.68	
				6			.48	2.16		.56	1.76	
				10			.67	2.35		.67	1.87	
				18			.93	2.61		.82	2.02	
				30			1.21	2.89		.93	2.13	
				60			1.71	3.39		1.15	2.35	
				120			2.40	3.39		1.45	2.65	
				240			3.34	5.02		1.87	3.07	
				480			4.65	6.34		2.44	3.66	

Table 6c. Continued

Temp C	Ex10 ³ ksi	σ ksi	$\frac{\sigma}{\sigma_{yRT}}$	t mins	calculated strains %				measured strains %			
					ϵ_e	ϵ_p	ϵ_c	ϵ_T	ϵ_e	ϵ_p	ϵ_c	ϵ_T
450	23.6	45.1	1.27	2	.19	2.38	0	2.57	.19	1.71	0	1.90
				4			.50	3.08			.35	2.23
				6			.70	3.27			.45	2.35
				10			.97	3.55			.58	2.48
				18			1.35	3.93			.75	2.65
				30			1.76	4.33			1.05	2.95
				60			2.49	5.07			1.31	3.21
				120			3.49	6.06			1.73	3.63
				240			4.87	7.45			2.28	4.18
450	23.6	46.7	1.32	2	.20	2.94	0	3.14	.20	2.11	0	2.31
				4			.60	3.74			.44	2.75
				6			.83	3.97			.56	2.87
				10			1.16	4.30			.73	3.04
				18			1.61	4.75			.97	3.28
				30			2.10	5.24			1.22	3.53
				60			2.97	6.11			1.64	3.95
				120			4.16	7.30			2.27	4.58
				450	23.6	48.1	1.35	2	.20	3.52	0	3.72
4			.69					4.41			.78	3.53
6			.96					4.68			1.06	3.81
10			1.33					5.05			2.75	4.10
18			1.85					5.57			1.80	4.55
30			2.42					6.13			2.25	5.00

Table 6d. Measured and Calculated Strains During Loading at 500C

Temp C	Ex10 ³ ksi	σ ksi	$\frac{\sigma}{\sigma_{yRT}}$	t mins	calculated strains %				measured strains %			
					ϵ_e	ϵ_p	ϵ_c	ϵ_T	ϵ_e	ϵ_p	ϵ_c	ϵ_T
500	23.0	21.0	.59	2	.09	.03	0	.12	.09	.06	0	.15
				4			.02	.14		.01	.16	
				6			.03	.15		.01	.16	
				10			.04	.16		.01	.16	
				18			.06	.18		.02	.17	
				30			.09	.21		.02	.17	
				60			.14	.27		.04	.19	
				120			.23	.35		.10	.25	
				240			.36	.49		.16	.31	
				480			.57	.69		.20	.35	
500	23.0	23.4	.66	2	.10	.07	0	.17	.10	.10	0	.20
				4			.03	.20		.04	.24	
				6			.04	.22		.05	.25	
				10			.07	.25		.08	.28	
				18			.11	.29		.10	.30	
				30			.16	.33		.13	.33	
				60			.26	.43		.20	.40	
				120			.41	.58		.30	.50	
				240			.64	.82		.48	.68	
				480			1.00	1.18		.70	.90	
960			1.58	1.76		1.08	1.28					
500	23.0	28.1	.79	2	.12	.29	0	.41	.12	.25	0	.37
				4			.08	.49		.13	.50	
				6			.12	.53		.17	.54	
				10			.19	.60		.23	.60	
				18			.29	.71		.31	.68	
				30			.42	.84		.39	.76	
				60			.68	1.09		.55	.92	
				120			1.07	1.48		.77	1.14	
				240			1.69	2.10		1.04	1.41	
				480			2.65	3.07		1.37	1.74	
960			4.18	4.59		1.99	2.36					
500	23.0	31.1	.88	2	.14	.62	0	.76	.14	.46	0	.60
				4			.20	.96		.23	.83	
				6			.27	1.03		.33	.93	
				10			.37	1.13		.43	1.03	
				18			.54	1.30		.51	1.19	
				30			.76	1.46		.75	1.35	
				60			1.19	1.95		1.03	1.63	
				120			1.87	2.63		1.60	2.30	
				240			2.93	3.69		2.05	2.65	
				480			4.60	5.36		3.28	3.88	

Table 6d. Continued

Temp C	Ex10 ³ ksi	σ ksi	$\frac{\sigma}{\sigma_{yRT}}$	t mins	calculated strains %				measured strains %			
					ϵ_e	ϵ_p	ϵ_c	ϵ_T	ϵ_e	ϵ_p	ϵ_c	ϵ_T
500	23.0	32.2	.91	2	.14	.81	0	.95	.14	.68	0	.82
				4			.16	1.11			.35	1.17
				6			.24	1.19			.46	1.28
				10			.38	1.33			.60	1.42
				18			.60	1.55			.82	1.64
				30			.87	1.82			1.00	1.82
				60			1.39	2.34			1.48	2.30
				120			2.20	3.16			2.15	2.97
				240			3.47	4.43			3.31	4.13
500	23.0	34.0	.96	2	.15	1.22	0	1.37	.15	.89	0	1.04
				4			.21	1.58			.21	1.25
				6			.33	1.69			.33	1.37
				10			.51	1.88			.78	1.82
				18			.80	2.17			1.09	2.13
				30			1.15	2.52			1.41	2.45
				60			1.85	3.22			2.16	3.20
				120			2.94	4.31			3.31	4.35
				500	23.0	37.0	1.04	2	.16	2.30	0	2.46
4			.32					2.79			.57	1.85
6			.51					2.98			.77	2.05
10			.80					3.27			1.05	2.35
18			1.25					3.72			1.46	2.74
30			1.81					4.27			1.97	3.25
60			2.91					5.37			2.88	4.16

Table 6e. Measured and Calculated Strains During Loading at 550C

Temp C	Ex10 ³ ksi	σ ksi	$\underline{\sigma}$ σ_{yRT}	t mins	calculated strains %				measured strains %			
					ϵ_e	ϵ_p	ϵ_c	ϵ_T	ϵ_e	ϵ_p	ϵ_c	ϵ_T
550	22.4	16.1	.45	2	.07	.01	0	.08	.07	.02	0	.09
				4			.03	.11		.06	.15	
				6			.05	.13		.07	.16	
				10			.09	.17		.09	.18	
				18			.16	.24		.10	.19	
				30			.26	.33		.15	.24	
				60			.47	.55		.25	.34	
				120			.84	.92		.44	.53	
				240			1.49	1.57		.81	.90	
480			2.66	2.73		1.39	1.48					
550	22.4	18.5	.52	2	.08	.04	0	.12	.08	.04	0	.12
				4			.04	.16		.13	.25	
				6			.11	.23		.18	.30	
				10			.20	.32		.26	.38	
				18			.35	.47		.43	.55	
				30			.56	.68		.57	.68	
				60			1.02	1.13		.82	.94	
				120			1.83	1.94		1.23	1.35	
				240			3.26	3.37		1.93	2.05	
480			5.78	5.91		3.23	3.35					
550	22.4	20.8	.59	2	.09	.11	0	.20	.09	.15	0	.24
				4			.12	.32		.19	.43	
				6			.22	.42		.29	.53	
				10			.38	.58		.44	.68	
				18			.68	.88		.68	.92	
				30			1.08	1.28		.94	1.18	
				60			1.96	2.16		1.46	1.70	
				120			3.53	3.73		2.29	2.53	
				240			6.29	6.49		3.81	4.05	
550	22.4	23.4	.66	2	.10	.33	0	.43	.10	.19	0	.29
				4			.24	.67		.38	.67	
				6			.42	.85		.55	.84	
				10			.74	1.17		.85	1.13	
				18			1.31	1.74		1.33	1.62	
				30			2.09	2.52		1.54	1.83	
				60			3.80	4.24		2.76	3.05	

Table 6e. Continued

Temp C	Ex10 ³ ksi	σ ksi	$\frac{\sigma}{\sigma_{yRT}}$	t mins	calculated strains %				measured strains %			
					ϵ_e	ϵ_p	ϵ_c	ϵ_T	ϵ_e	ϵ_p	ϵ_c	ϵ_T
550	22.4	23.4	.66	2	.10	.33	0	.43	.10	.25	0	.35
				4			.24	.67			.42	.79
				6			.42	.85			.65	1.00
				10			.74	1.17			.97	1.32
				18			1.31	1.74			1.22	1.57
				30			2.09	2.52			2.10	2.45
				60			3.80	4.24			3.46	3.81
550	22.4	25.0	.70	2	.11	.61	0	.72	.11	.32	0	.43
				4			.34	1.06			.35	.78
				6			.61	1.33			.60	1.03
				10			1.08	1.80			.89	1.32
				18			1.90	2.63			1.50	1.93
				30			3.02	3.74			1.95	2.38
				60			5.52	6.24			2.95	4.38
550	22.4	26.7	.75	2	.12	1.13	0	1.25	.12	.58	0	.70
				4			.50	1.74			.85	1.55
				6			.88	2.12			1.31	2.01
				10			1.56	2.80			2.05	2.75
				18			2.77	4.01			3.30	4.00

Table 6f. Measured and Calculated Strains During Loading at 600C

Temp C	Ex10 ³ ksi	σ ksi	\underline{g} σ_{yRT}	t mins	calculated strains %				measured strains %			
					ϵ_e	ϵ_p	ϵ_c	ϵ_T	ϵ_e	ϵ_p	ϵ_c	ϵ_T
600	21.7	9.7	.27	2	.04	0	0	.04	.04	0	0	.03
				4			.01	.06		.02	.05	
				6			.02	.07		.03	.06	
				10			.04	.09		.05	.08	
				18			.08	.13		.06	.09	
				30			.15	.19		.09	.12	
				60			.30	.35		.15	.18	
				120			.62	.66		.26	.29	
				240			1.24	1.29		.51	.54	
				480			2.49	2.53		1.00	1.03	
600	21.7	12.0	.34	2	.06	0	0	.06	.06	.04	0	.10
				4			.04	.09		.04	.14	
				6			.07	.13		.07	.17	
				10			.15	.21		.13	.23	
				18			.30	.35		.26	.36	
				30			.52	.57		.34	.44	
				60			1.07	1.12		.58	.68	
				120			2.18	2.24		.95	1.15	
				240			4.39	4.45		1.93	2.03	
				480			8.83	8.88		2.85	3.95	
600	21.7	12.8	.36	2	.06	.01	0	.06	.06	.09	0	.15
				4			.05	.12		.07	.22	
				6			.11	.17		.13	.28	
				10			.22	.28		.20	.35	
				18			.43	.50		.39	.52	
				30			.76	.82		.60	.75	
				60			1.57	1.64		1.10	1.25	
				120			3.20	3.26		2.20	2.35	
				240			6.25	6.51		4.33	4.48	
				600	21.7	16.5	.46	2	.08	.12	0	.19
4			.24					.44		.20	.41	
6			.49					.68		.38	.59	
10			.98					1.17		.79	1.00	
18			1.96					2.15		1.44	1.65	
30			3.43					3.62		2.54	2.75	
600	21.7	17.6	.50	2	.08	.25	0	.33	.08	.33	0	.41
				4			.36	.69		.73	1.14	
				6			.71	1.05		1.24	1.65	
				10			1.44	1.77		2.11	2.52	
				18			2.87	3.20		3.79	4.20	

Table 6g. Measured and Calculated Strains During Loading at 650C

Temp C	Ex10 ³ ksi	σ ksi	σ_{yRT}	t mins	calculated strains %				measured strains %							
					ϵ_e	ϵ_p	ϵ_c	ϵ_T	ϵ_e	ϵ_p	ϵ_c	ϵ_T				
650	21.1	4.8	.14	2	.02	0	0	.02	.02	.04	0	.06				
				4			0	.02		0	.06					
				6			0	.02		0	.06					
				10			0	.03		0	.06					
				18			.01	.03		0	.06					
				30			.02	.04		0	.06					
				60			.04	.06		0	.06					
				120			.10	.12		.07	.13					
				240			.22	.24		.13	.19					
				480			.49	.52		.46	.52					
650	21.1	6.4	.18	2	.03	0	0	.03	.03	.04	0	.07				
				4			0	.03		.02	.09					
				6			.01	.04		.03	.10					
				10			.02	.05		.06	.13					
				18			.06	.09		.10	.17					
				30			.11	.14		.33	.40					
				60			.25	.28		.38	.45					
				120			.58	.61		.42	.49					
				240			1.32	1.35		1.14	1.21					
				480			3.00	3.03		3.58	3.65					
650	21.1	8.8	.25	2	.04	0	0	.04	.04	.03	0	.07				
				4			.04	.08		.06	.13					
				6			.08	.12		.14	.21					
				10			.18	.22		.27	.34					
				18			.41	.45		.55	.62					
				30			.78	.83		.96	1.03					
				60			1.84	1.89		1.96	2.03					
				120			4.25	4.29		4.19	4.26					
				650	21.1	11.2	.31	2	.05	.03	0	.08	.05	.15	.09	.20
								4			.16	.24		.27	.47	
6			.36					.45		.45	.65					
10			.81					.90		.93	1.13					
18			1.83					1.92		1.85	2.05					
30			3.54					3.63		3.35	3.55					

Table 7. Calculated Values of Plastic Strain

Temp. C	σ ksi	ϵ_p %
350	25.0	.11
	32.1	.29
	40.2	.70
	47.9	1.37
	52.3	1.92
	56.2	2.54
	60.1	3.29
	61.0	3.48
	62.5	4.45
	65.0	4.45
66.0	4.72	
400	27.0	.12
	31.0	.20
	35.0	.37
	38.8	.60
	48.6	1.80
	51.7	2.42
	56.0	3.56
	58.0	4.23
	60.0	4.99
450	27.0	.11
	31.9	.29
	34.0	.43
	37.0	.72
	40.0	1.16
	41.8	1.51
	45.1	2.38
	46.7	2.94
	48.1	3.52
	49.0	3.94
	50.0	4.45
	50.5	4.72
500	24.5	.10
	28.1	.29
	31.1	.62
	32.2	.81
	34.0	1.22
	37.0	2.30
	39.0	3.42
550	20.8	.11
	23.4	.33
	25.0	.61
	26.7	1.13

Table 7. (continued) Calculated Values of Plastic Strain

Temp. C	σ ksi	ϵ_p %
600	16.5	.12
	17.0	.16
	17.6	.25
650	11.2	.03

Table 8. Measured and Calculated Plastic and Total Strains for SS41 Steel

Temp. C	σ ksi	Ex10 ³ ksi	$\epsilon_p + \epsilon_e$ %	$\epsilon_e = \frac{\sigma}{E}$ %	ϵ_p % Fujimoto	ϵ_p % Fields	ϵ_T %* Fujimoto	ϵ_T %* Fields
350	35.5	24.9	1.13	.14	.99	.43	1.20	.68
	39.0		1.52	.16	1.36	.62	1.62	.89
	42.6		1.82	.17	1.65	.87	1.95	1.19
400	21.3	24.3	.18	.09	.09	.03	.23	.14
	24.9		.35	.10	.25	.07	.43	.21
	28.4		.53	.12	.41	.13	.63	.33
	32.0		.88	.13	.75	.24	1.03	.51
	35.5		1.27	.15	1.12	.39	1.51	.77
450	17.8	23.6	.09	.07	.02	.01	.11	.10
	21.3		.18	.09	.09	.03	.28	.18
	24.9		.37	.11	.26	.07	.55	.30
	28.4		.69	.12	.57	.15	1.0	.51
	32.0		1.02	.14	.88	.30	1.43	.88
500	14.2	23.0	.06	.06	.00	.00	.09	.08
	17.8		.11	.08	.03	.01	.22	.15
	21.3		.24	.09	.15	.04	.59	.28
	24.9		.44	.11	.33	.12	1.08	.58
	28.4		.88	.12	.76	.32	--	--
550	10.7	22.4	.05	.05	.00	.00	.11	.10
	14.2		.07	.06	.01	.00	.29	.30
	17.8		.18	.08	.10	.02	--	--
	21.3		.50	.10	.40	.13	--	--
600	7.1	21.1	.03	.03	.00	.00	.06	.08
	10.7		.06	.05	.01	.00	.42	.59
	14.2		.17	.07	.10	.02	--	--

* ϵ_T - total strain after 60 min. at temperature.

-- - these specimens fractured before 60 minutes at temperature.

The values of strain are those measured by Fujimoto and calculated by Fields.

Table 9a. Measured and Calculated Creep Strains for SS41 During Loading at 350°C

Temp C	σ ksi	t mins.	ϵ_c % measured by Fujimoto	ϵ_c % calculated by Fields	ϵ_c % calculated by Fujimoto
350	35.5	2	.028	.045	.023
		5	.036	.051	.029
		10	.042	.056	.034
		20	.049	.061	.042
		37	.054	.065	.048
		62	.068	.070	.055
		99	.081	.074	.062
		156	.097	.078	.070
		250	.12	.083	.078
		355	.13	.087	.086
350	39.1	2	.036	.069	.036
		5	.050	.077	.045
		10	.056	.084	.054
		20	.070	.092	.064
		37	.082	.099	.076
		63	.10	.106	.087
		99	.12	.11	.097
		159	.14	.12	.11
		249	.16	.13	.12
		370	.19	.13	.14
350	42.6	2	.046	.10	.054
		5	.064	.11	.069
		10	.073	.12	.082
		20	.085	.13	.097
		37	.10	.14	.11
		63	.13	.15	.13
		100	.15	.16	.15
		155	.18	.17	.16
		248	.21	.18	.18
		354	.24	.19	.20

Table 9b. Measured and Calculated Creep Strains for SS41 During Loading at 450°C

Temp. C	σ ksi	t mins.	ϵ_c % measured by Fujimoto	ϵ_c % calculated by Fields	ϵ_c % calculated by Fujimoto
450	17.8	2	.019	.005	.016
		5	.025	.008	.021
		10	.031	.011	.026
		19	.034	.014	.032
		33	.039	.019	.038
		58	.044	.024	.046
		91	.046	.030	.053
		144	.050	.037	.061
		227	.055	.046	.071
		350	.058	.057	.081
450	21.3	2	.03	.012	.034
		4	.05	.017	.043
		10	.06	.026	.057
		19	.07	.035	.070
		33	.09	.045	.084
		58	.10	.059	.10
		90	.11	.073	.12
		144	.13	.091	.13
		232	.14	.114	.16
450	24.9	2	.059	.026	.067
		5	.090	.040	.089
		9	.11	.053	.11
		19	.13	.076	.14
		32	.15	.097	.16
		56	.18	.12	.19
		90	.20	.16	.22
		143	.23	.20	.26
		226	.25	.25	.30
450	28.4	2	.074	.05	.12
		5	.11	.08	.16
		9	.15	.10	.19
		19	.20	.15	.24
		32	.26	.19	.28
		56	.31	.24	.34
		88	.36	.30	.39
		144	.43	.38	.46
		228	.48	.47	.53
		336	.55	.57	.60

Table 9b. (continued) Measured and Calculated Creep Strains for SS41 During Loading at 450°C

Temp. C	σ ksi	t mins.	ϵ_c % measured by Fujimoto	ϵ_c % calculated by Fields	ϵ_c % calculated by Fujimoto
450	32.0	2	.11	.09	.20
		5	.17	.14	.26
		9	.22	.19	.31
		18	.28	.26	.39
		32	.35	.34	.47
		56	.41	.44	.56
		90	.49	.55	.65
		141	.59	.68	.75
		225	.67	.85	.87
		333	.75	1.03	.99

Table 9c. Measured and Calculated Creep Strains for SS41 During Loading at 550°C

Temp. C	σ ksi	t mins.	ϵ_c % measured by Fujimoto	ϵ_c % calculated by Fields	ϵ_c % calculated by Fujimoto
550	10.7	2	.015	0	.018
		5	.023	.006	.026
		10	.028	.011	.033
		19	.036	.019	.043
		34	.044	.030	.053
		57	.055	.046	.065
		93	.065	.069	.078
		147	.077	.10	.093
		236	.086	.15	.11
		349	.097	.20	.13
550	14.2	2	.044	.014	.057
		5	.071	.030	.081
		10	.098	.054	.11
		19	.14	.092	.13
		33	.18	.14	.17
		56	.22	.22	.20
		91	.27	.33	.24
		142	.33	.48	.29
		230	.42	.72	.35
		345	.54	1.00	.41
550	17.8	2	.18	.051	.14
		5	.33	.11	.20
		9	.48	.18	.25
		19	.70	.32	.33
		32	.98	.51	.40
		60	--	.85	.51
		90	--	1.19	.59
		120	--	1.51	.66
		247	--	--	.92
		362	--	--	1.00
550	21.3	2	.41	.14	.29
		5	.78	.30	.41
		9	1.2	.49	.51
		20	--	.94	.69
		30	--	1.31	.80
		60	--	2.33	1.05

Table 9d. Measured and Calculated Creep Strains for SS41 During Loading at 600°C

Temp. C	σ ksi	t mins.	ϵ_c % measured by Fujimoto	ϵ_c % calculated by Fields	ϵ_c % calculated by Fujimoto
600	7.1	2	.013	.002	.010
		5	.016	.004	.015
		10	.021	.008	.019
		20	.024	.016	.026
		35	.028	.033	.032
		60	.032	.049	.040
		99	.035	.081	.050
		155	.040	.13	.060
		247	.042	.20	.073
		378	.046	.31	.087
600	10.7	2	.054	.019	.048
		5	.090	.047	.070
		10	.12	.094	.093
		19	.18	.18	.12
		34	.25	.32	.15
		58	.36	.55	.19
		93	.50	.88	.23
		146	.68	1.38	.28
		238	.87	2.24	.34
600	14.2	2	.28	.10	.14
		5	.61	.25	.21
		9	.96	.45	.27
		15	--	.75	.33
		20	--	1.00	.37
		30			.44
		60			.59

Table 10. Construction of a Deformation Mechanism Map for a Loading Time of 60 mins.

Table 10a. The Boundary at Which Fracture Occurs

Temp. C	σ_T ksi	$\frac{\sigma_T}{\sigma_{YRT}}$	Reference
350*	70.6	1.99	(5)
400*	62.5	1.76	
450*	51.8	1.46	
500	40.6	1.14	
550	26.9	.76	
600	17.3	.49	
650	11.3	.32	

* Estimated from Figure 2 (reproduced from Skinner⁽⁵⁾) by extrapolating the curve to lower temperatures by eye.

Table 10b. The Boundary between ELASTIC and Elastic PLASTIC

Temp. C	σ ksi	$\frac{\sigma}{\sigma_{YRT}}$	ϵ_e %	ϵ_p %	ϵ_c %	Reference
20	35.5	1.0	.12	.10	0	(5)
49	34.8	.98	.12	.10	0	
98	33.4	.94	.12	.10	0	
150	31.7	.89	.11	.10	0	
198	30.0	.85	.11	.10	0	
250	27.5	.77	.10	.10	0	
301	26.1	.73	.10	.10	0	
350	24.1	.68	.10	.10	.01	Equation (16)
400	26.8	.75	.11	.10	.06	
410	27.0	.76	.11	.10	.08	
420	27.1	.76	.11	.10	.10	

Table 10c. The Boundary between Elastic CREEP
Elastic Plastic CREEP

Temp. C	σ ksi	$\frac{\sigma}{\sigma_{YRT}}$	ϵ_e %	ϵ_p %	ϵ_c %	Reference
425	27.0	.76	.11	.10	.11	Equation (16)
450	26.7	.75	.11	.10	.18	Equation (16)
475	25.8	.73	.11	.10	.27	Equation (16)
500	24.4	.69	.11	.10	.33	Equation (17)
550	20.6	.58	.09	.10	1.92	Equation (17)
600	16.3	.46	.07	.10	6.84	Equation (17)
625	>UTS					

Table 10d. The Boundary between ELASTIC and Elastic CREEP

Temp. C	σ ksi	$\frac{\sigma}{\sigma_{YRT}}$	ϵ_e %	ϵ_p %	ϵ_c %	Reference
420	27.1	.76	.11	.10	.10	Equation (16)
425	26.5	.75	.11	.09	.10	Equation (16)
450	23.7	.67	.10	.05	.10	Equation (16)
475	21.3	.60	.09	.03	.10	Equation (16)
500	19.6	.55	.09	.02	.10	Equation (17)
525	15.4	.43	.07	0	.10	Equation (17)
550	12.2	.34	.05	0	.10	Equation (17)
575	9.8	.28	.04	0	.10	Equation (17)
600	8.0	.23	.04	0	.10	Equation (17)
650	5.5	.15	.03	0	.10	Equation (17)

Table 10e. The Boundary between Elastic PLASTIC and Elastic PLASTIC Creep

Temp. C	σ ksi	$\frac{\sigma}{\sigma_{YRT}}$	ϵ_e %	ϵ_p %	ϵ_c %	Reference
267*	70.6	1.99				Equation (16)
287*	57.5	1.62				Equation (16)
306*	50.1	1.41				Equation (16)
325	44.8	1.26	.18	1.12	.10	Equation (16)
350	39.0	1.10	.16	.62	.10	Equation (16)
400	29.7	.84	.12	.17	.10	Equation (16)

* curve extrapolated backwards by eye

Table 10f. The Boundary between Elastic PLASTIC Creep and Elastic Plastic CREEP

Temp. C	σ ksi	$\frac{\sigma}{\sigma_{YRT}}$	ϵ_e %	ϵ_p %	ϵ_c %	Reference
420	27.8	.78	.12	.12	.12	Equation (16)
425	33.3	.93	.14	.31	.31	Equation (16)
430	37.8	1.06	.16	.64	.64	Equation (16)
440	44.2	1.24	.19	1.78	1.78	Equation (16)
450	46.8	1.32	.20	2.98	2.98	Equation (16)
460	49.0	1.38	.21	4.98	4.98	Equation (16)

Table 10g. Total Strain Contours of 1%, 2%, and 5%

$\epsilon_T = 1\%$			$\epsilon_T = 2\%$			$\epsilon_T = 5\%$			Ref.
Temp. C.	σ ksi	$\frac{\sigma}{\sigma_{YRT}}$	Temp. C.	σ ksi	$\frac{\sigma}{\sigma_{YRT}}$	Temp. C.	σ ksi	$\frac{\sigma}{\sigma_{YRT}}$	
20	38.3	1.08	23	45.8	1.29	21	58.2	1.64	(5)
47	38.8	1.09	49	46.2	1.30	47	59.2	1.67	
99	39.7	1.12	99	47.3	1.33	99	61.7	1.74	
145	41.3	1.16	147	50.3	1.42	115	63.0	1.77	
197	42.5	1.20	197	54.1	1.52	146	66.8	1.88	
245	41.6	1.17	246	51.7	1.46	167	70.3	1.97	
297	40.0	1.13	297	49.8	1.40	174	70.9	2.00	
350	40.5	1.14	350	49.2	1.39	350	62.8	1.77	Eq. (16)
400	37.5	1.07	400	44.5	1.25	400	54.4	1.53	Eq. (16)
450	32.9	.93	450	37.8	1.06	450	45.0	1.27	Eq. (16)
500	27.7	.78	500	31.3	.88	500	36.6	1.03	Eq. (17)
550	18.1	.51	550	20.5	.58	550	24.1	.68	Eq. (17)
600	11.7	.34	600	13.2	.37	600	15.5	.44	Eq. (17)
650	7.9	.22	650	8.9	.25	650	10.3	.29	Eq. (17)

A36 STEEL

NORMALIZED YIELD STRESS VERSUS TEMPERATURE

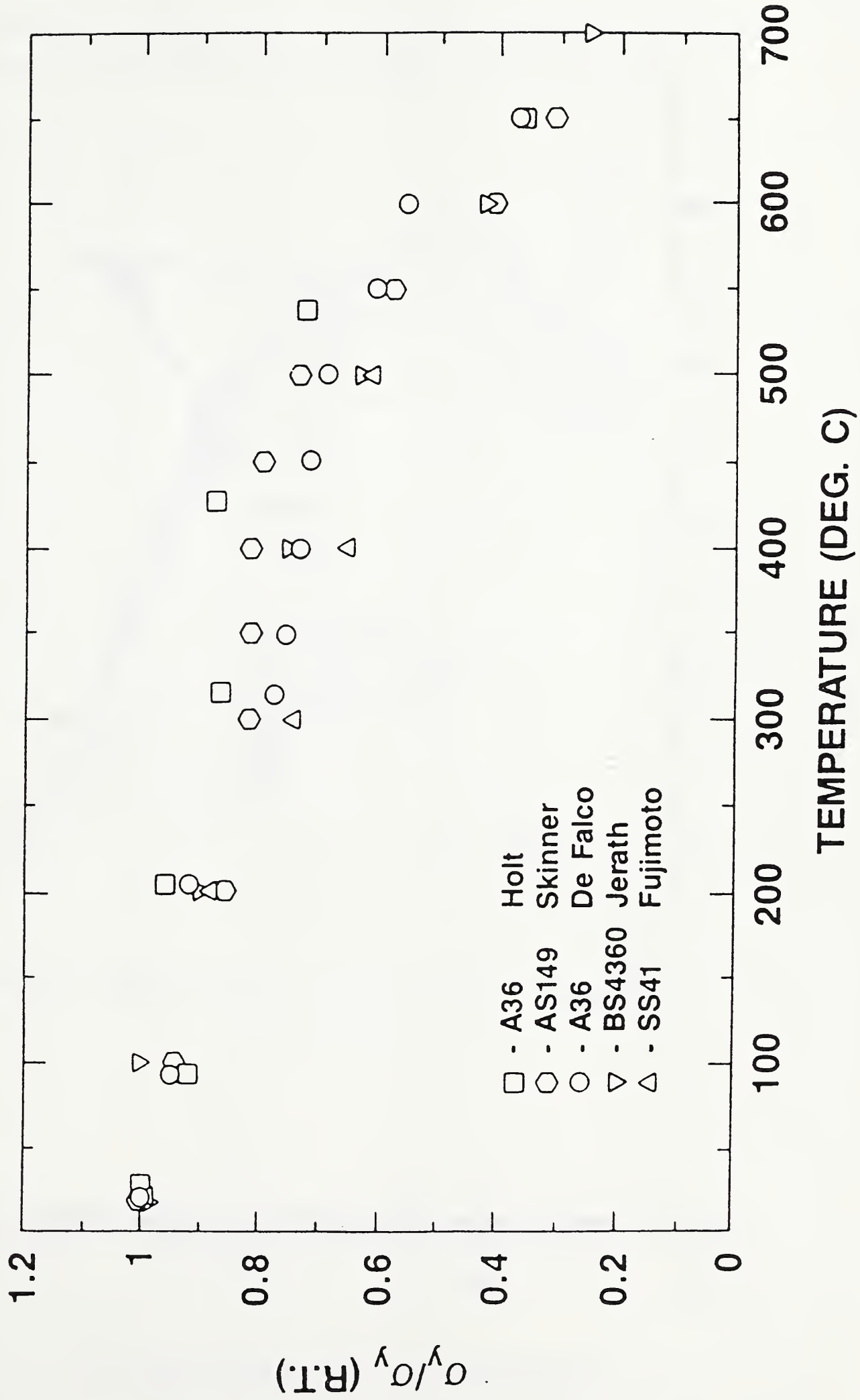


Figure 1. Normalized yield stress versus temperature for A36 and similar steels.

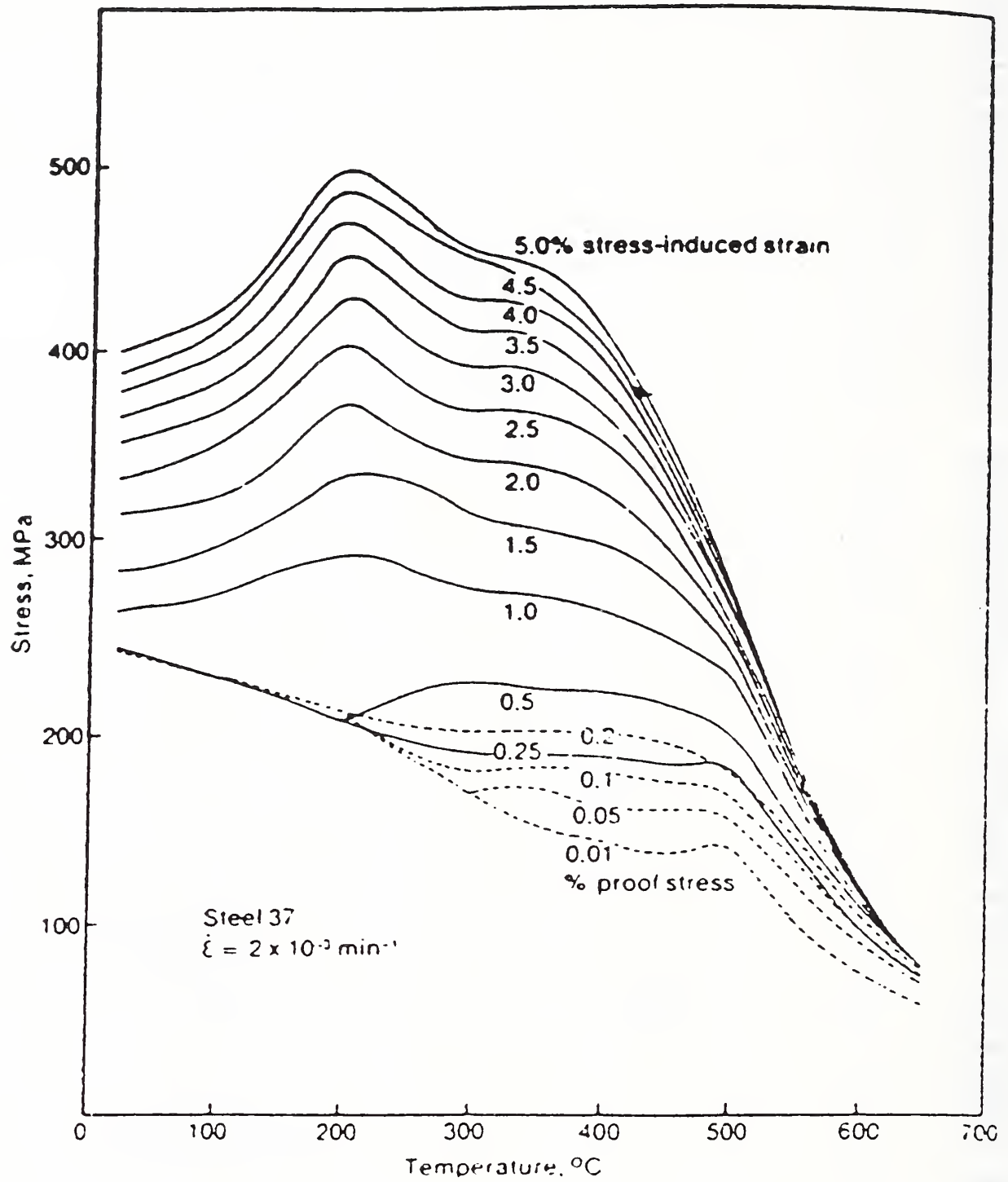


Figure 2. The effect of temperature on the proof and flow stress of AS Al49 steel at a strain rate of $2 \times 10^{-3} \text{ min}^{-1}$ (5).

PLASTIC STRAIN VS STRESS AT 400 DEG C

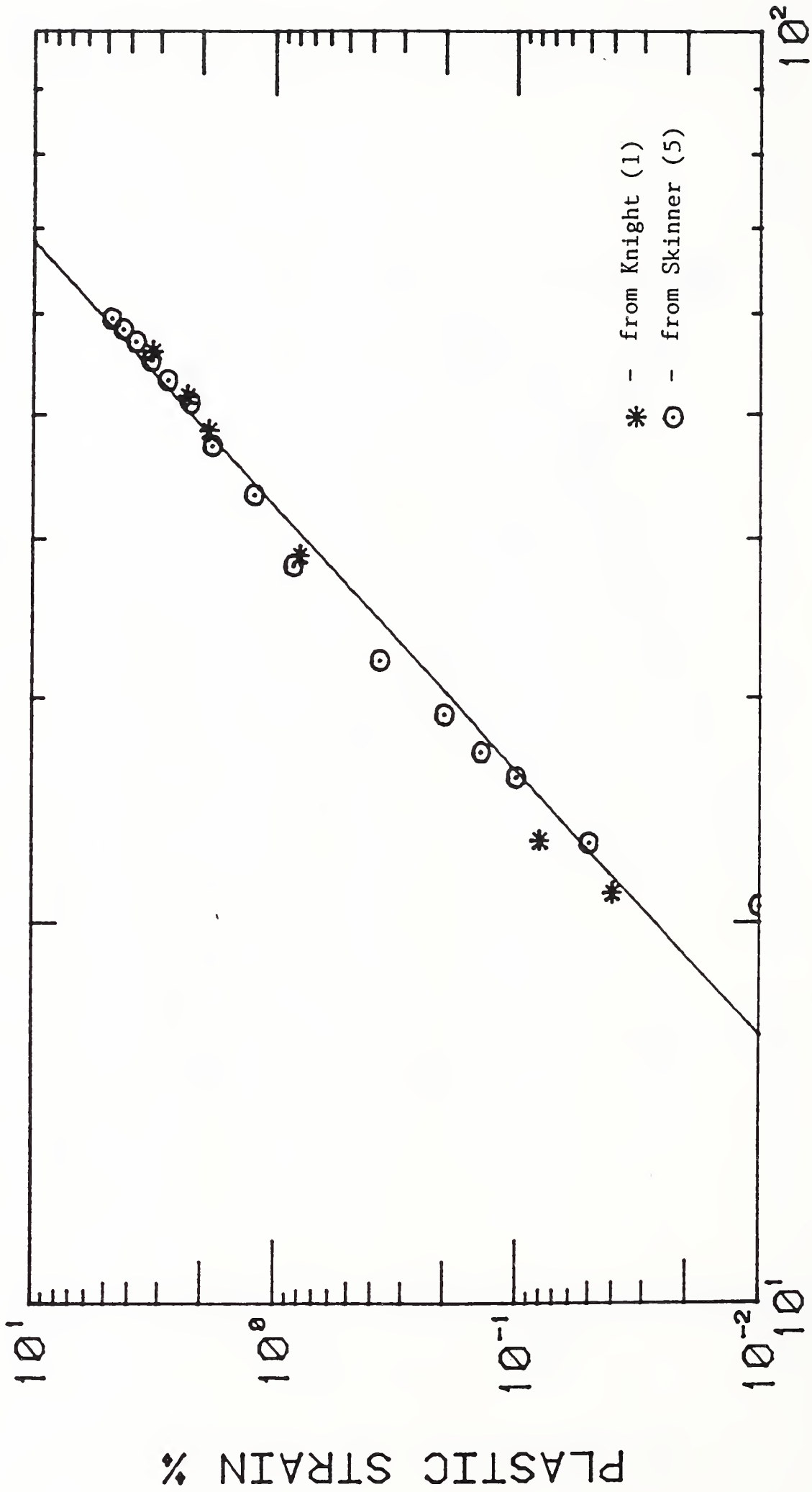


Figure 3b. Plastic strain versus stress at 400°C.

PLASTIC STRAIN VS STRESS AT 450 DEG C

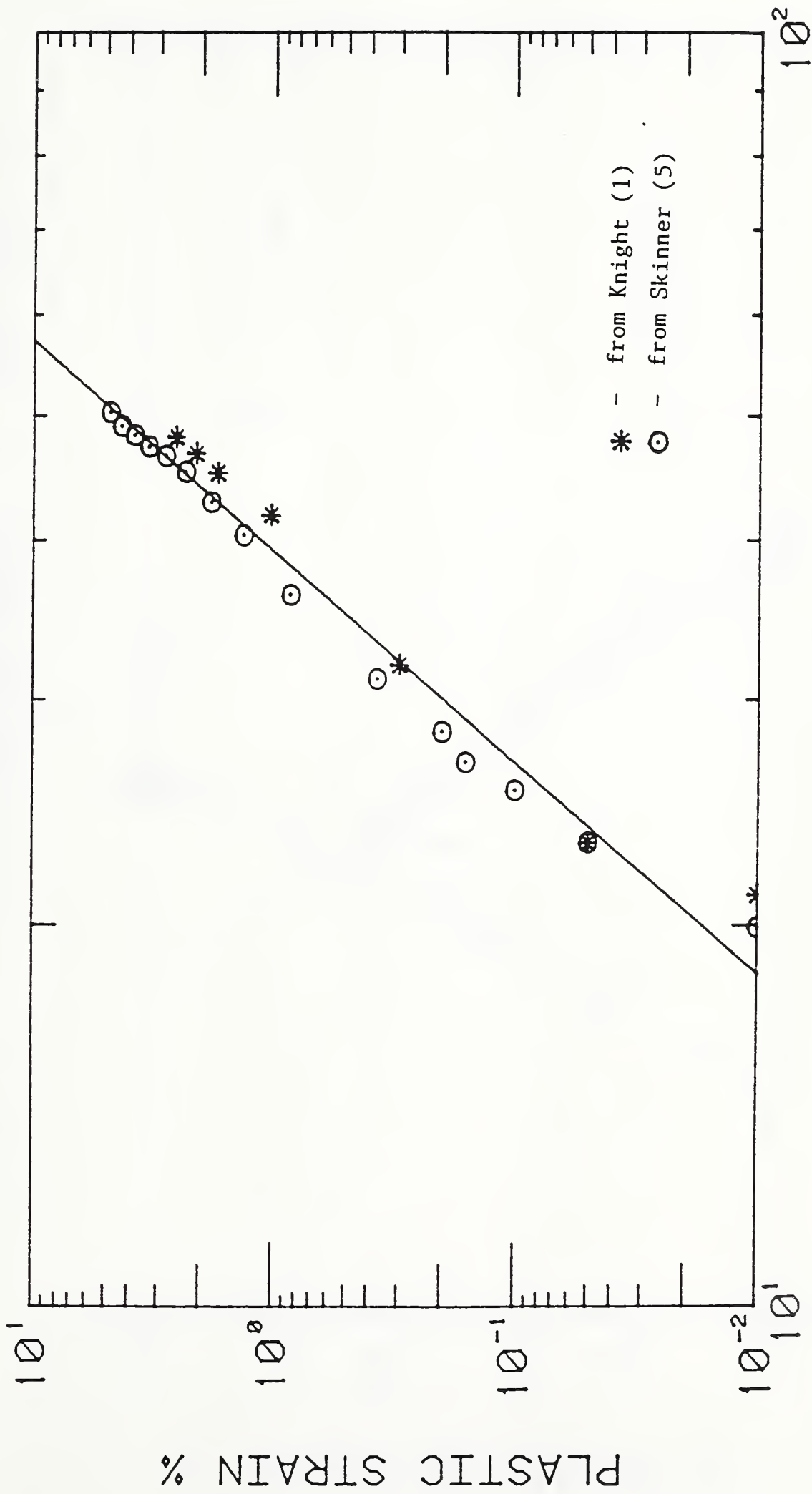
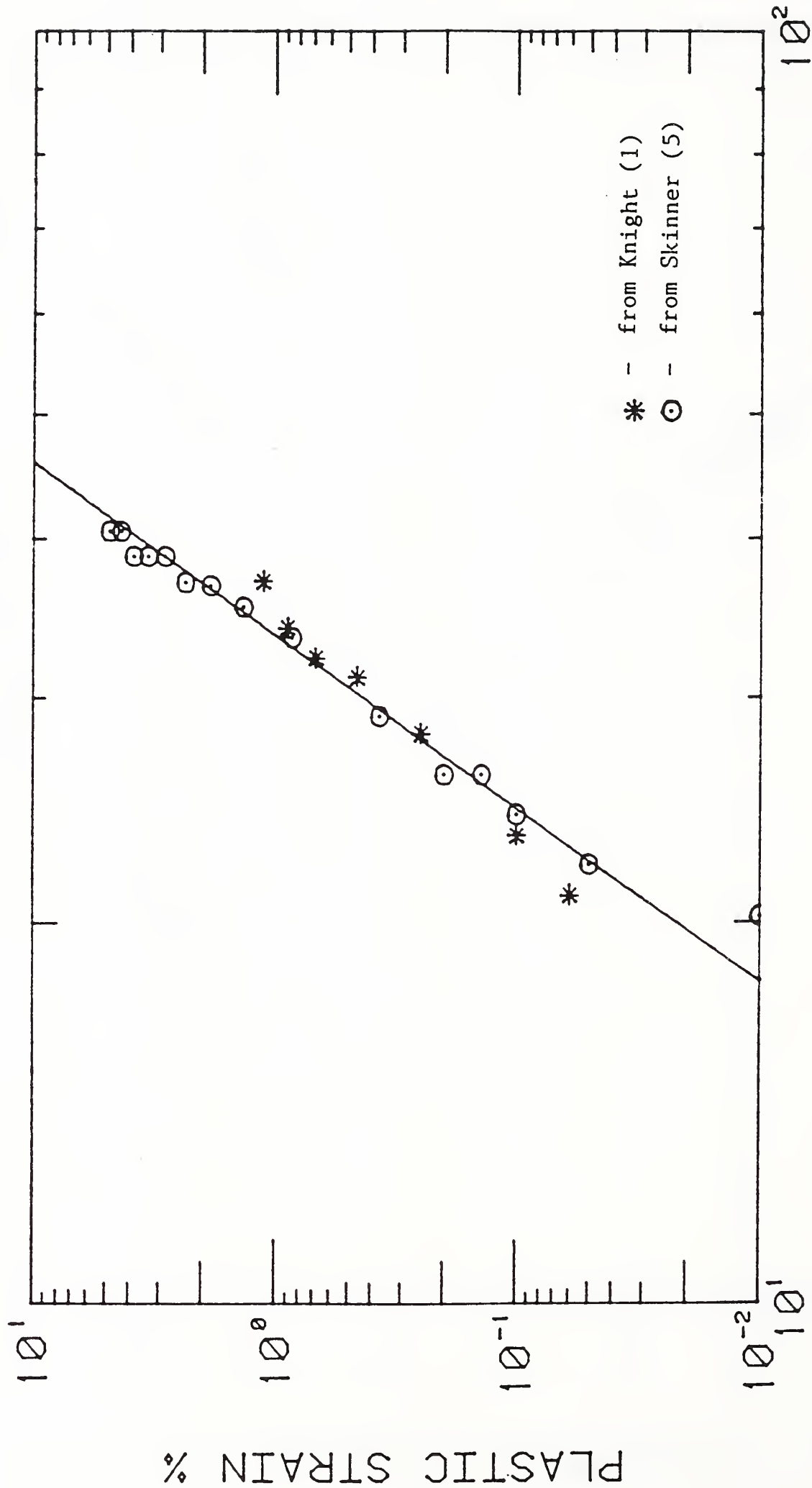


Figure 3c. Plastic strain versus stress at 450°C.

PLASTIC STRAIN VS STRESS AT 500 DEG C



STRESS KSI

Figure 3d. Plastic strain versus stress at 500°C.

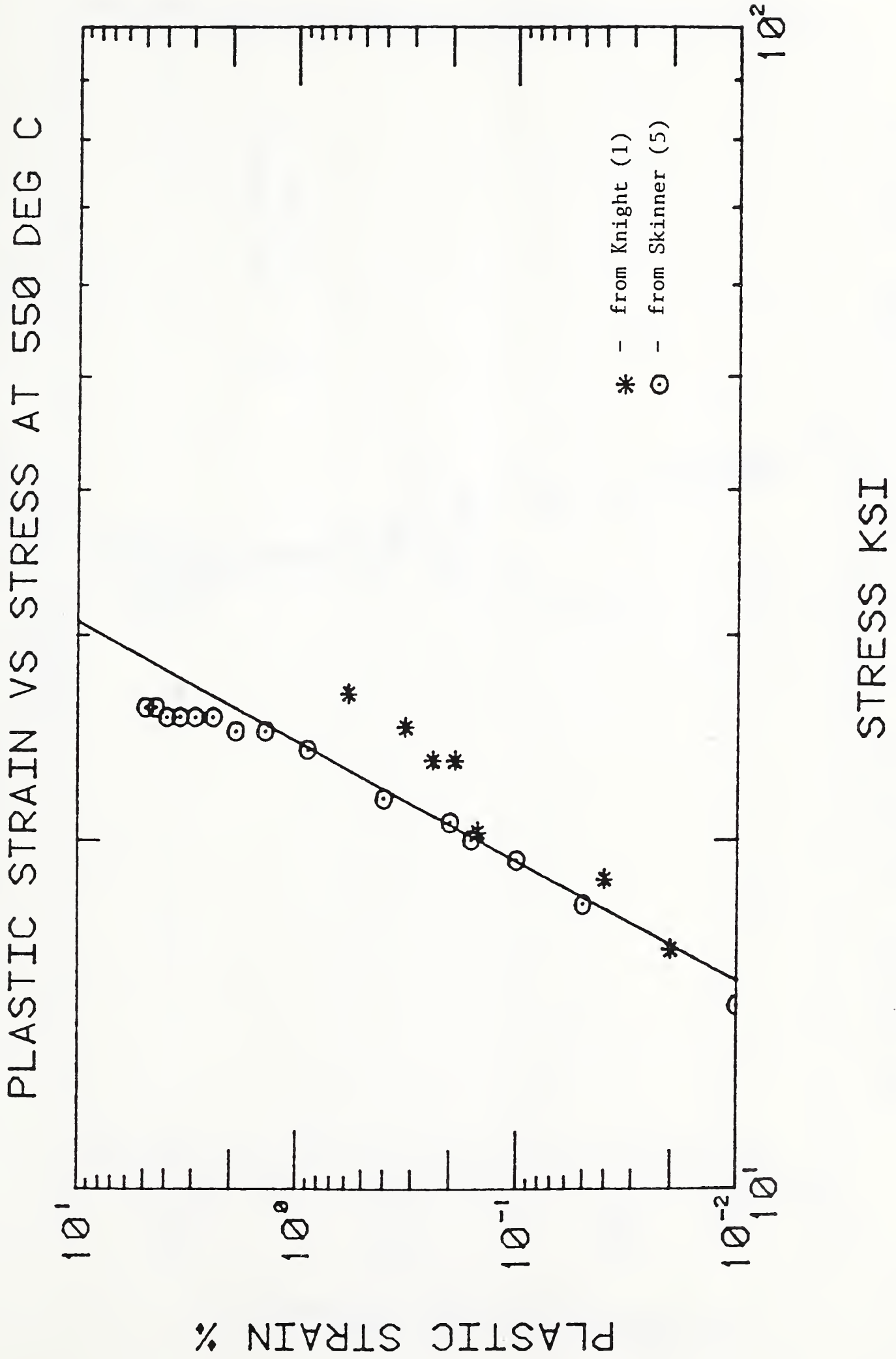


Figure 3e. Plastic strain versus stress at 550°C.

PLASTIC STRAIN VS STRESS AT 600 DEG C

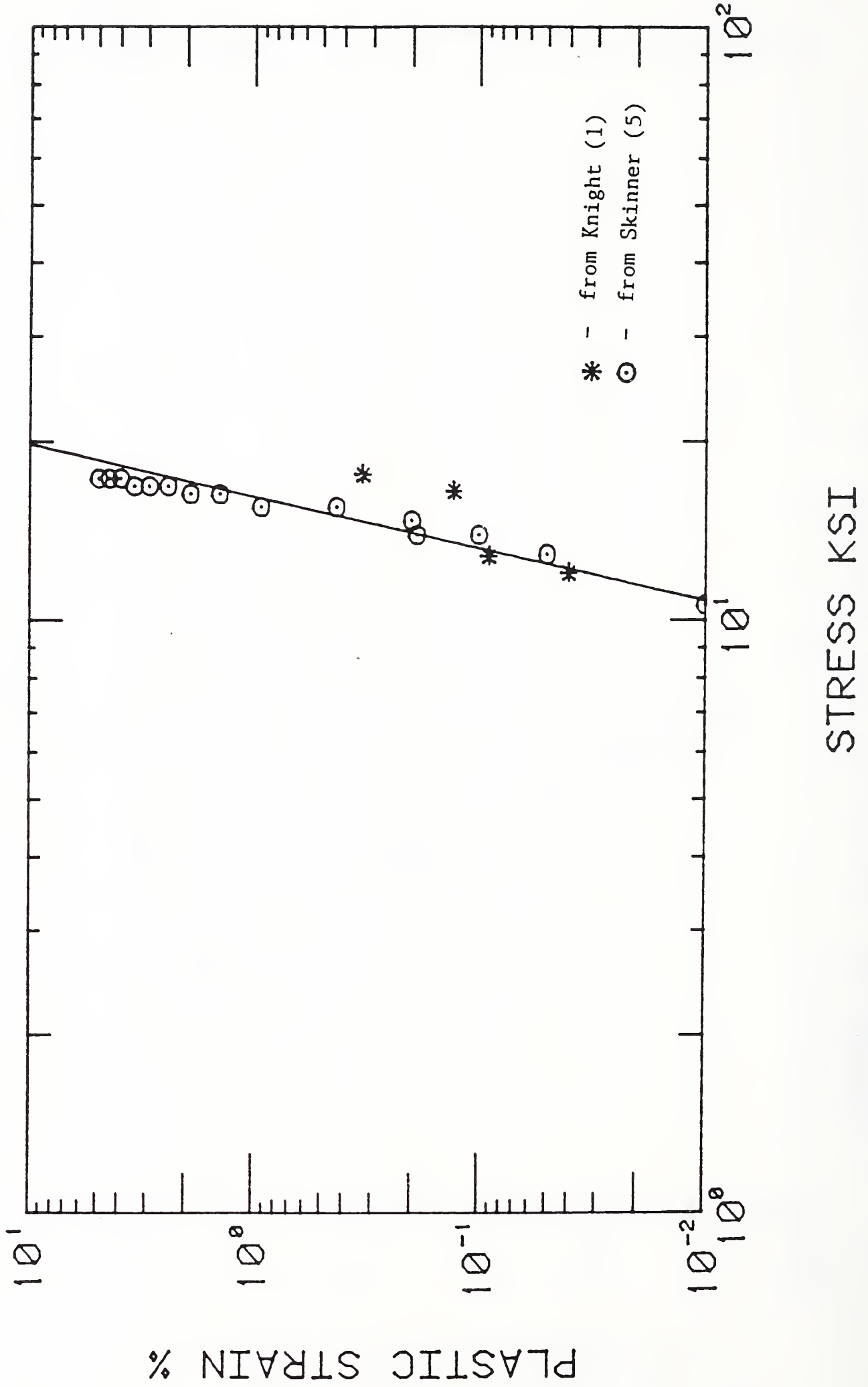


Figure 3f. Plastic strain versus stress at 600°C.

PLASTIC STRAIN VS STRESS AT 650 DEG C

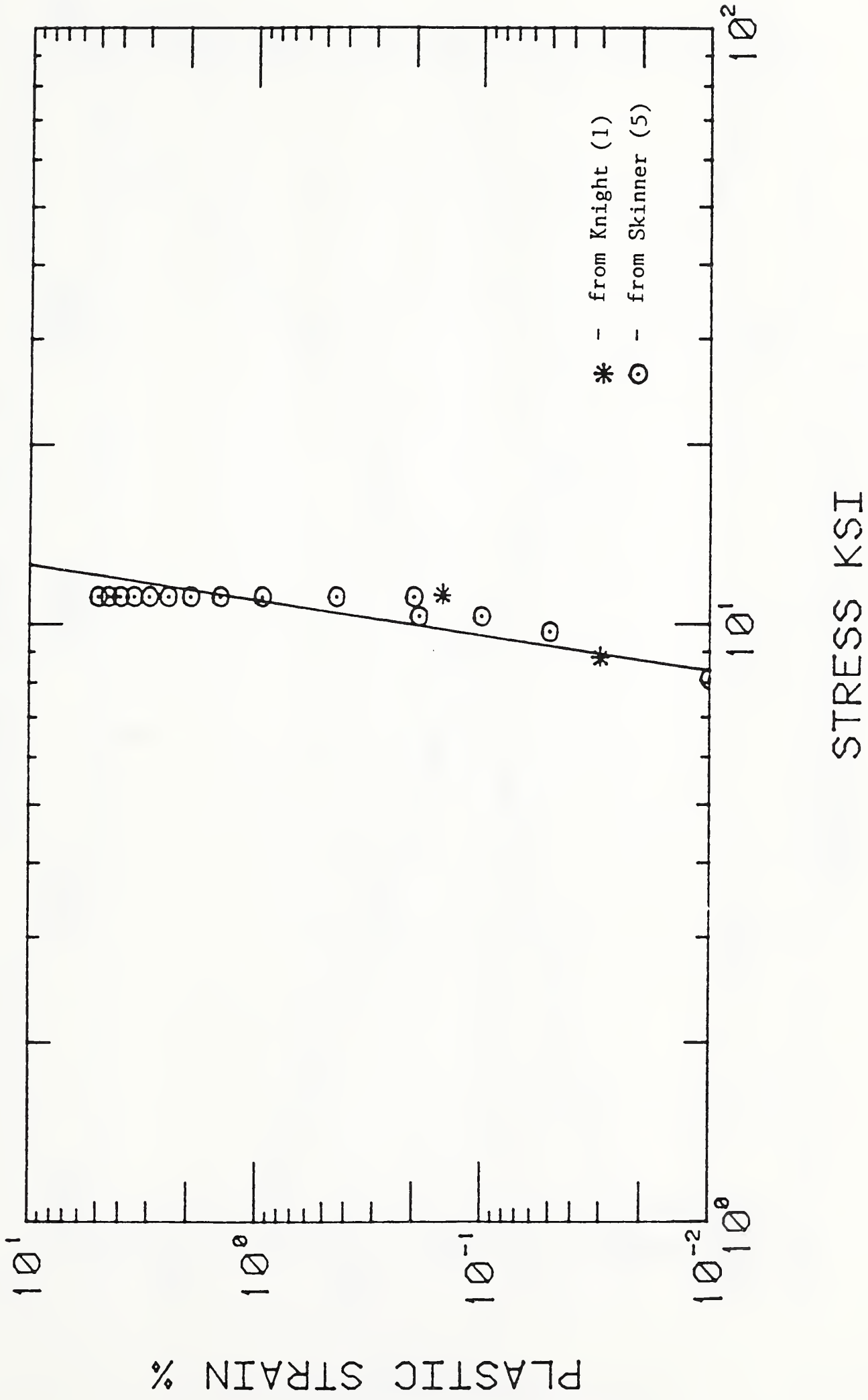
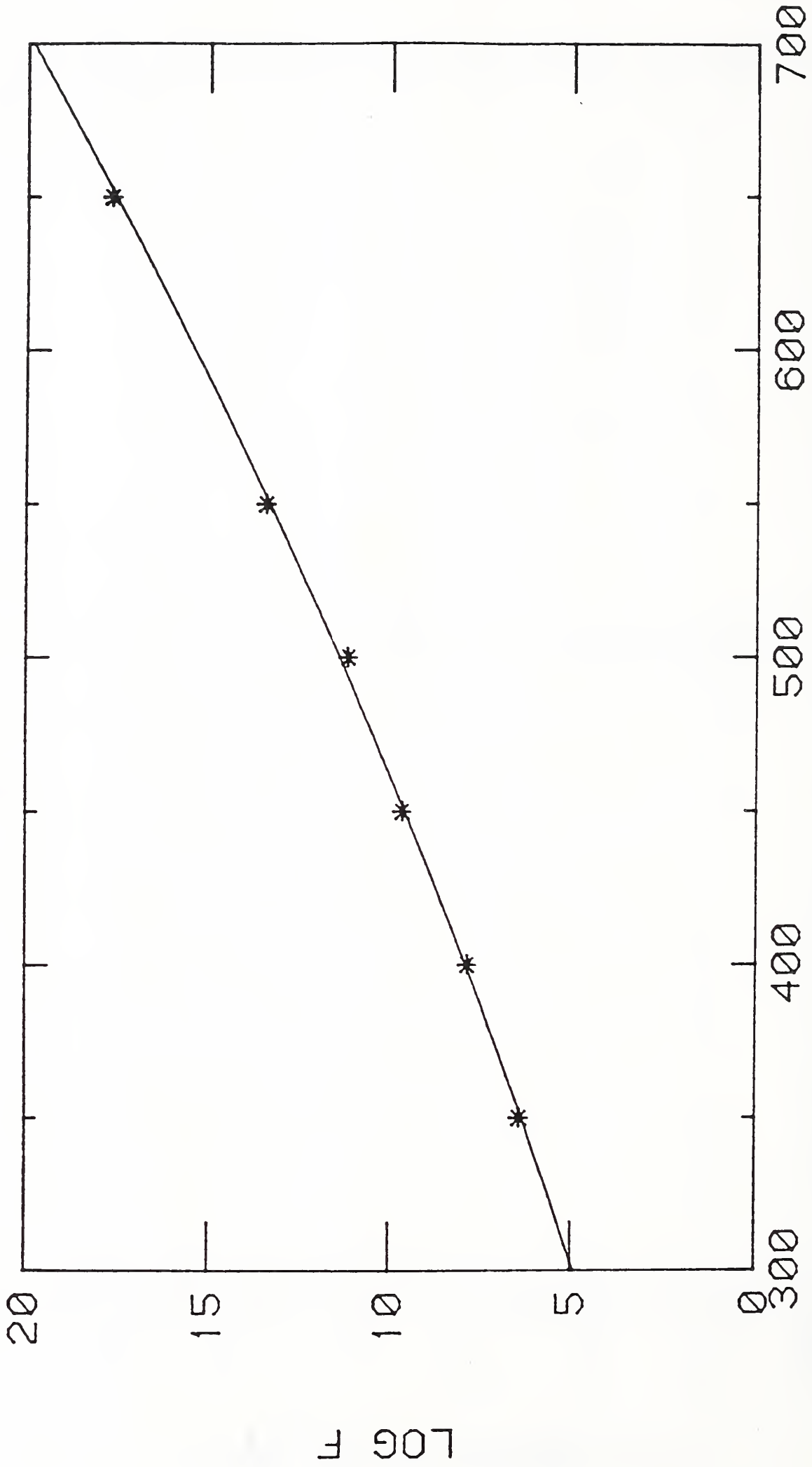


Figure 3g. Plastic strain versus stress at 650°C.

LOG F VS TEMPERATURE



TEMPERATURE DEG C

Figure 4. Log F versus temperature.

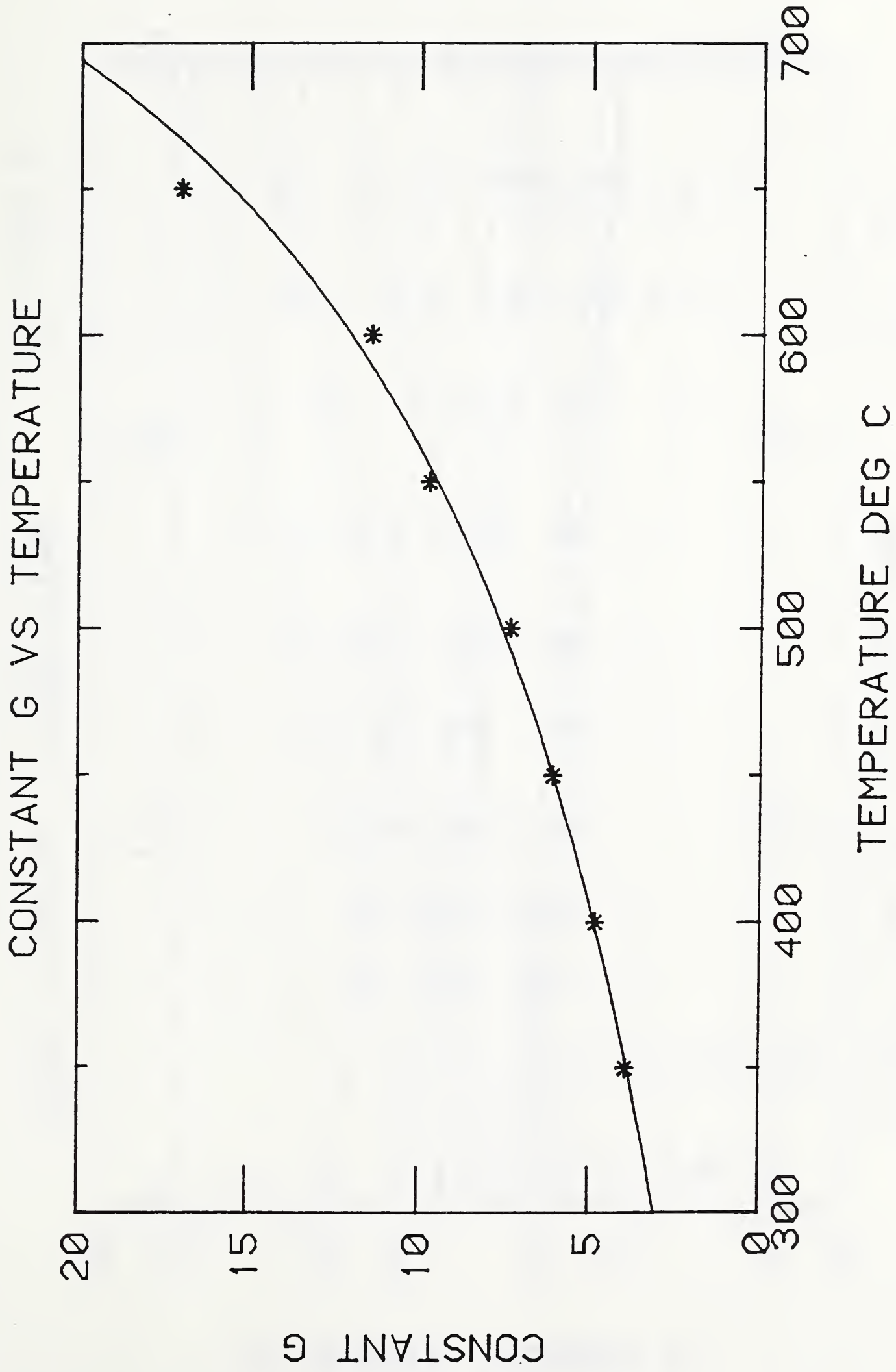
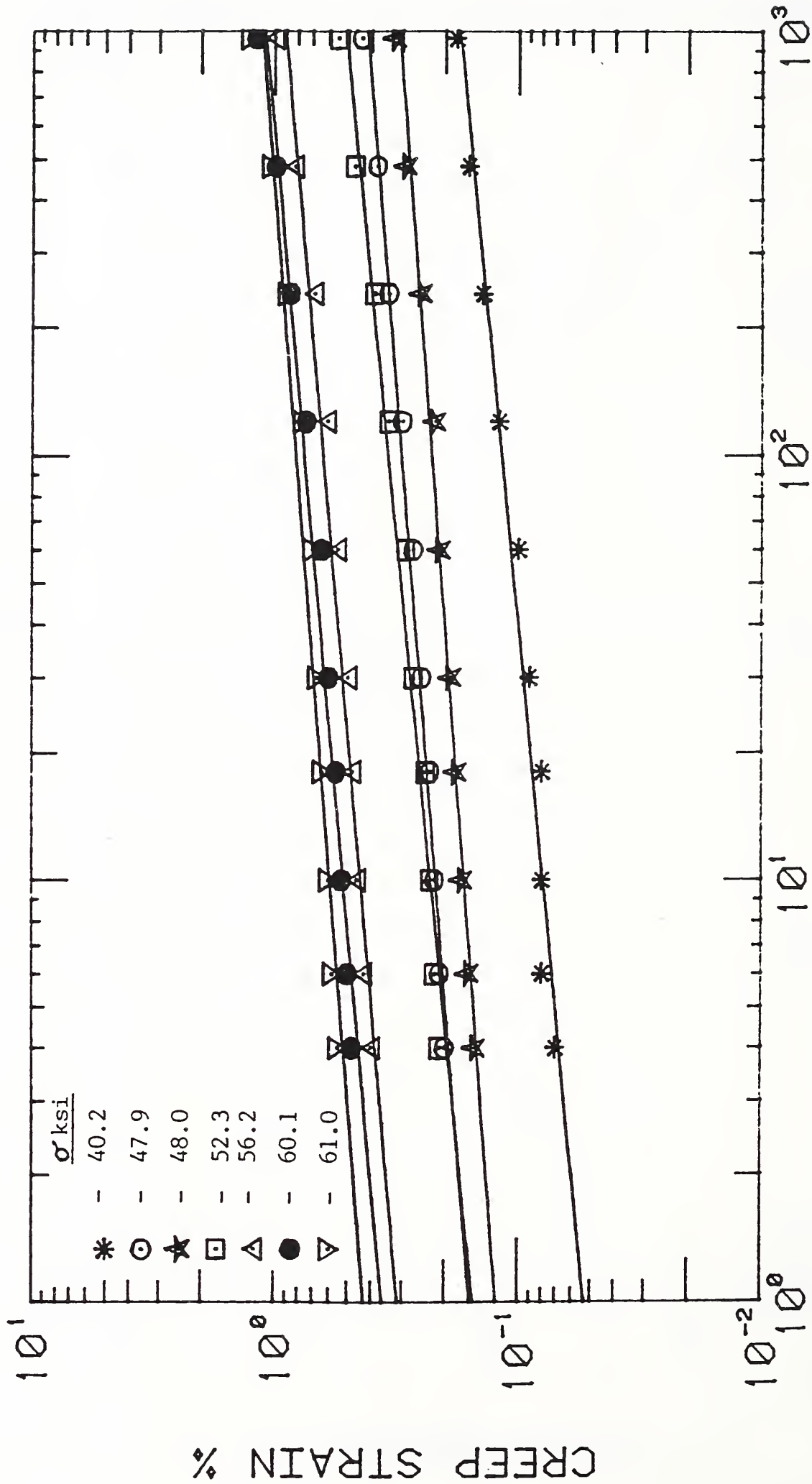


Figure 5. Constant G versus temperature.

CREEP STRAIN VS TIME FOR T = 350 DEG C



TIME MINS

Figure 6a. Creep strain versus time at 350°C.

CREEP STRAIN VS TIME FOR T = 400 DEG C

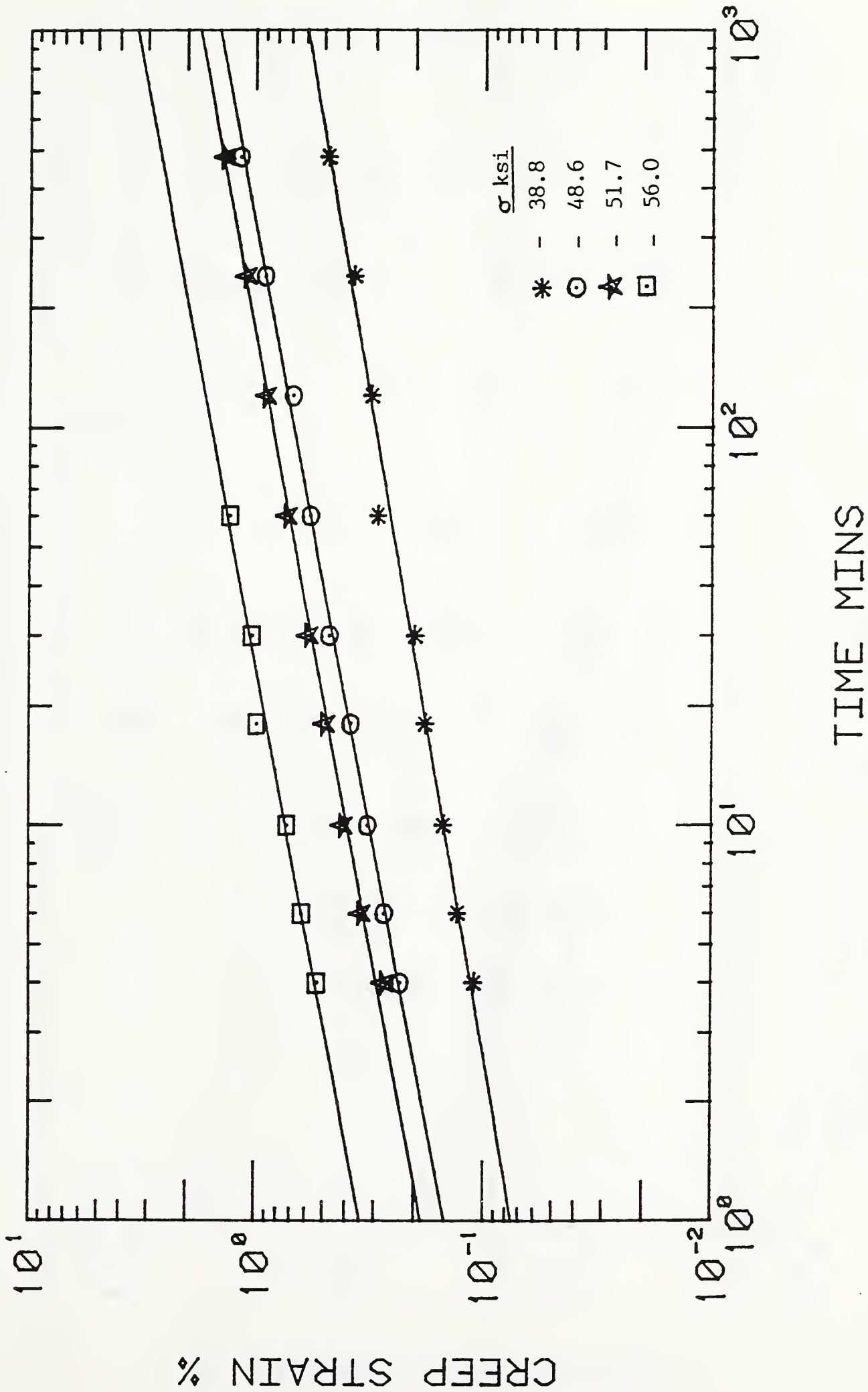
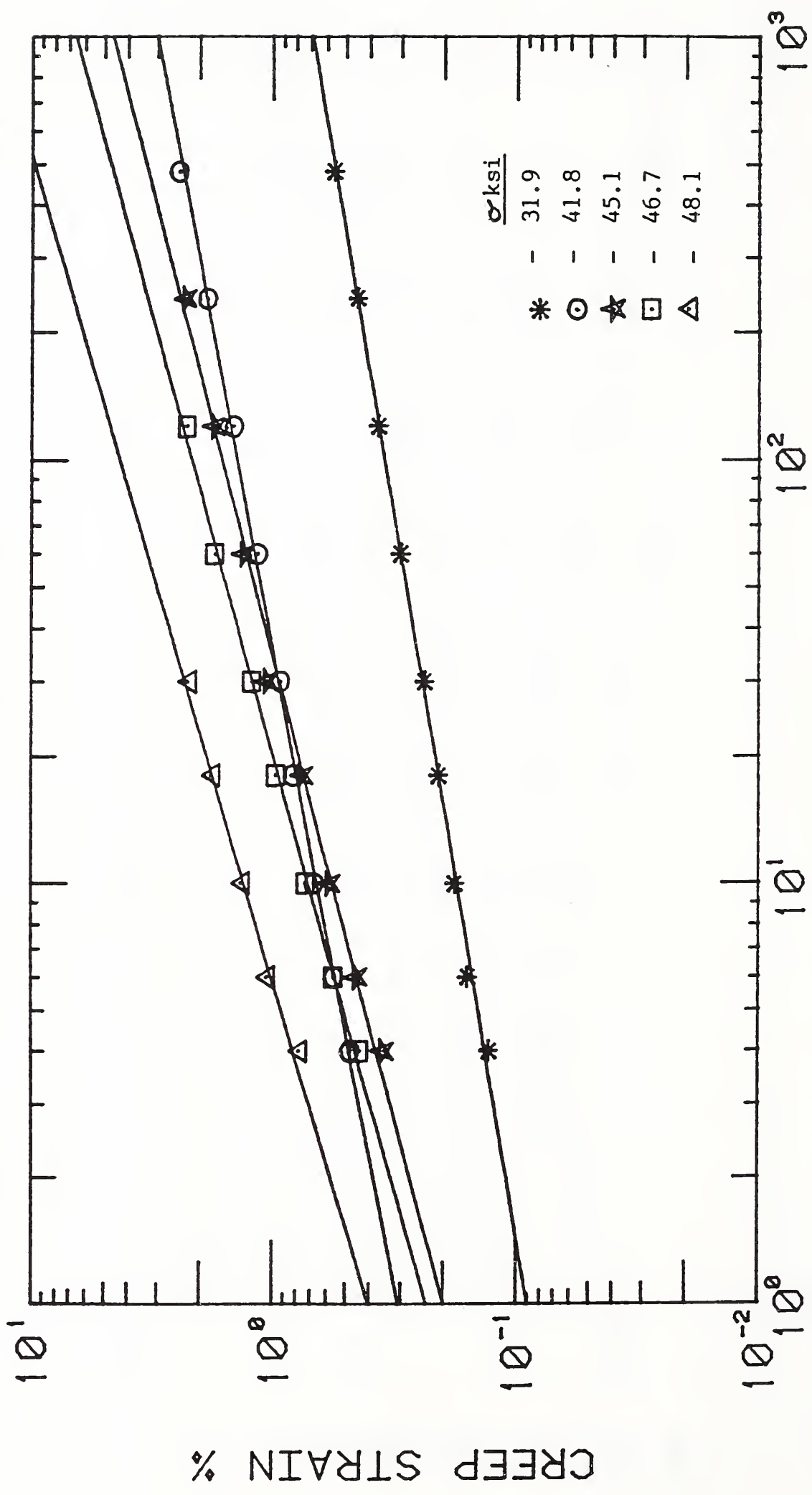


Figure 6b. Creep strain versus time at 400°C.

CREEP STRAIN VS TIME FOR T = 450 DEG C



TIME MINS

Figure 6c. Creep strain versus time at 450°C.

CREEP STRAIN VS TIME FOR T = 500 DEG C

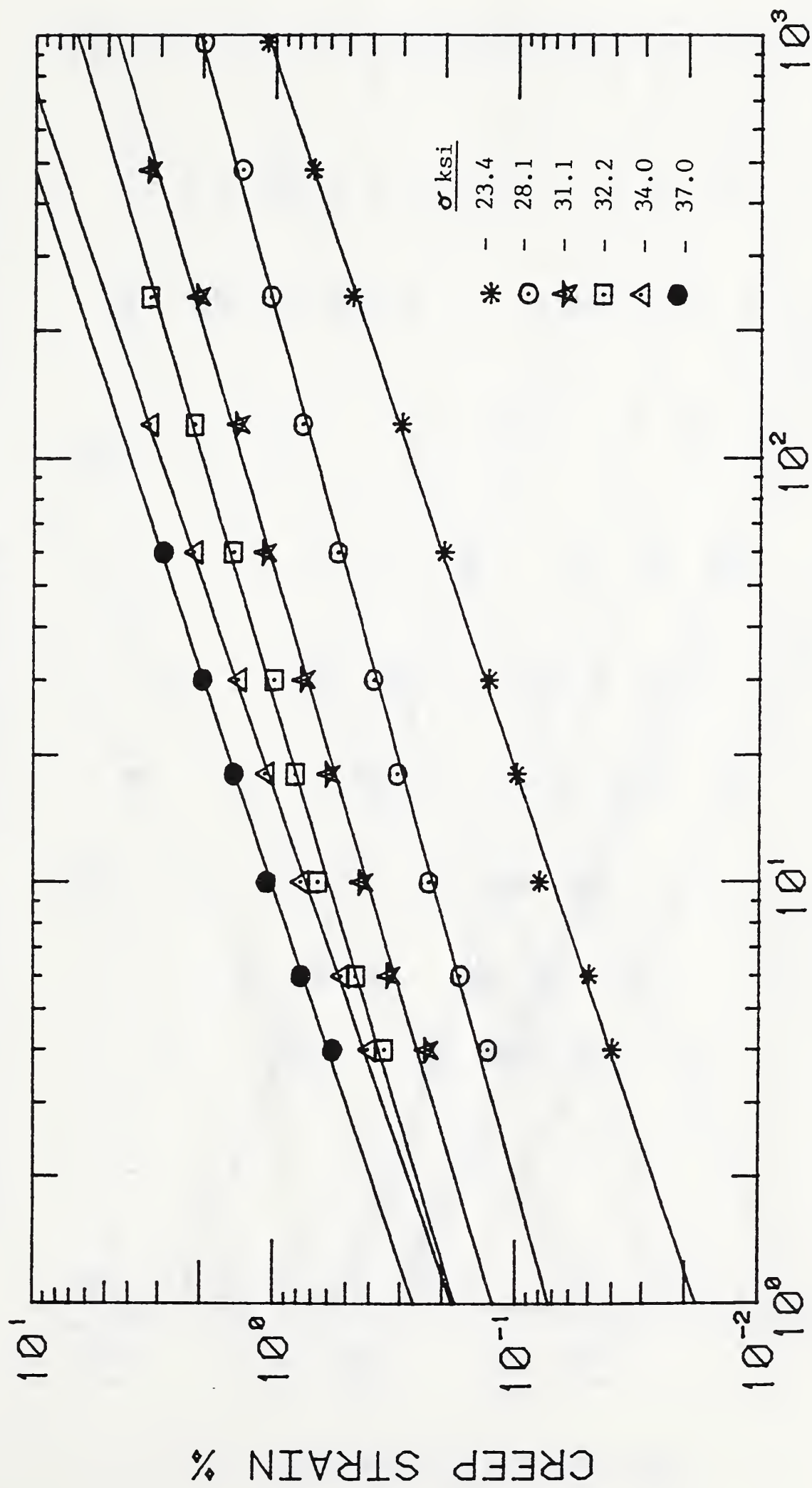
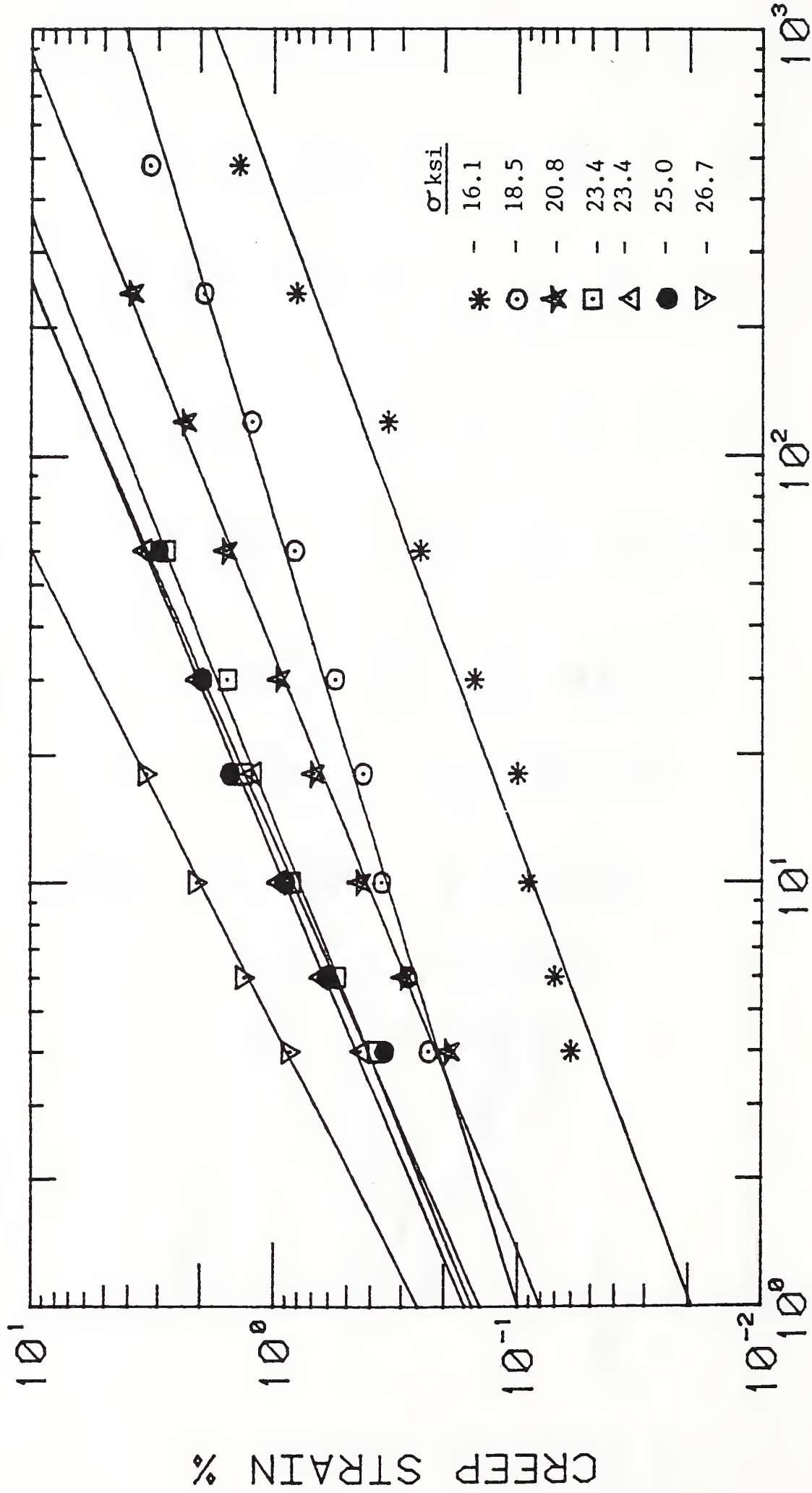


Figure 6d. Creep strain versus time at 500°C.

CREEP STRAIN VS TIME FOR T = 550 DEG C



TIME MINS

Figure 6e. Creep strain versus time at 550°C.

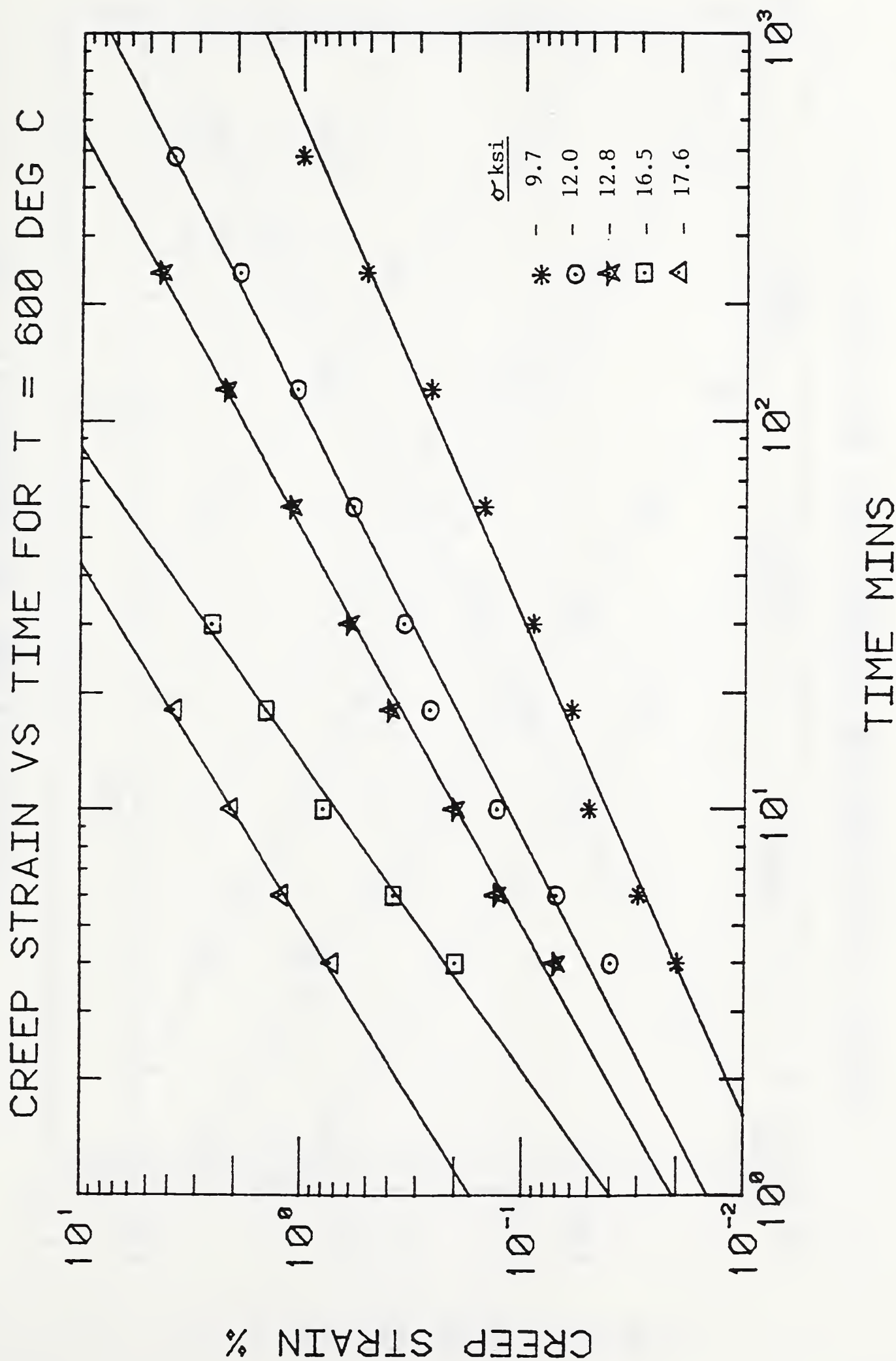


Figure 6f. Creep strain versus time at 600°C.

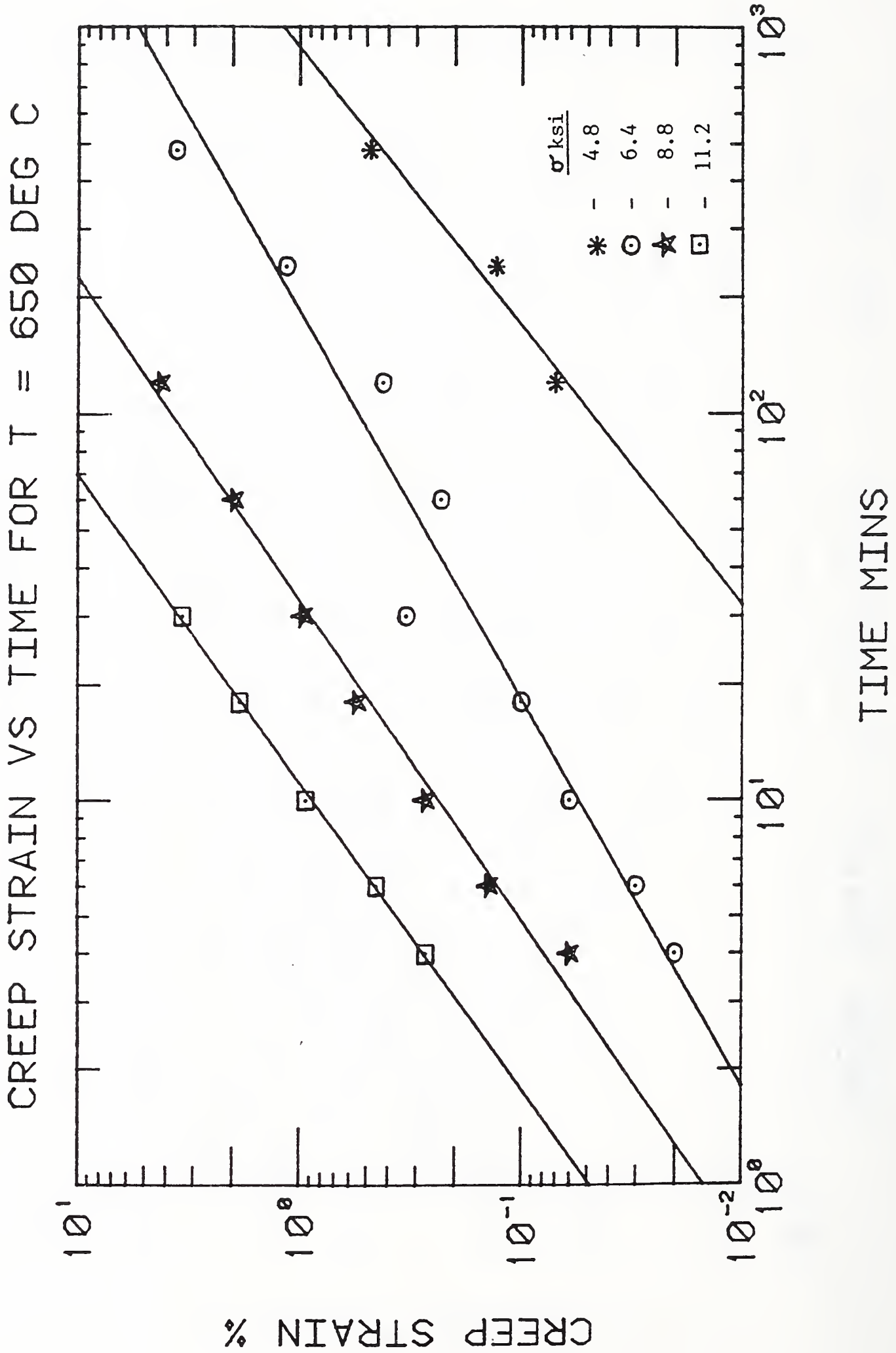
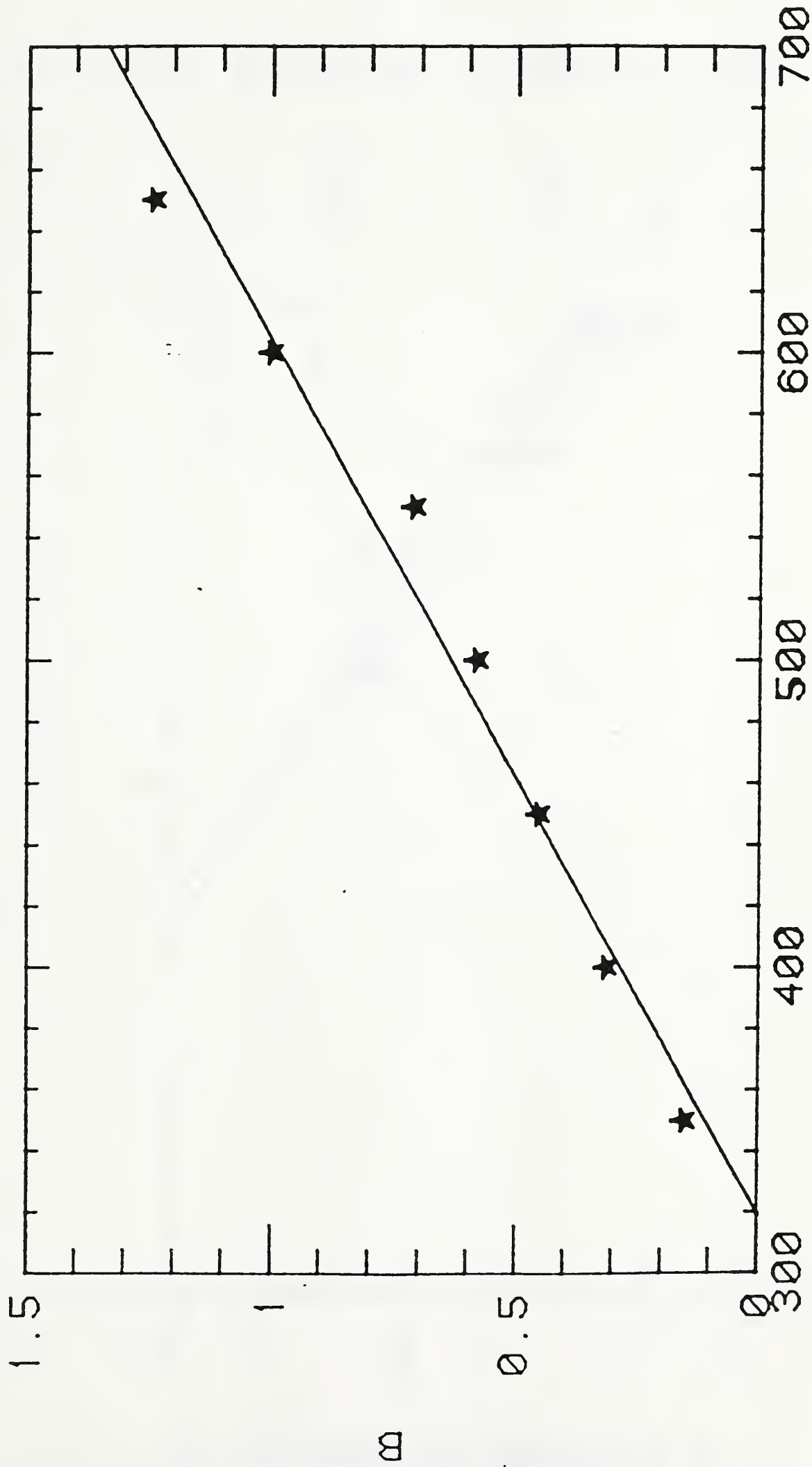


Figure 6g. Creep strain versus time at 650°C.

PARAMETER B VS TEMPERATURE



TEMPERATURE IN DEG C

Figure 7. Parameter B versus temperature.

CREEP STRAIN VS STRESS FOR T = 350 DEG C

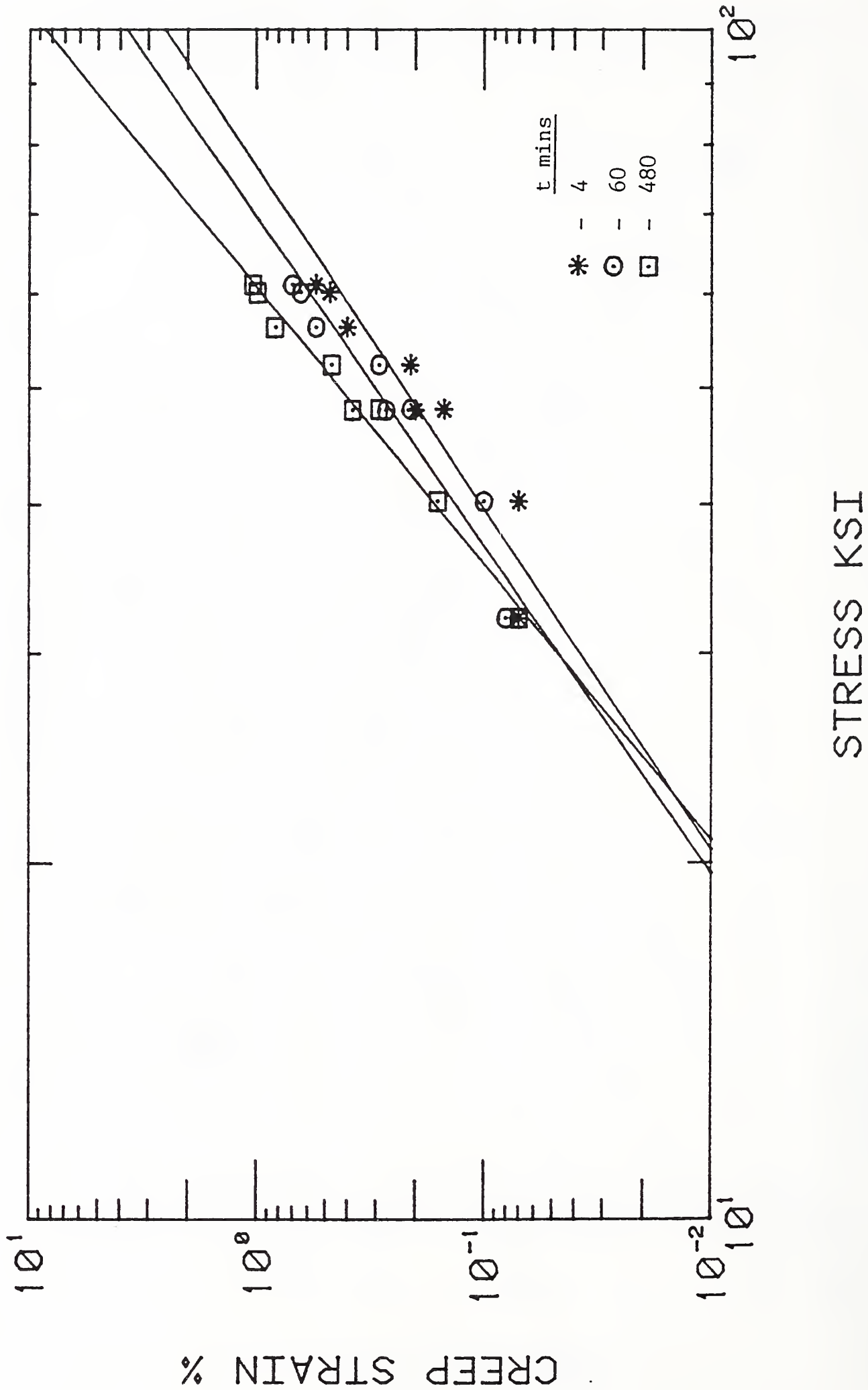


Figure 8a. Creep strain versus stress at 350°C.

CREEP STRAIN VS STRESS FOR T = 400 DEG C

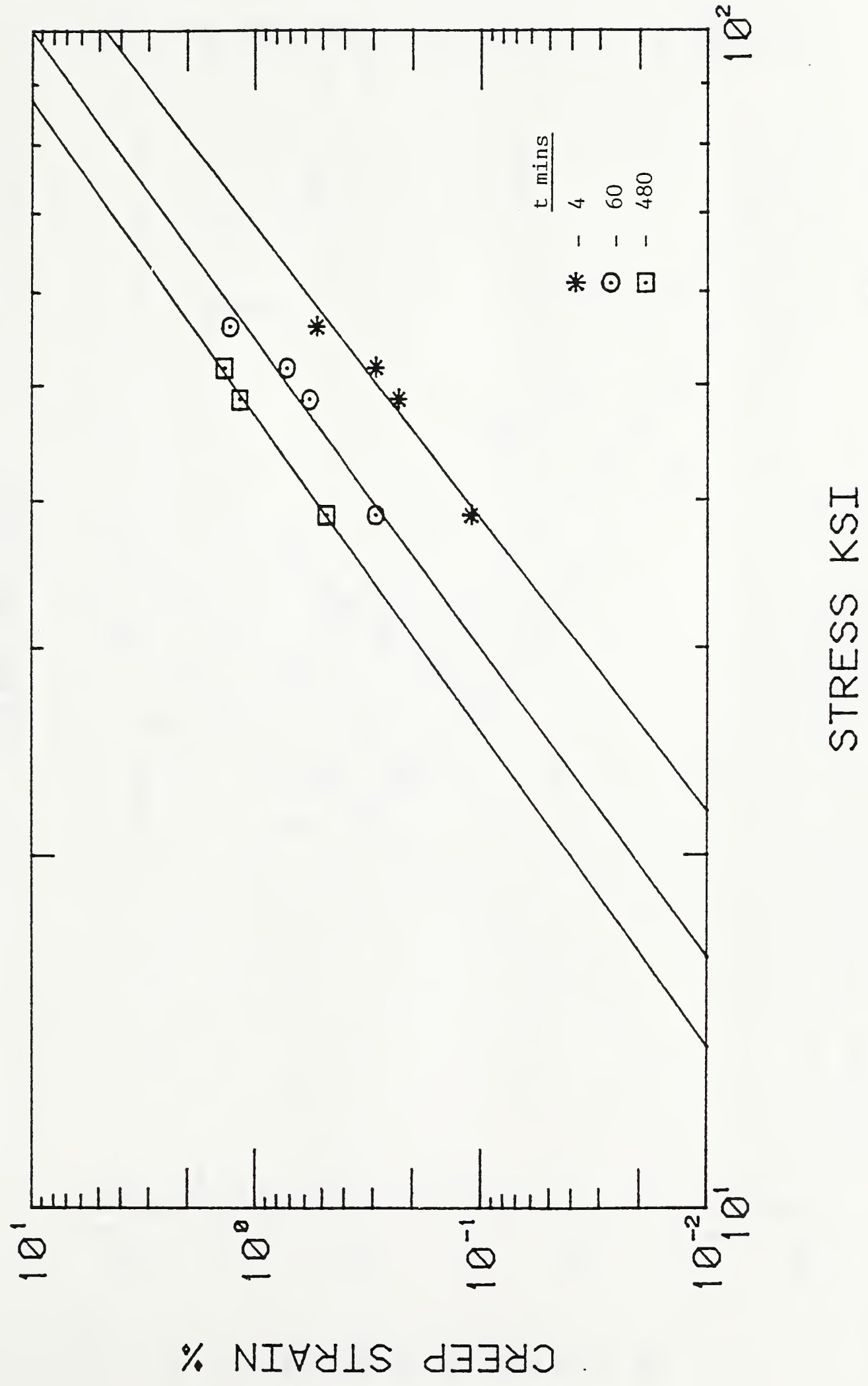


Figure 8b. Creep strain versus stress at 400°C.

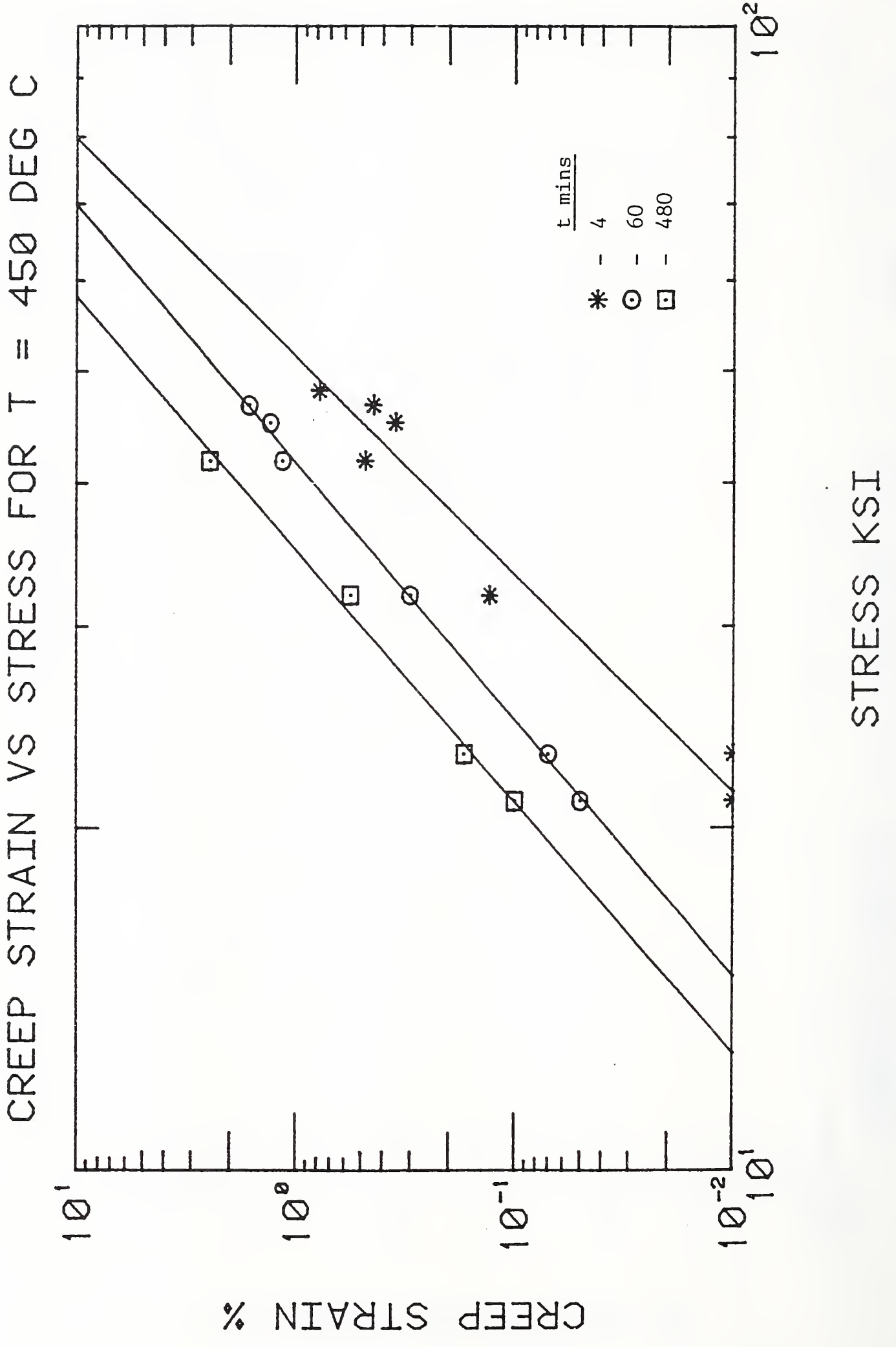


Figure 8c. Creep strain versus stress at 450°C.

CREEP STRAIN VS STRESS FOR T = 500 DEG C

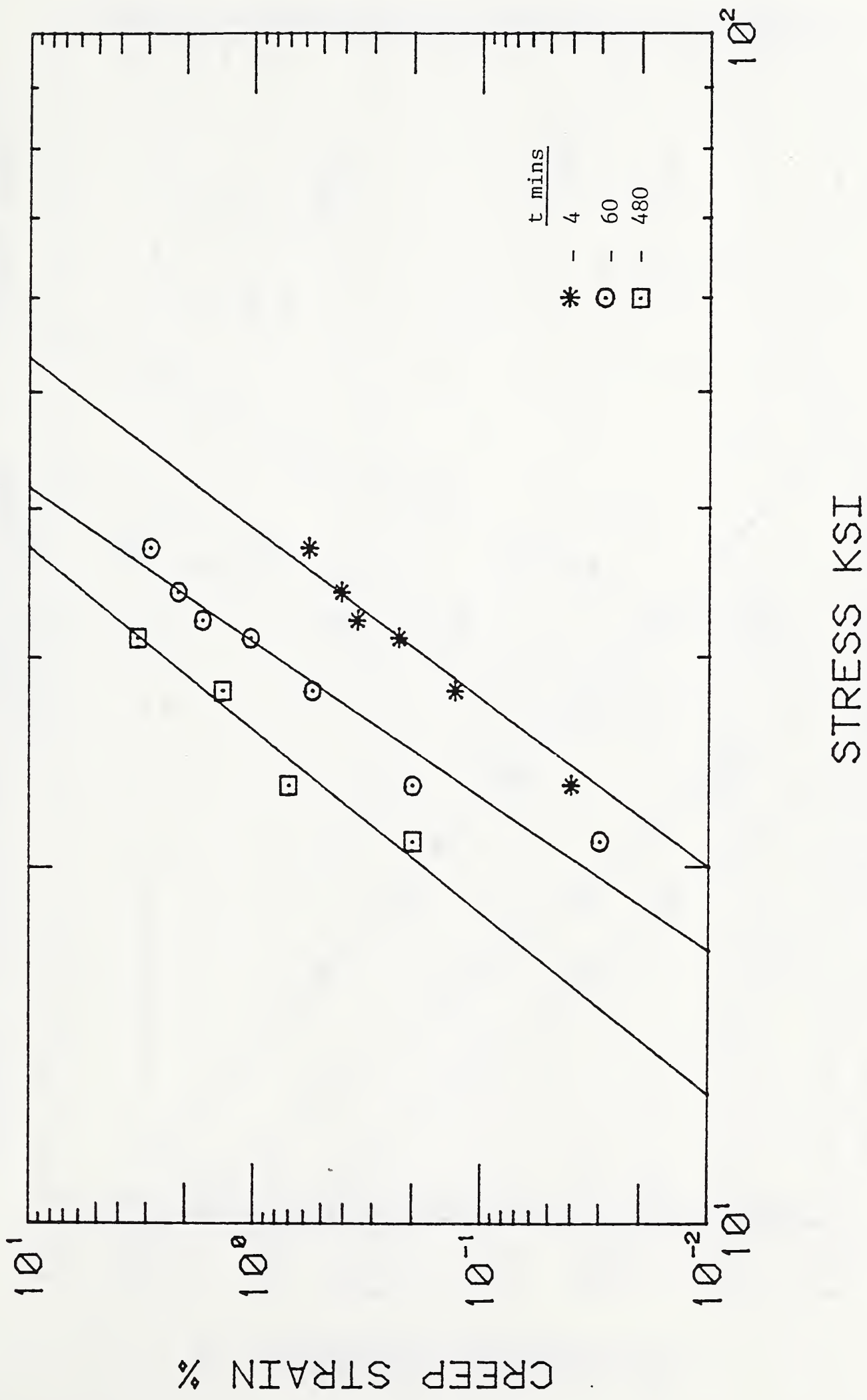
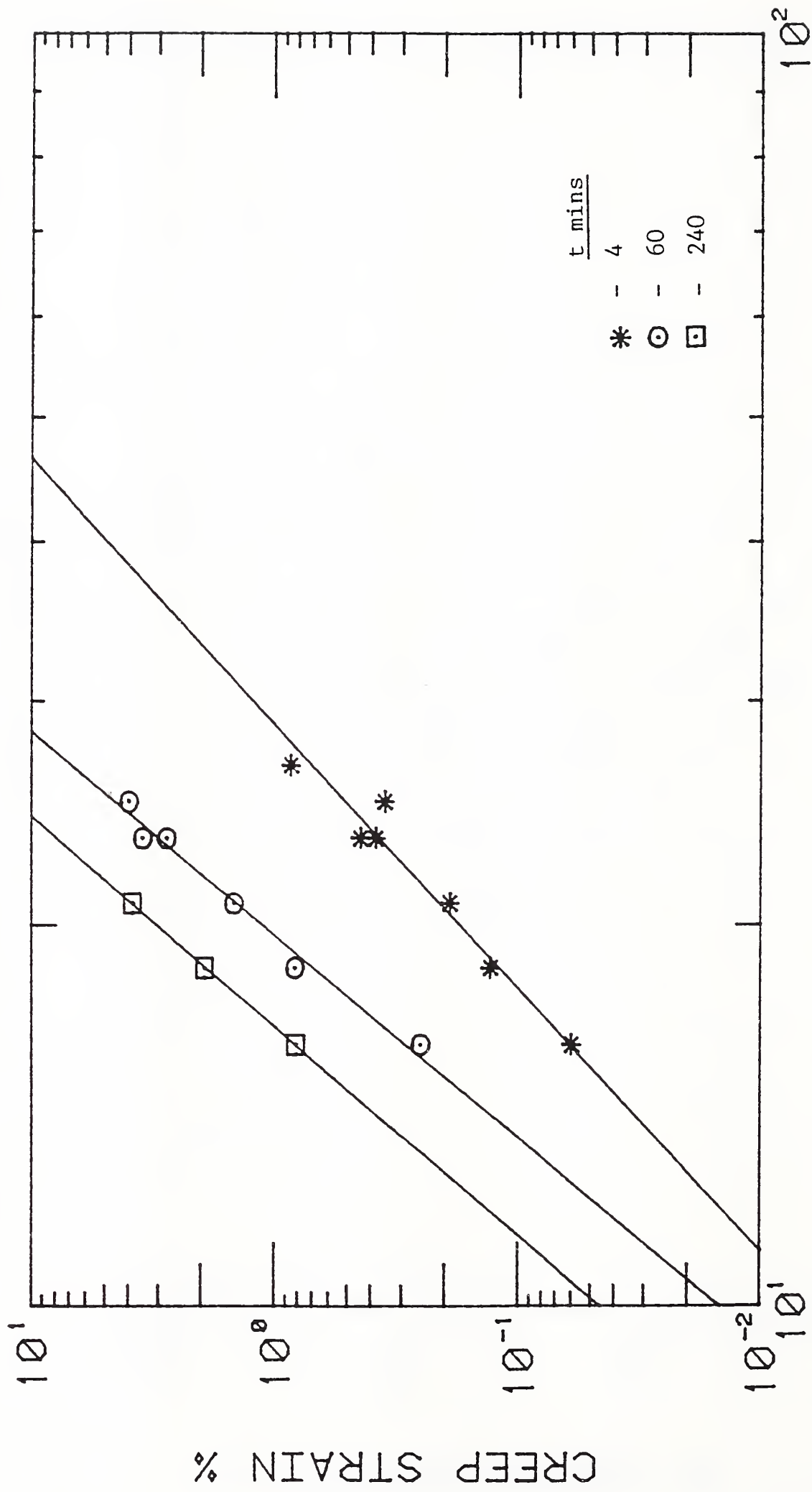


Figure 8d. Creep strain versus stress at 500°C.

CREEP STRAIN VS STRESS FOR T = 550 DEG C



STRESS KSI

Figure 8e. Creep strain versus stress at 550°C.

CREEP STRAIN VS STRESS FOR T = 600 DEG C

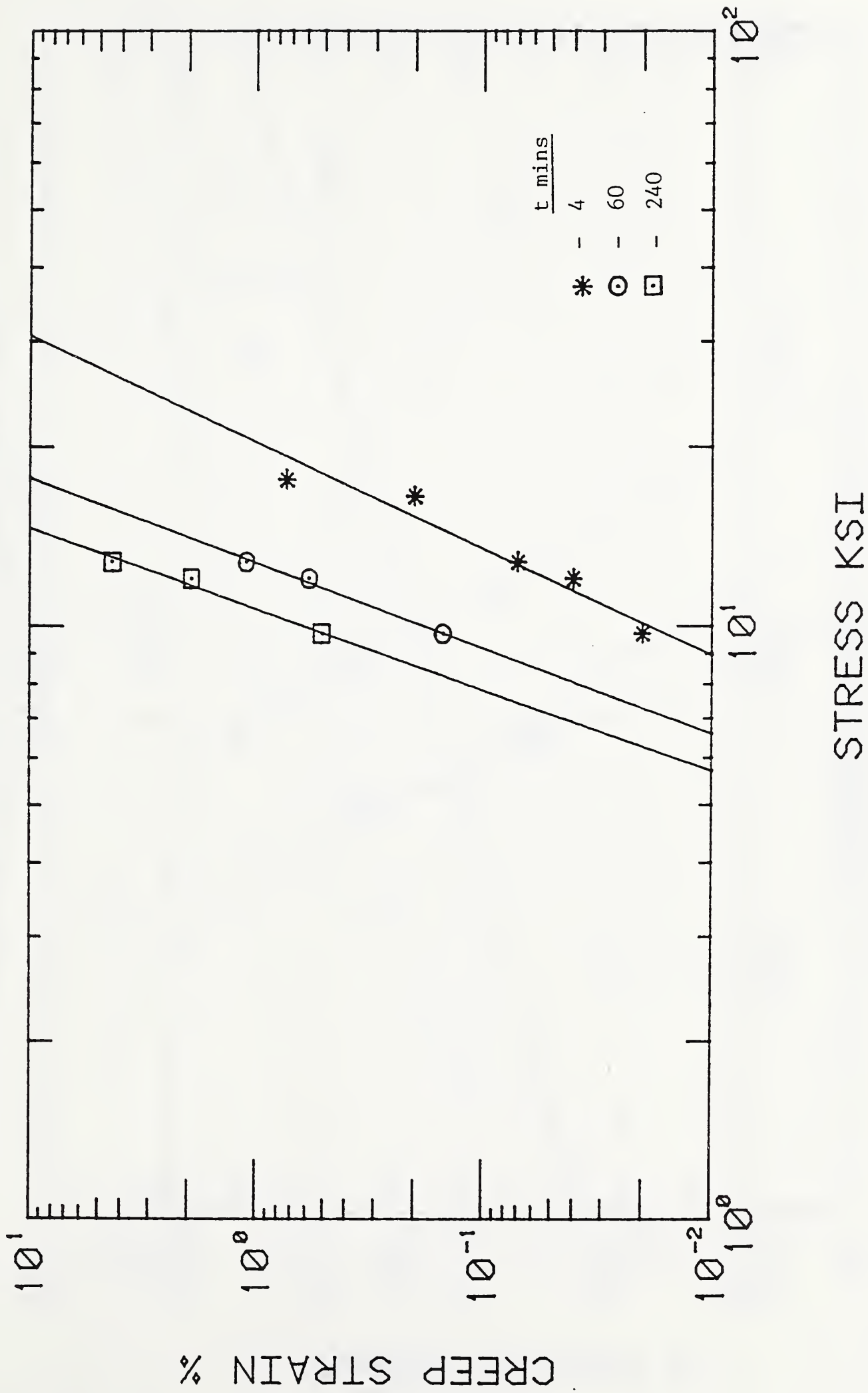


Figure 8f. Creep strain versus stress at 600°C.

CREEP STRAIN VS STRESS FOR T = 650 DEG C

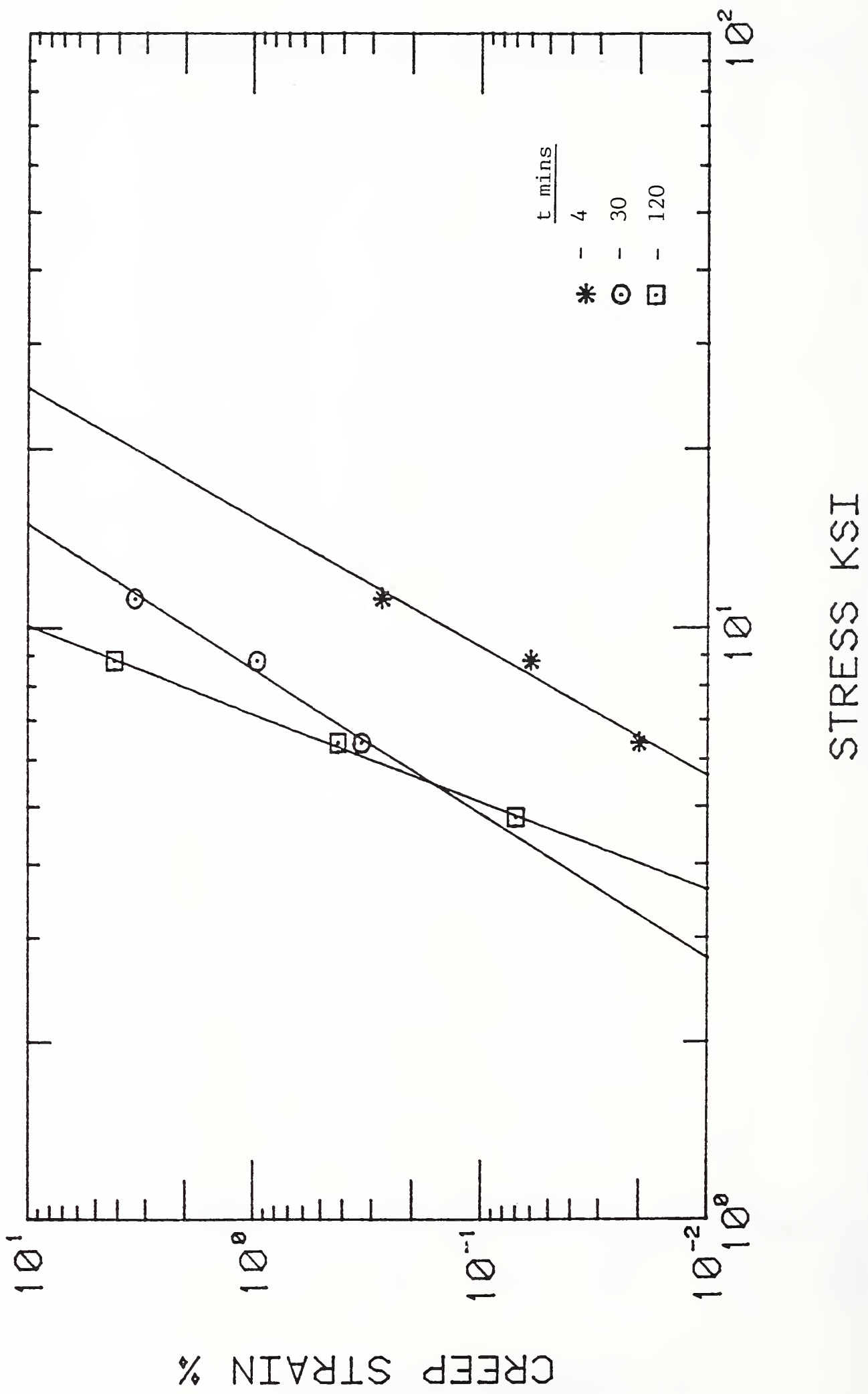


Figure 8g. Creep strain versus stress at 650°C.

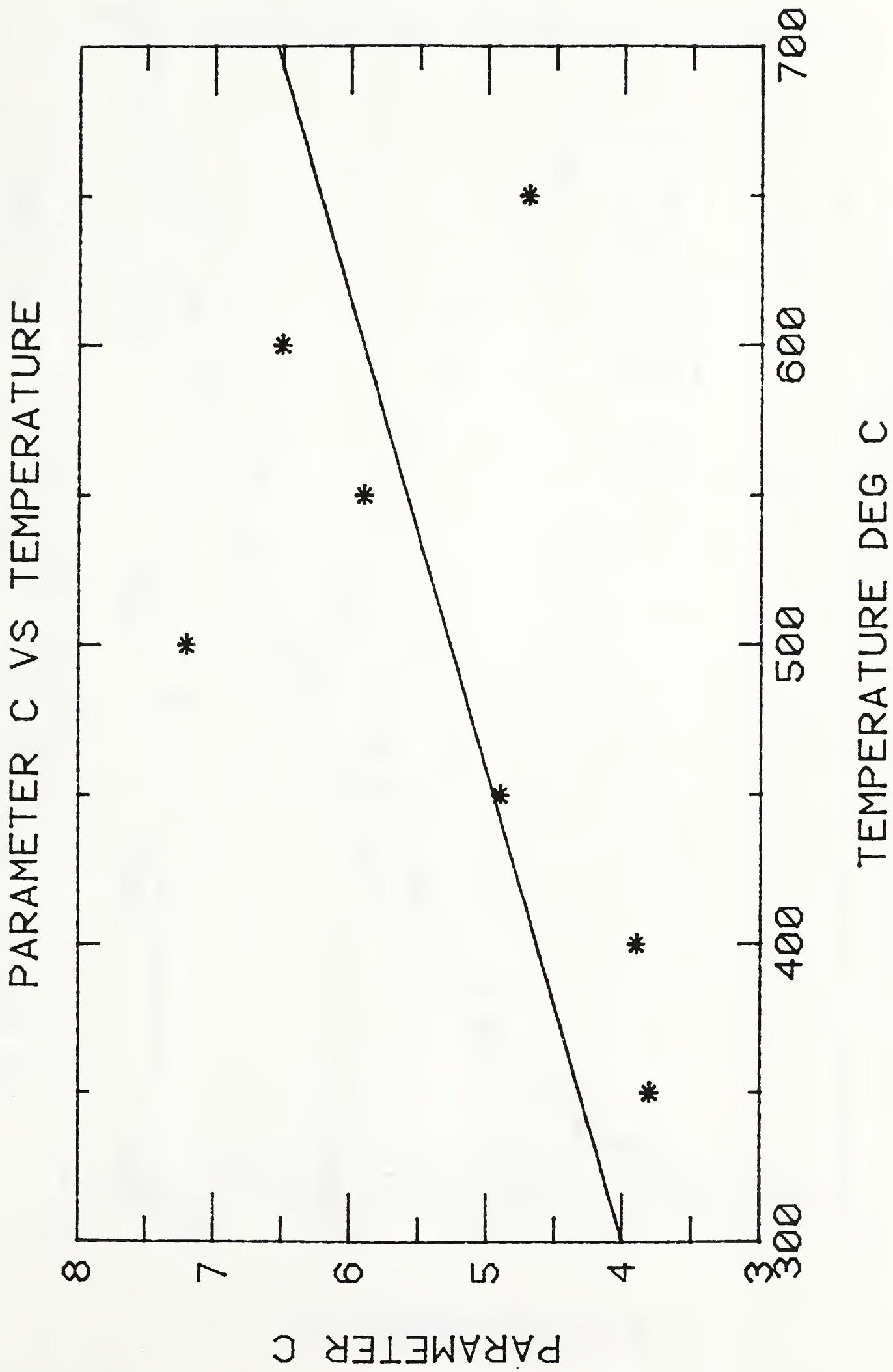
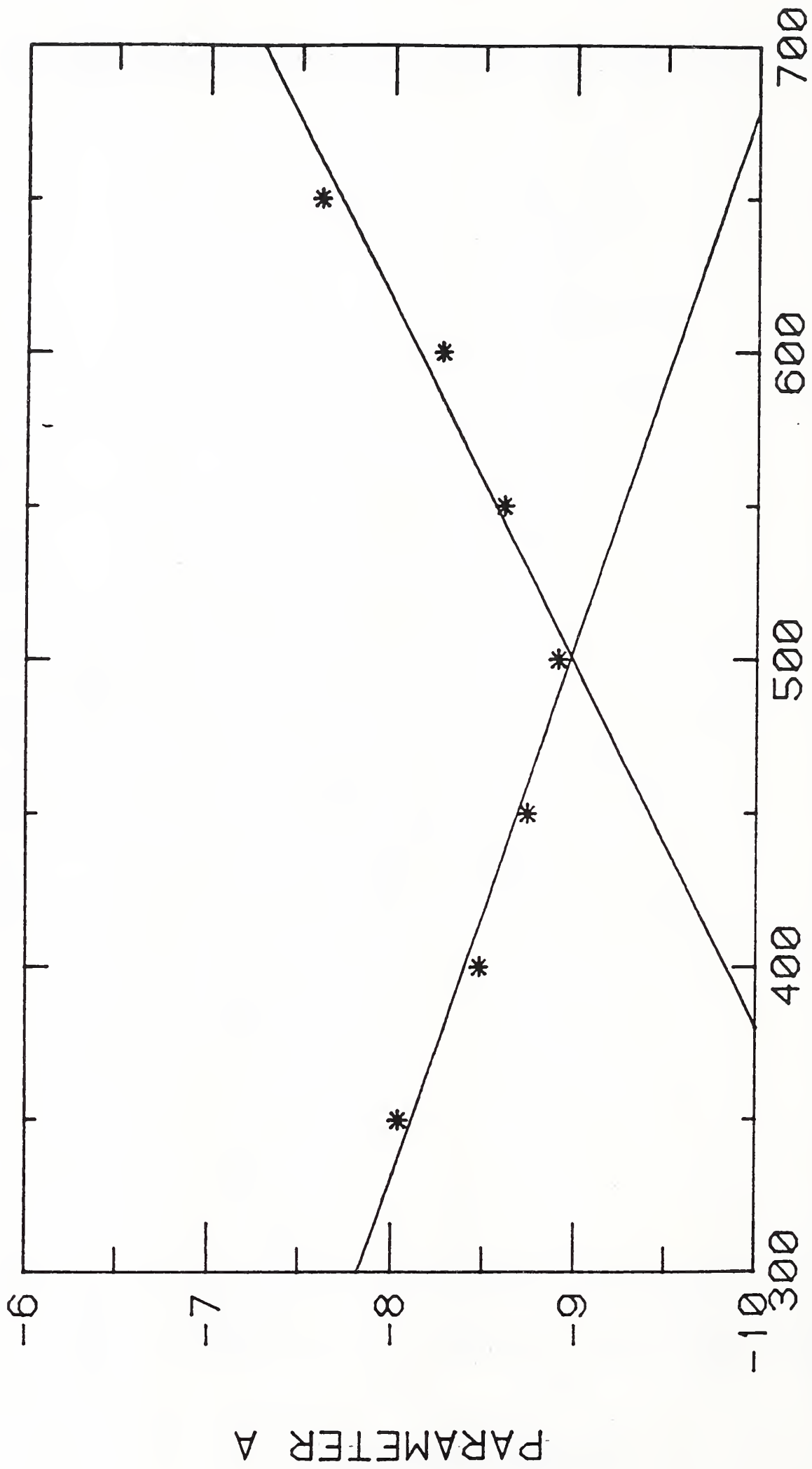


Figure 9. Parameter C versus temperature.

PARAMETER A VS TEMPERATURE



TEMPERATURE DEG C

Figure 10. Parameter A versus temperature.

PLASTIC STRAIN VS STRESS AT 350 DEG C

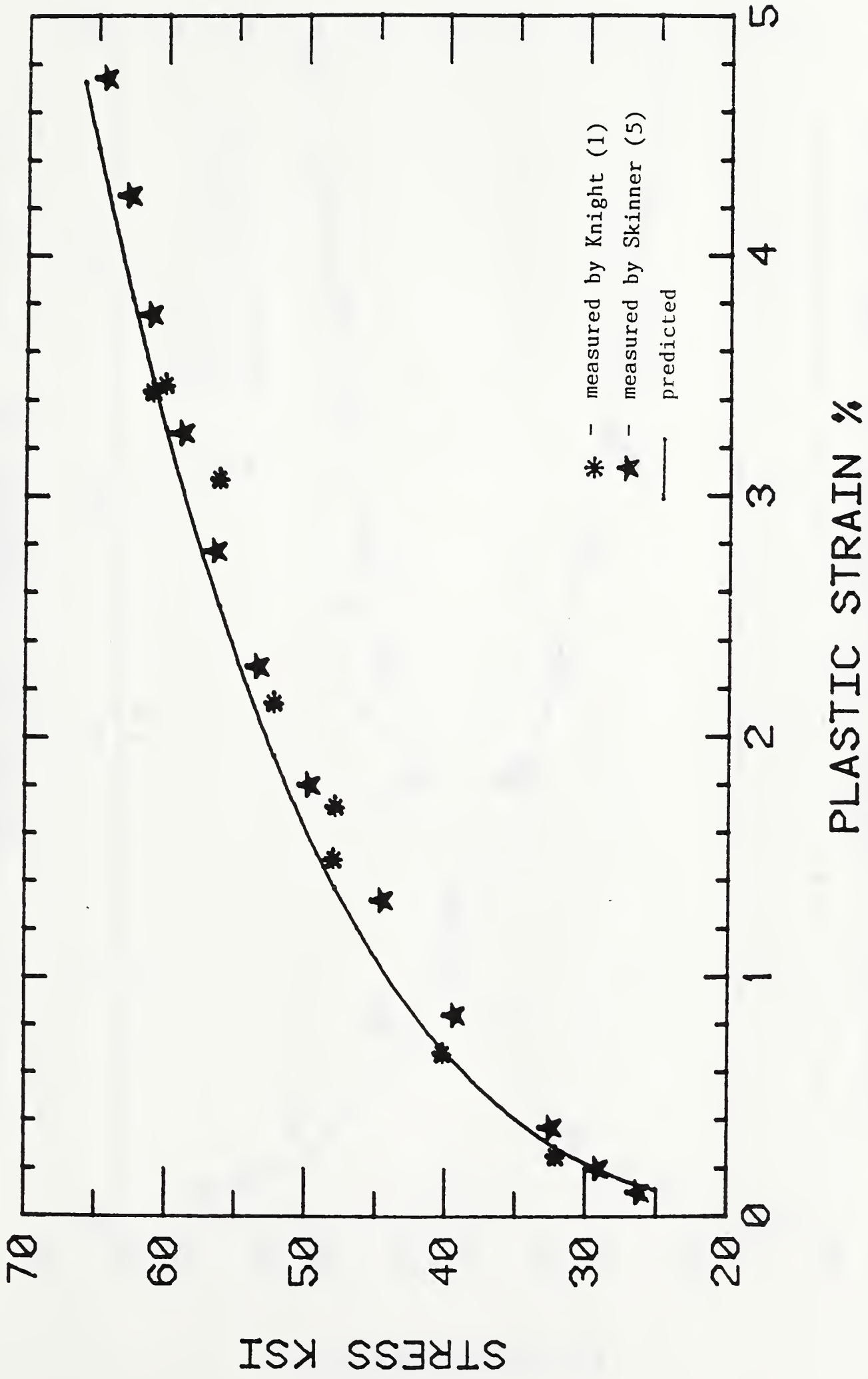
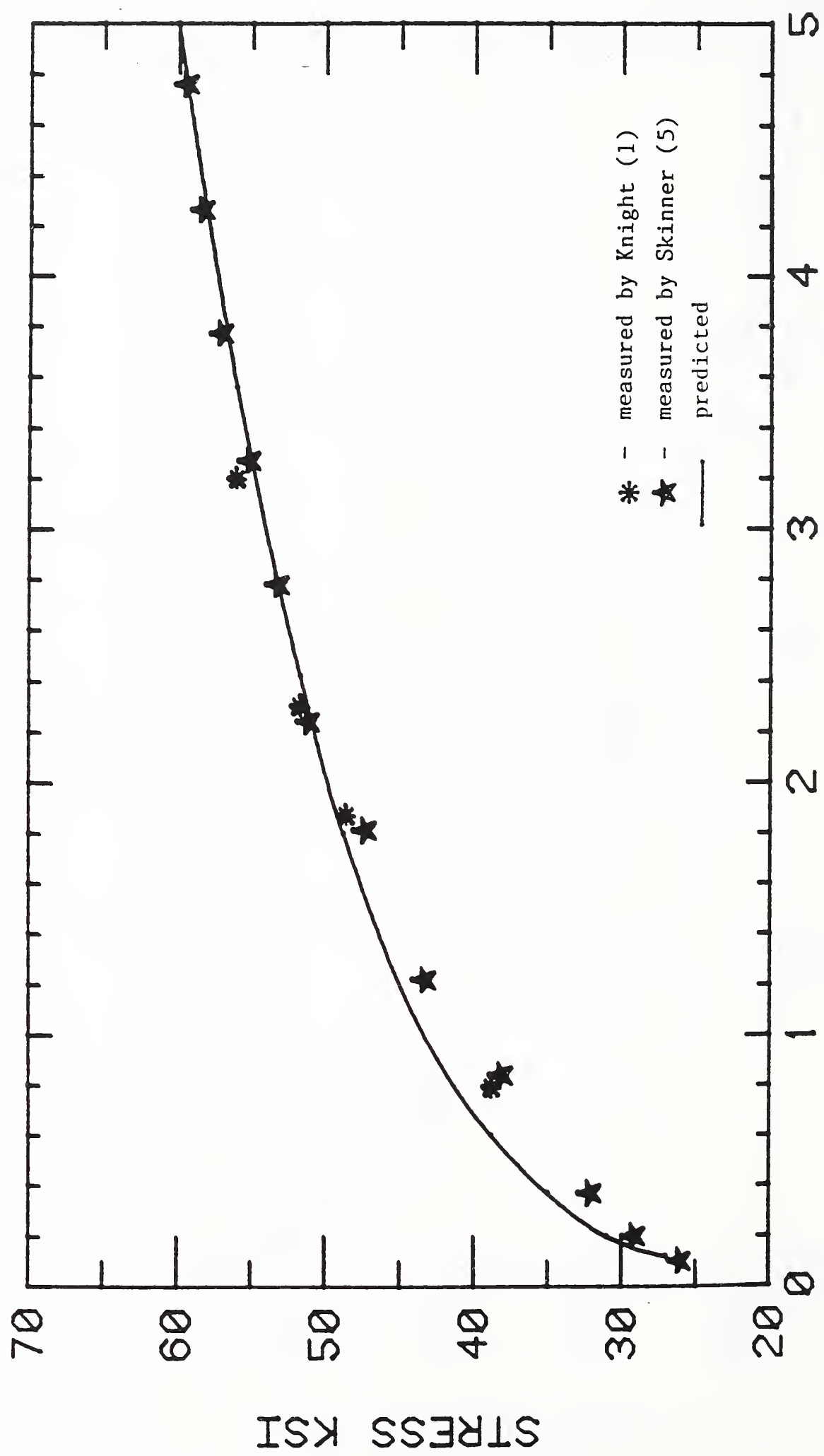


Figure 11a. Correlation of measured and calculated plastic strain at 350°C.

PLASTIC STRAIN VS STRESS AT 400 DEG C



PLASTIC STRAIN %

Figure 11b. Correlation of measured and calculated plastic strain at 400°C.

PLASTIC STRAIN VS STRESS AT 450 DEG C

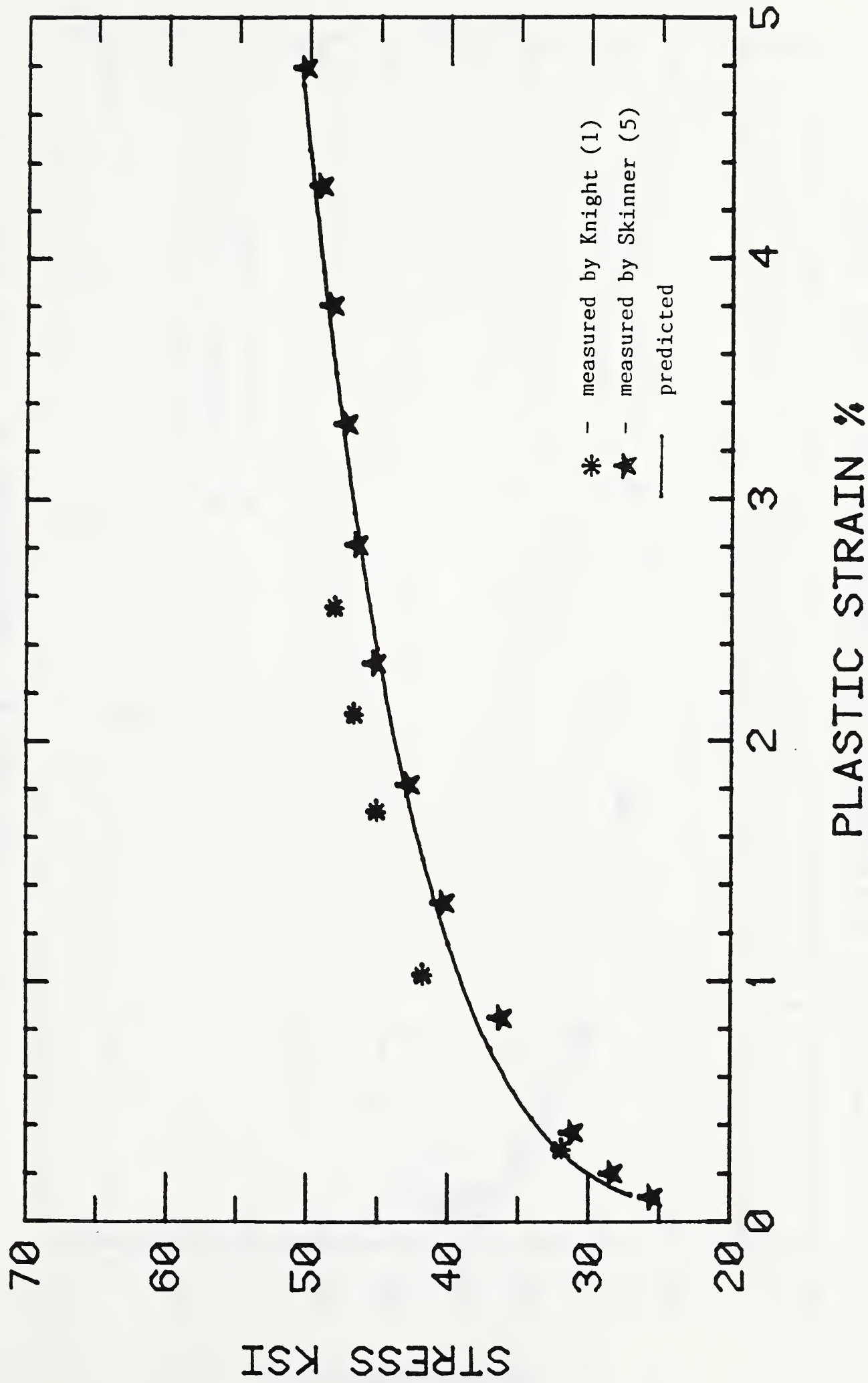
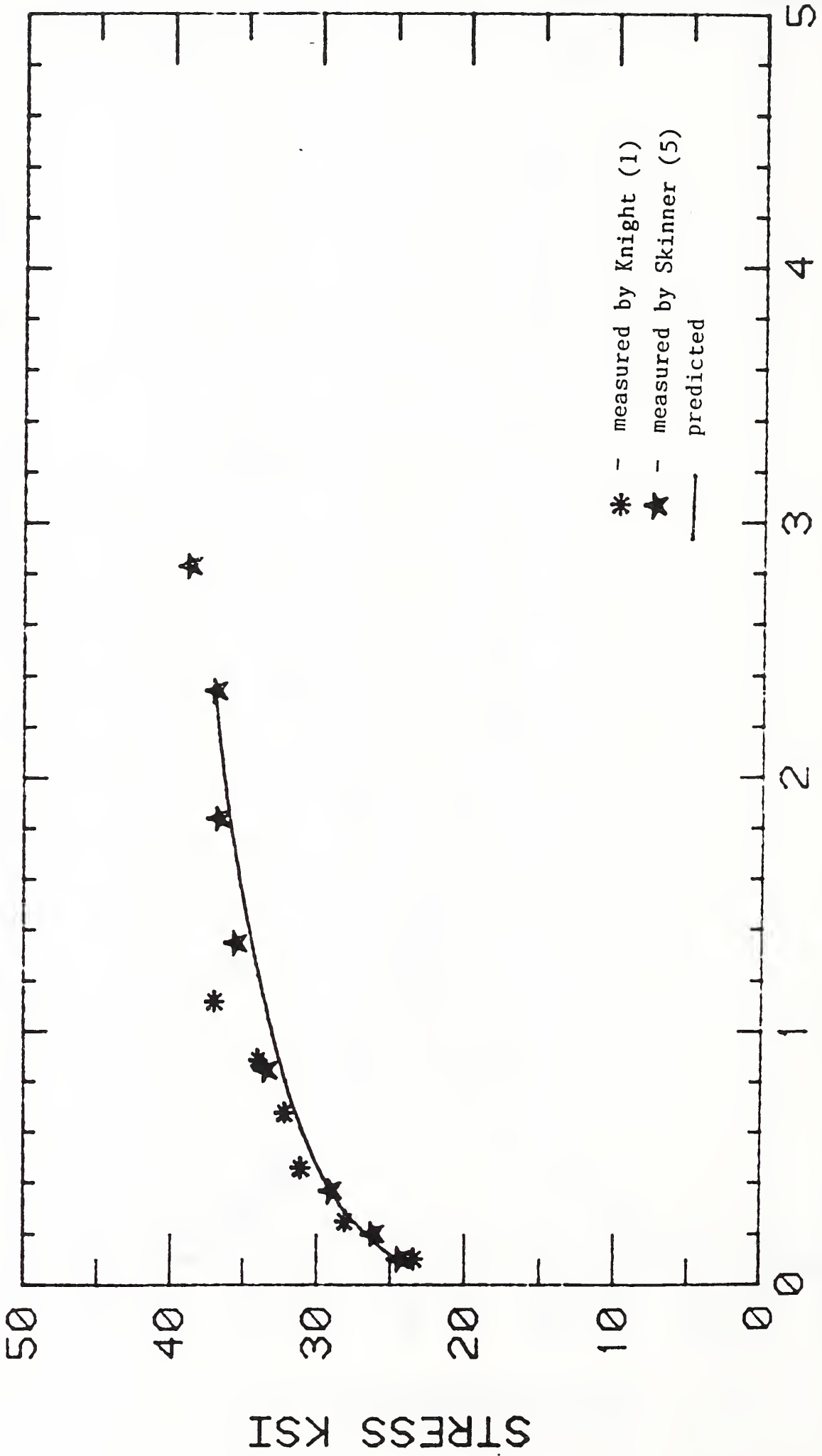


Figure 11c. Correlation of measured and calculated plastic strain at 450°C.

PLASTIC STRAIN VS STRESS AT 500 DEG C



PLASTIC STRAIN %

Figure 11d. Correlation of measured and calculated plastic strain at 500°C.

PLASTIC STRAIN VS STRESS AT 550 DEG C

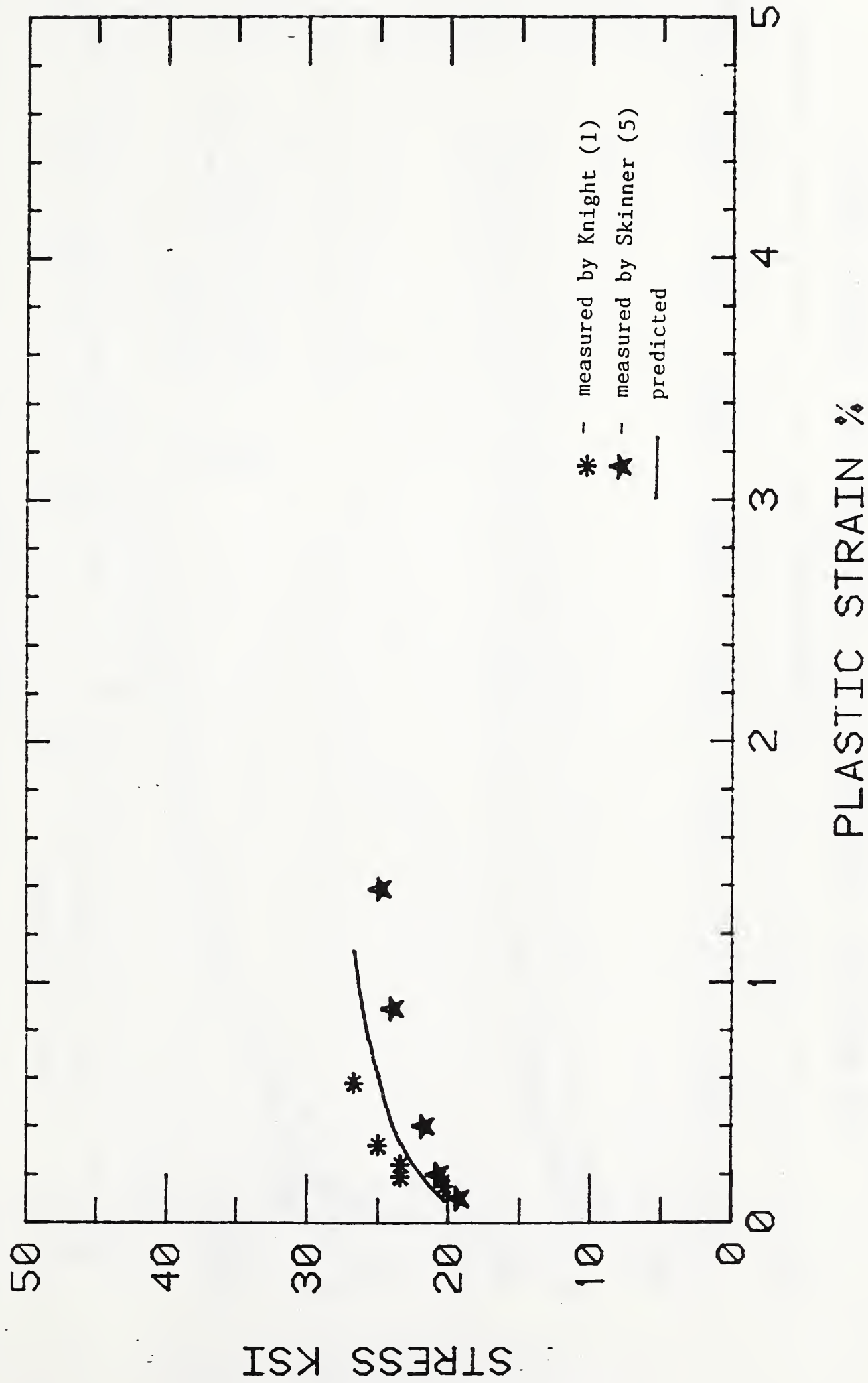


Figure 11e. Correlation of measured and calculated plastic strain at 550°C.

PLASTIC STRAIN VS STRESS AT 600 DEG C

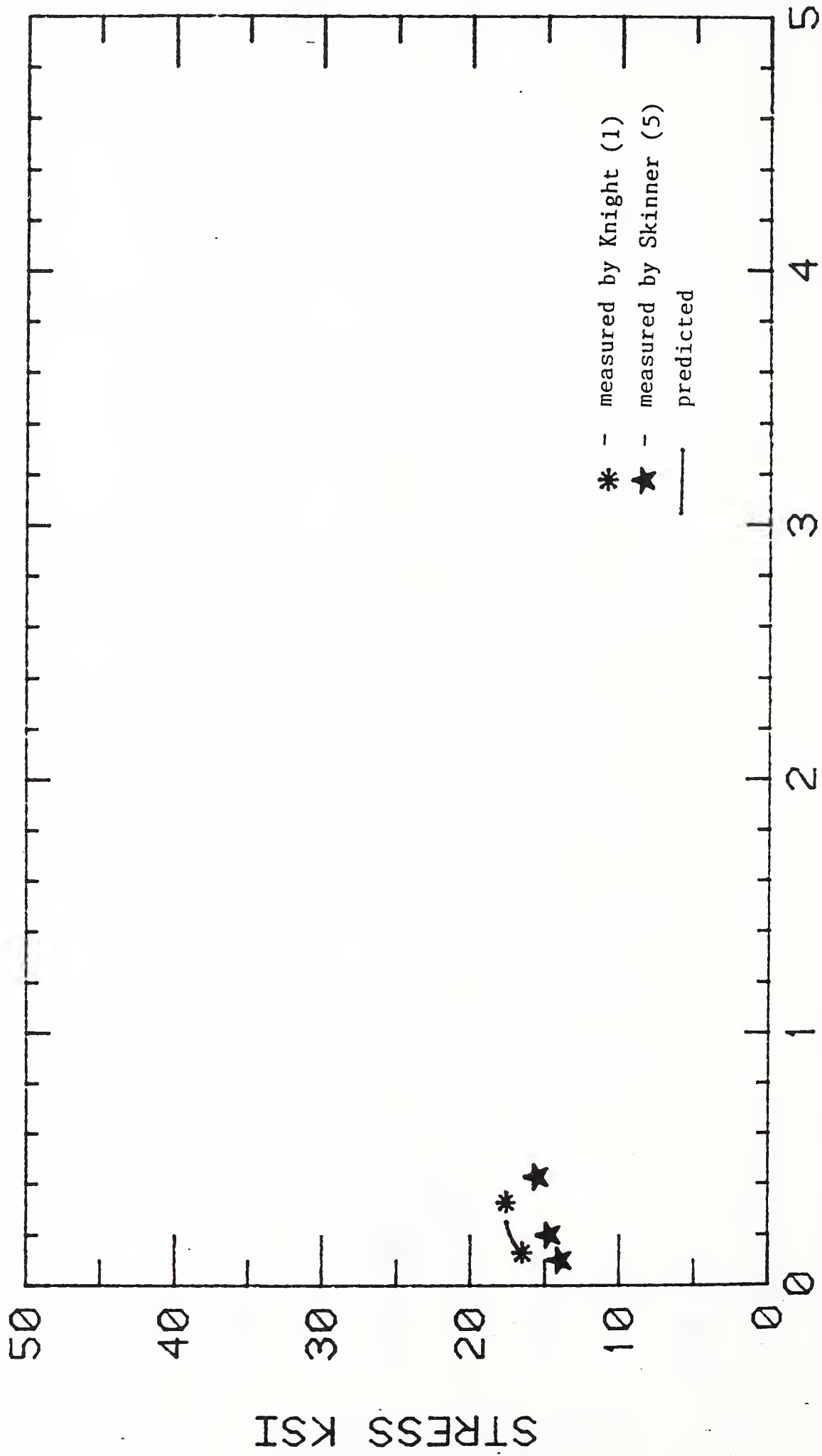


Figure 11f. Correlation of measured and calculated plastic strain at 600°C.

AS 149 STEEL - CREEP STRAIN VS TIME AT 350 DEG C

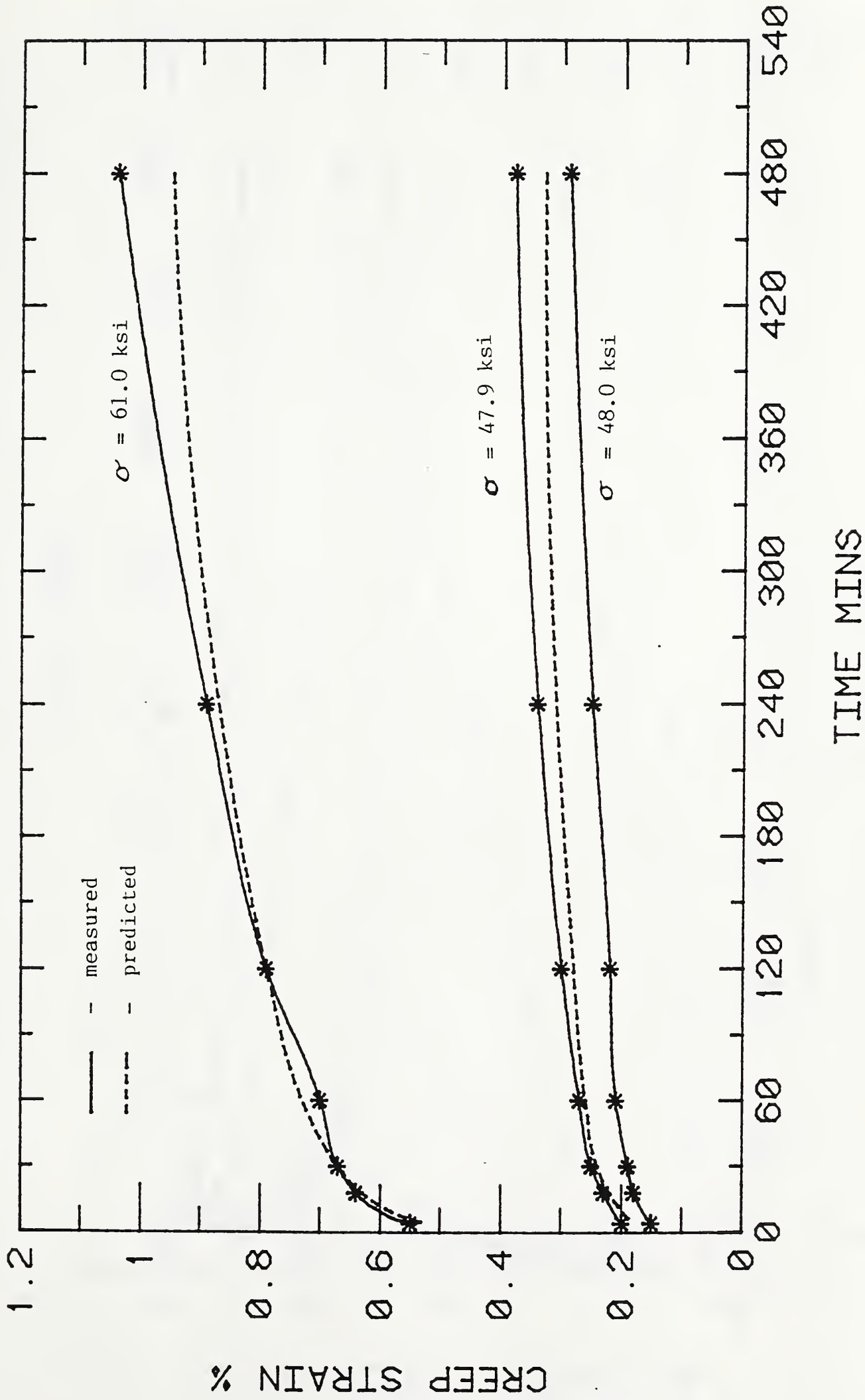


Figure 12a. Correlation of measured and calculated creep strain at 350°C.

AS 149 STEEL - CREEP STRAIN VS TIME AT 400 DEG C

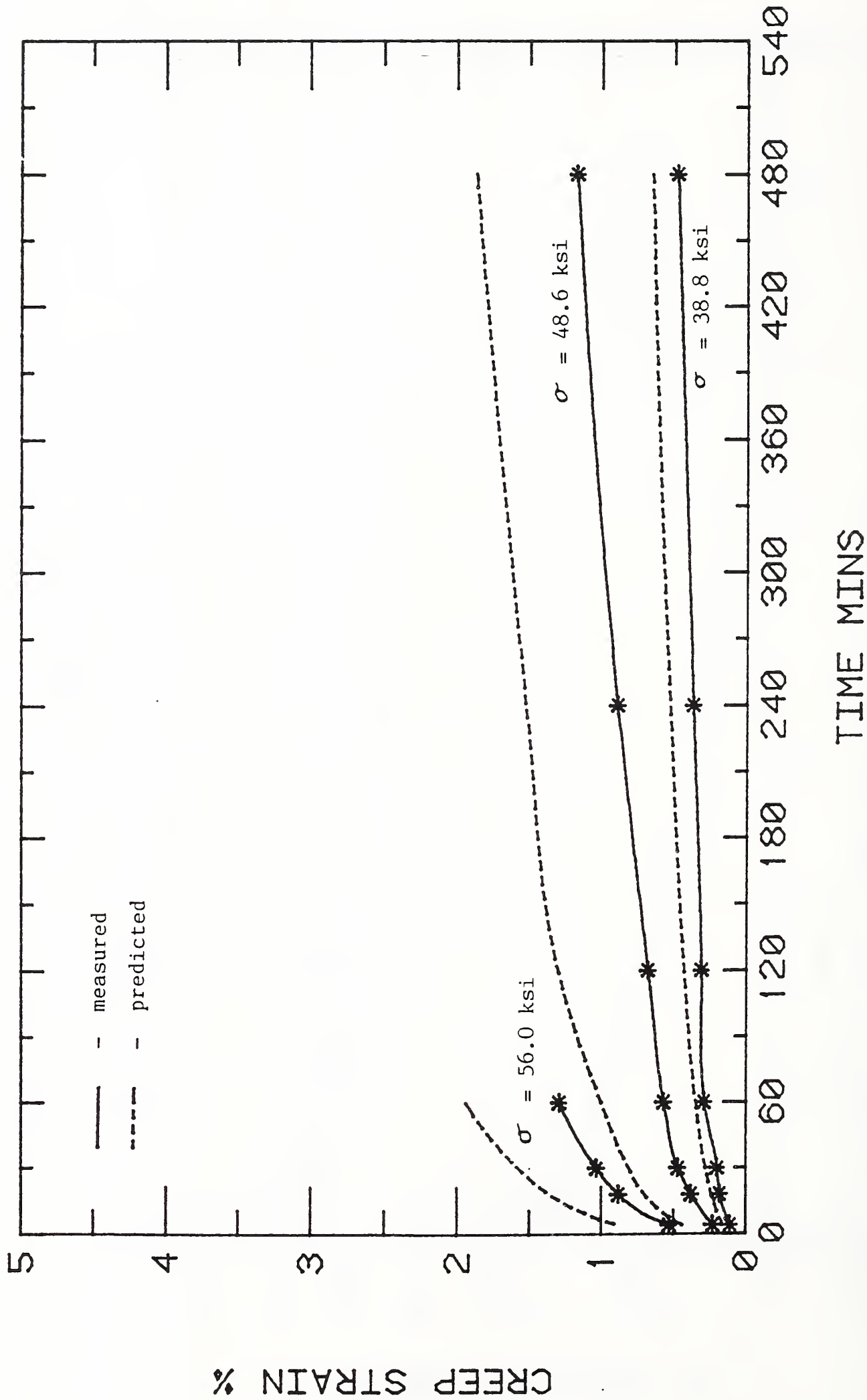


Figure 12b. Correlation of measured and calculated creep strain at 400°C.

AS 149 STEEL - CREEP STRAIN VS TIME AT 450 DEG C

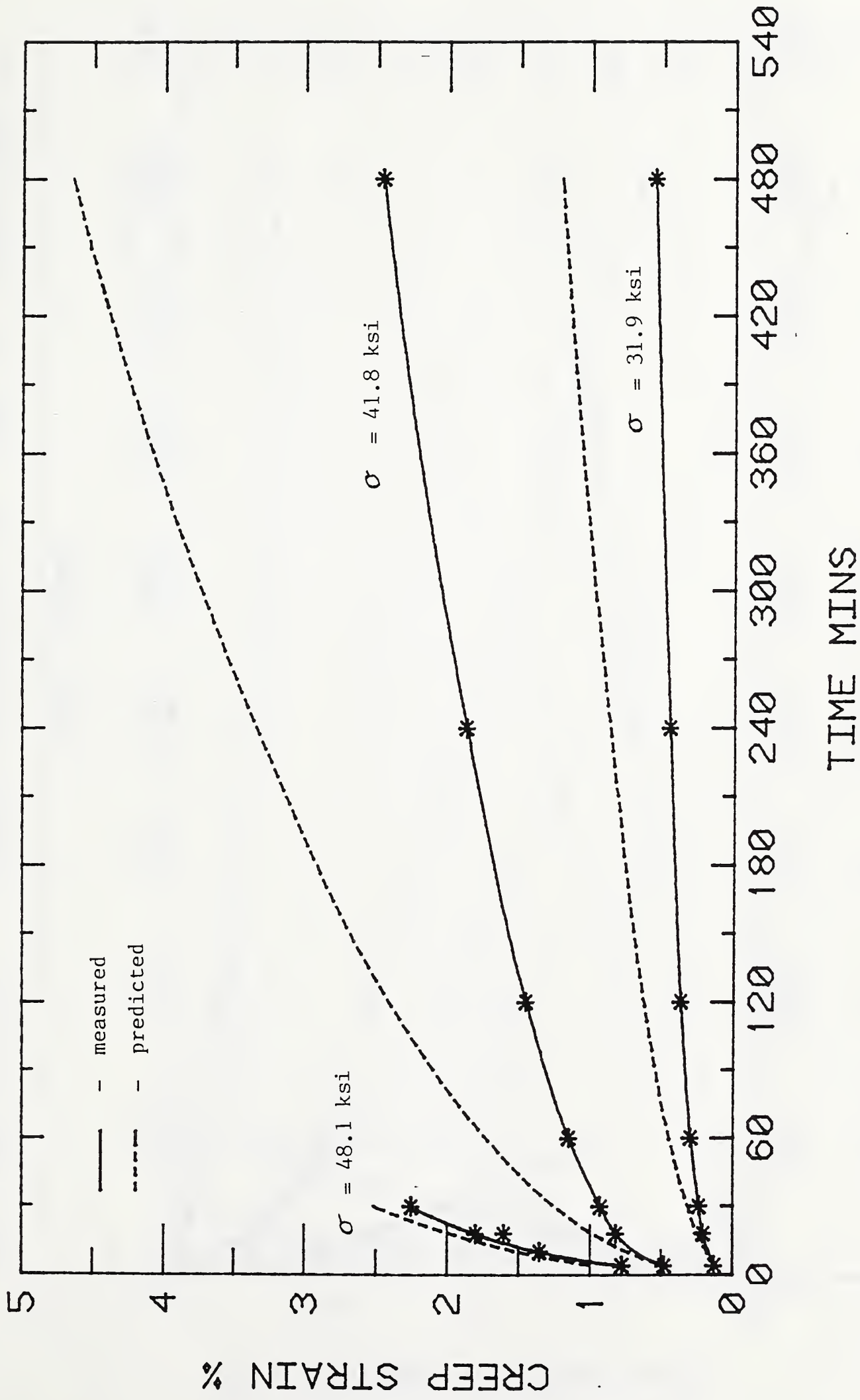


Figure 12c. Correlation of measured and calculated creep strain at 450°C.

AS 149 STEEL - CREEP STRAIN VS TIME AT 500 DEG C

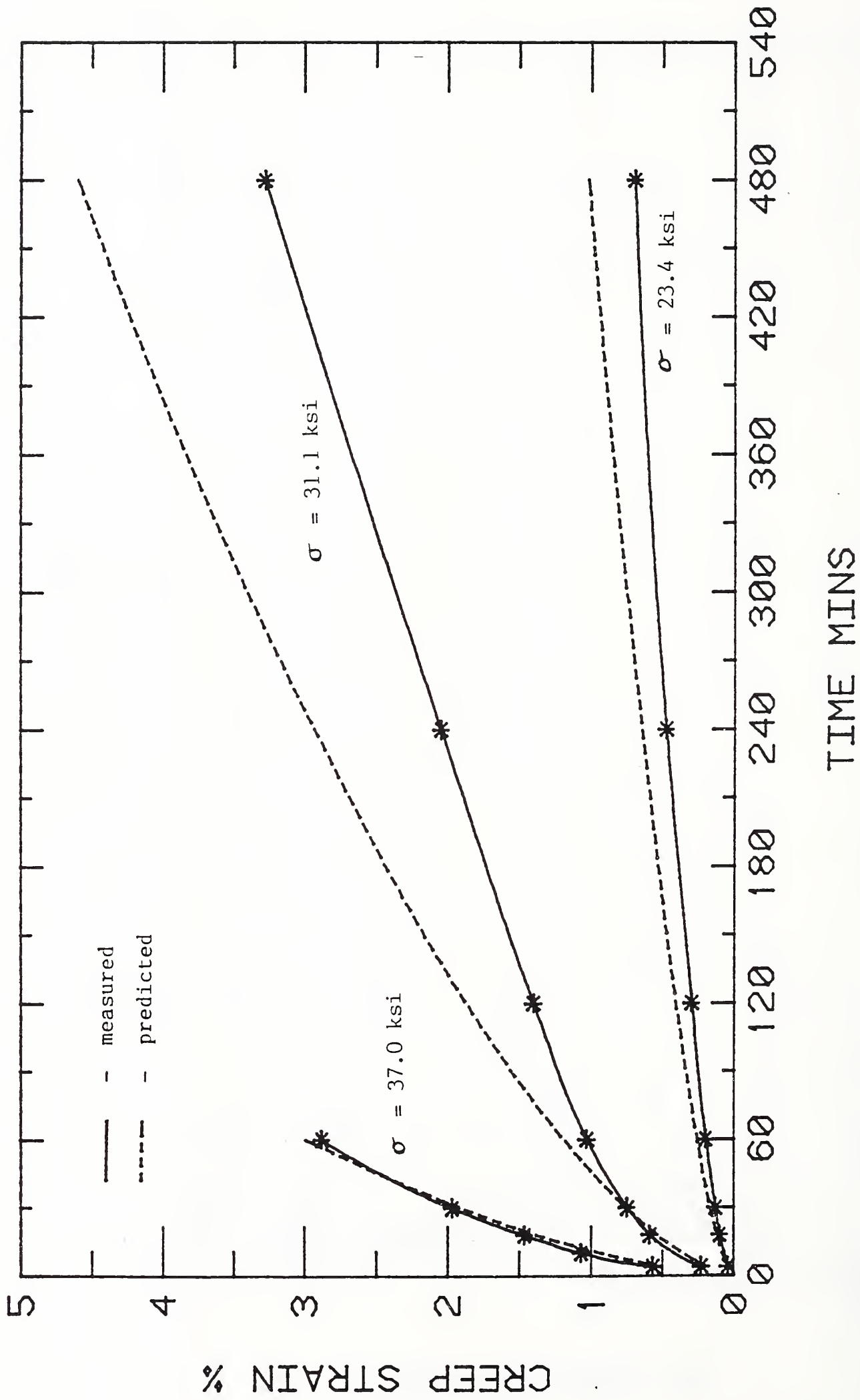


Figure 12d. Correlation of measured and calculated creep strain at 500°C.

AS 149 STEEL - CREEP STRAIN VS TIME AT 550 DEG C

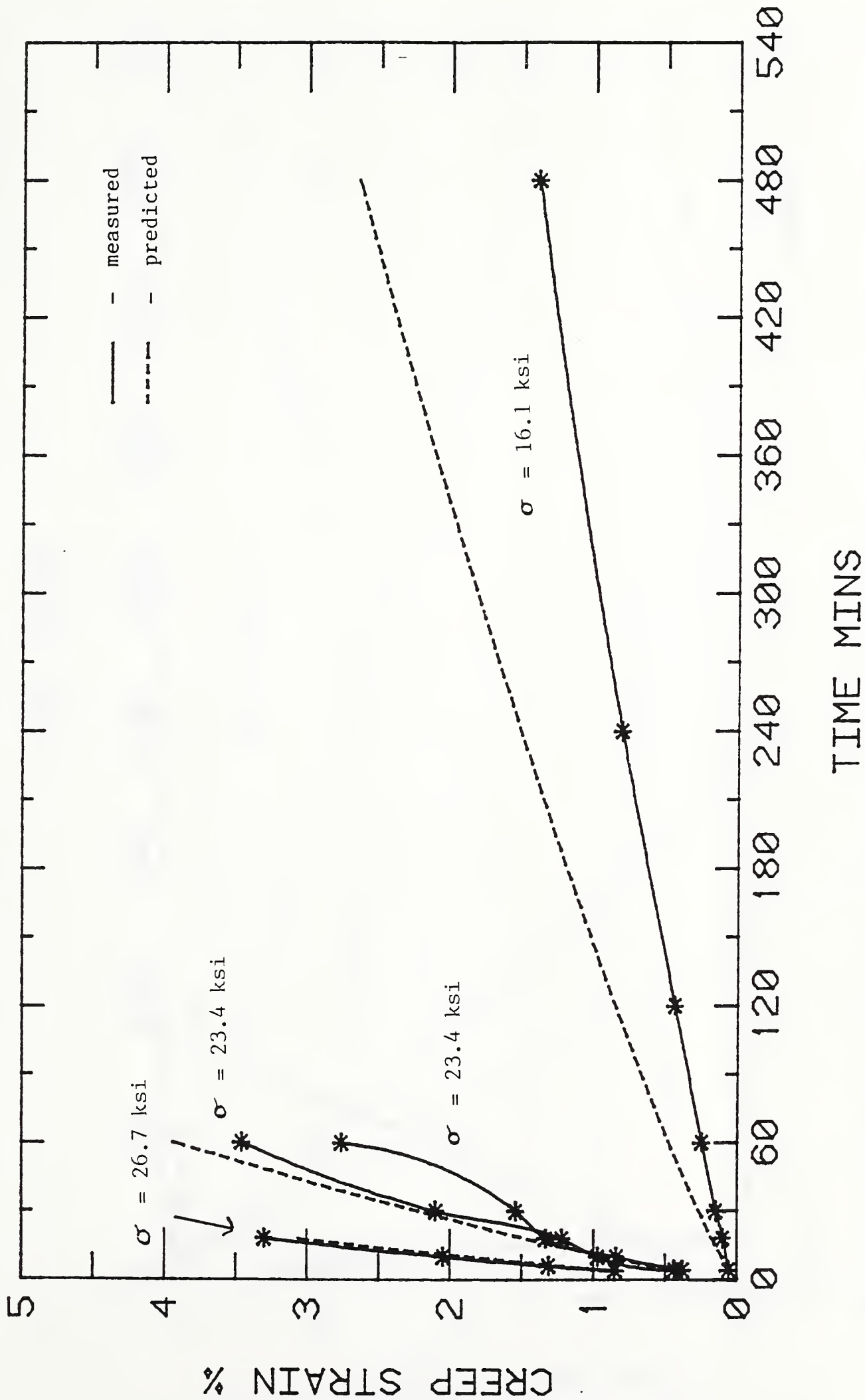


Figure 12e. Correlation of measured and calculated creep strain at 550°C.

AS 149 STEEL - CREEP STRAIN VS TIME AT 500 DEG C

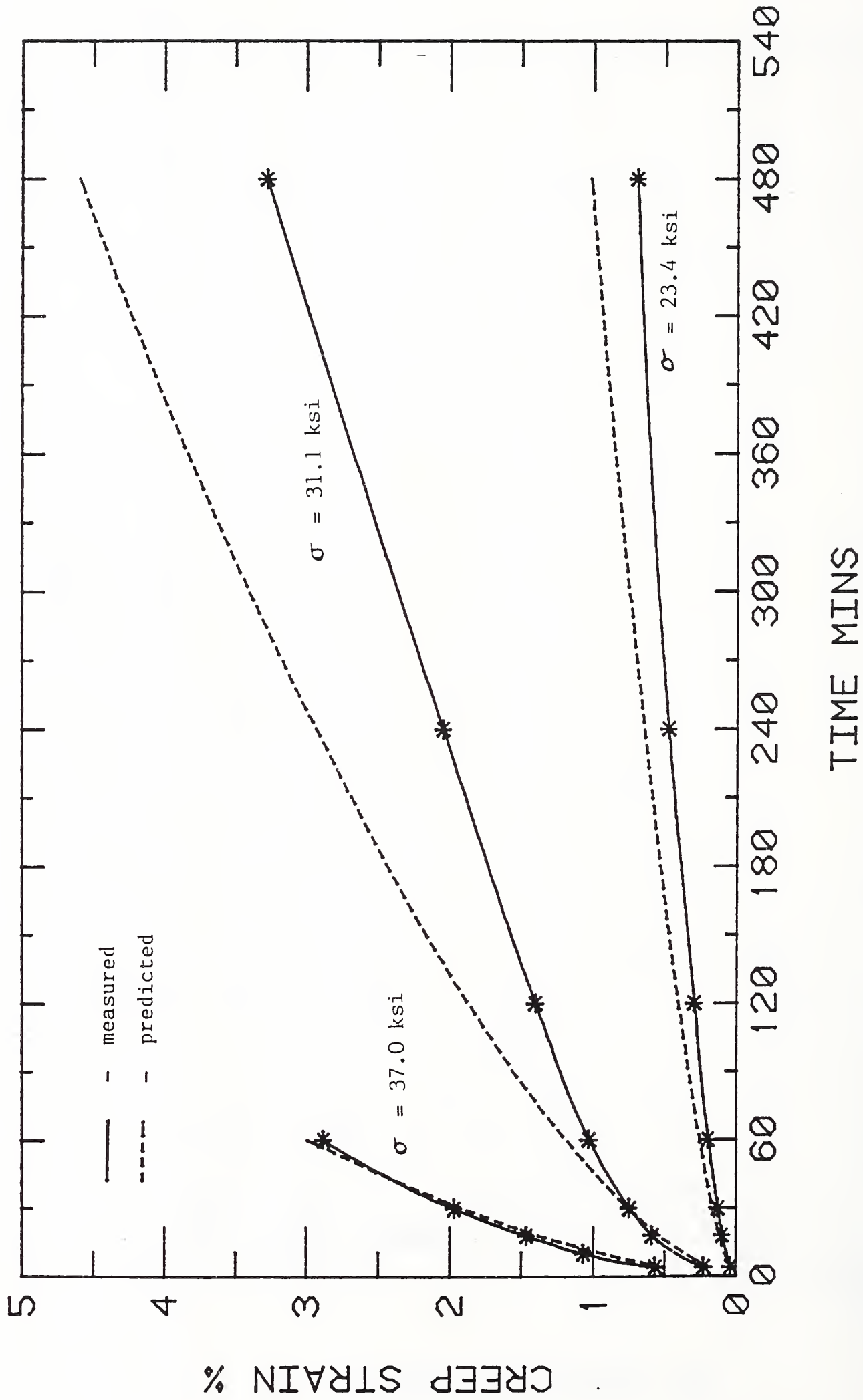


Figure 12d. Correlation of measured and calculated creep strain at 500°C.

AS 149 STEEL - CREEP STRAIN VS TIME AT 550 DEG C

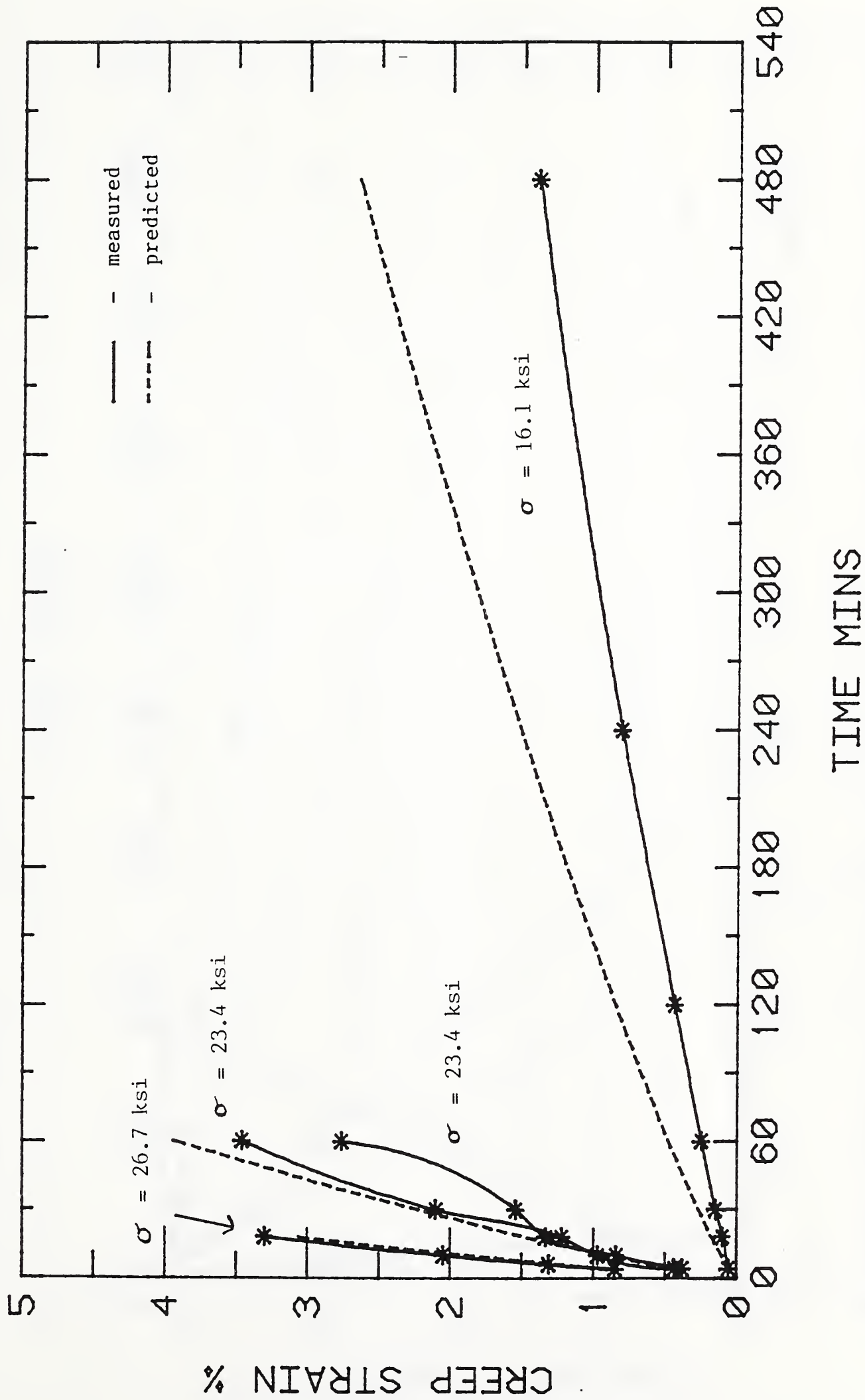


Figure 12e. Correlation of measured and calculated creep strain at 550°C.

AS A149 STEEL - TOTAL STRAIN VS TIME AT 350 DEG C

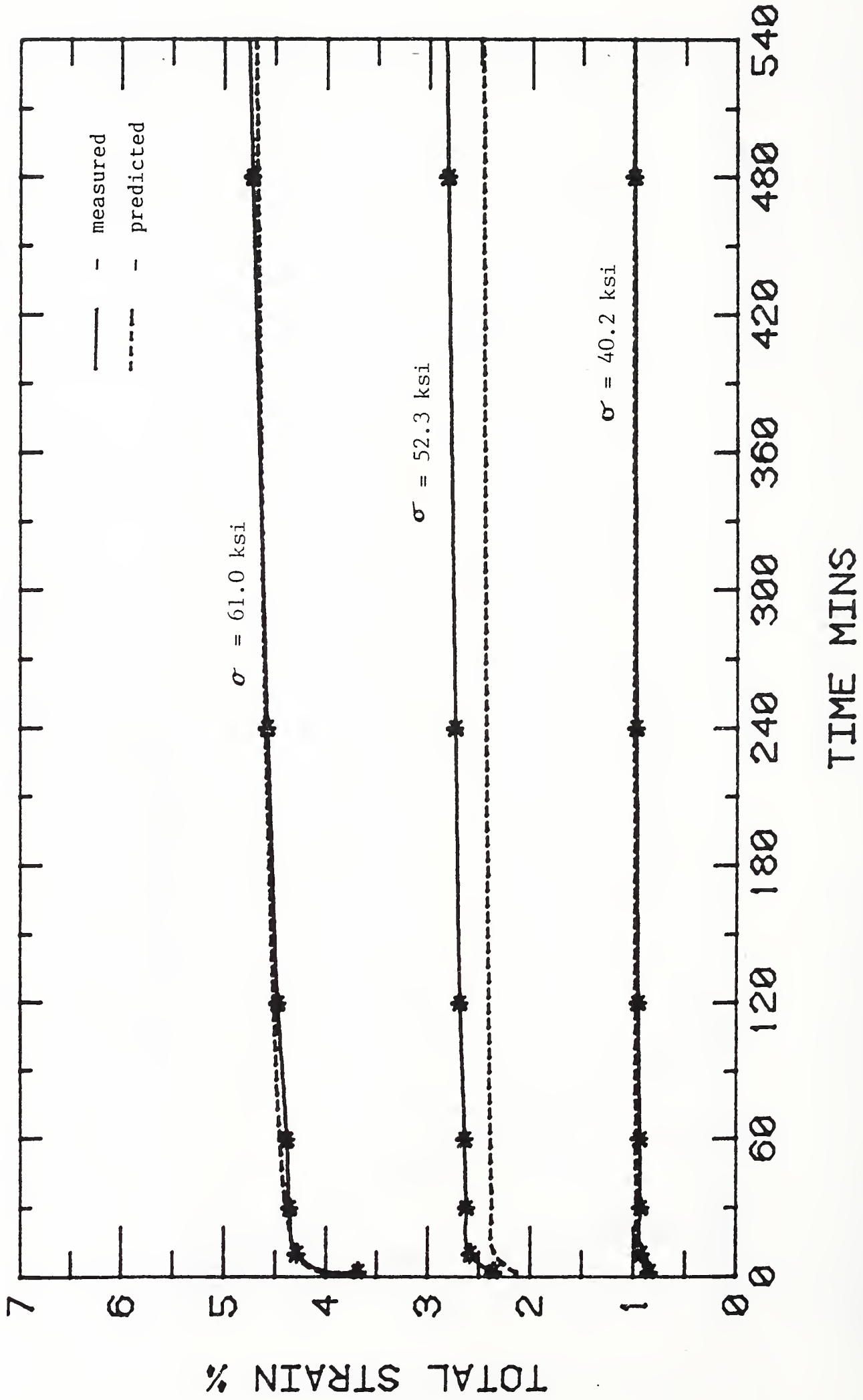


Figure 13a. Correlation of measured and calculated total strain at 350°C.

AS A149 STEEL - TOTAL STRAIN VS TIME AT 400 DEG C

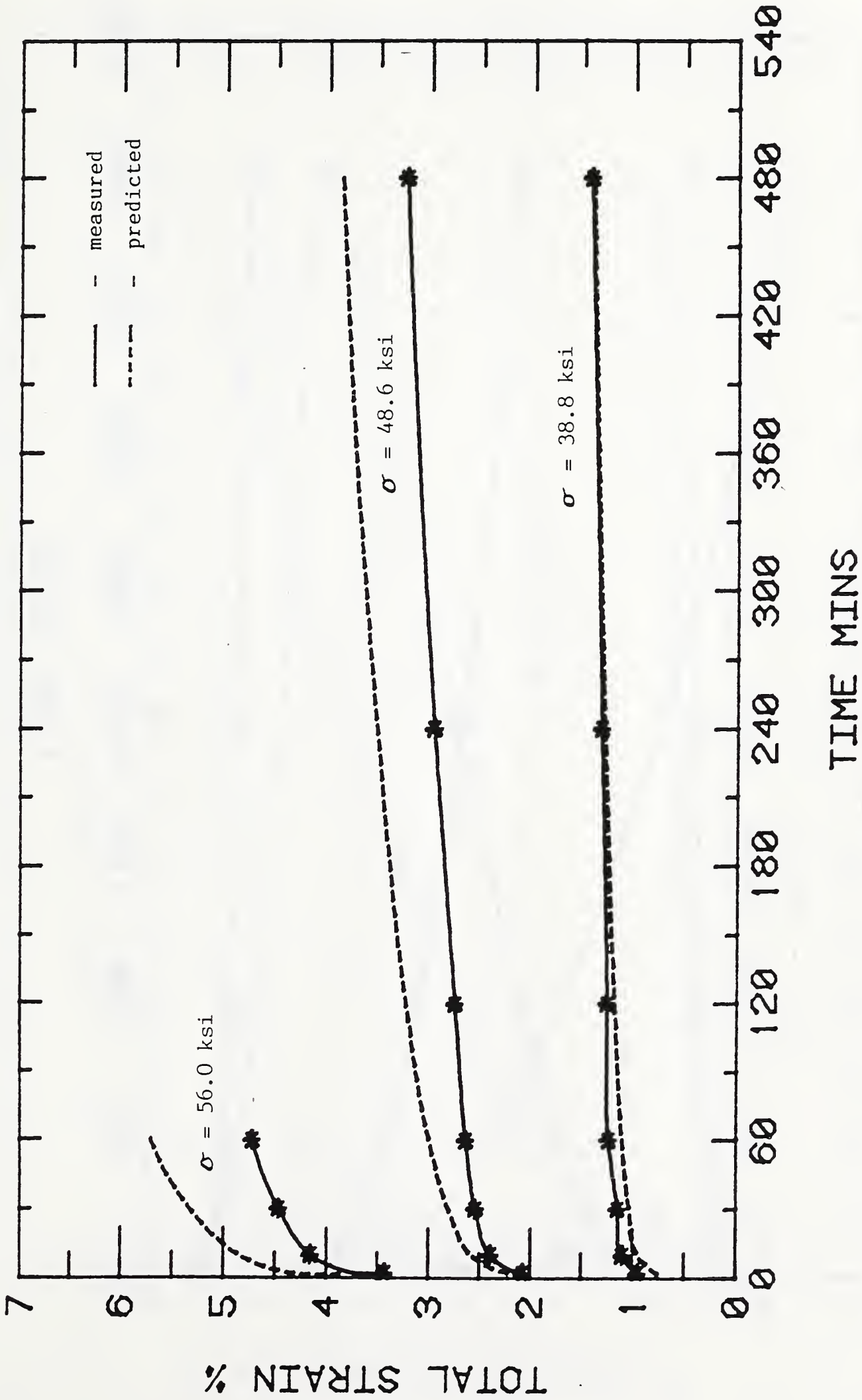


Figure 13b. Correlation of measured and calculated total strain at 400°C.

AS A149 STEEL - TOTAL STRAIN VS TIME AT 450 DEG C

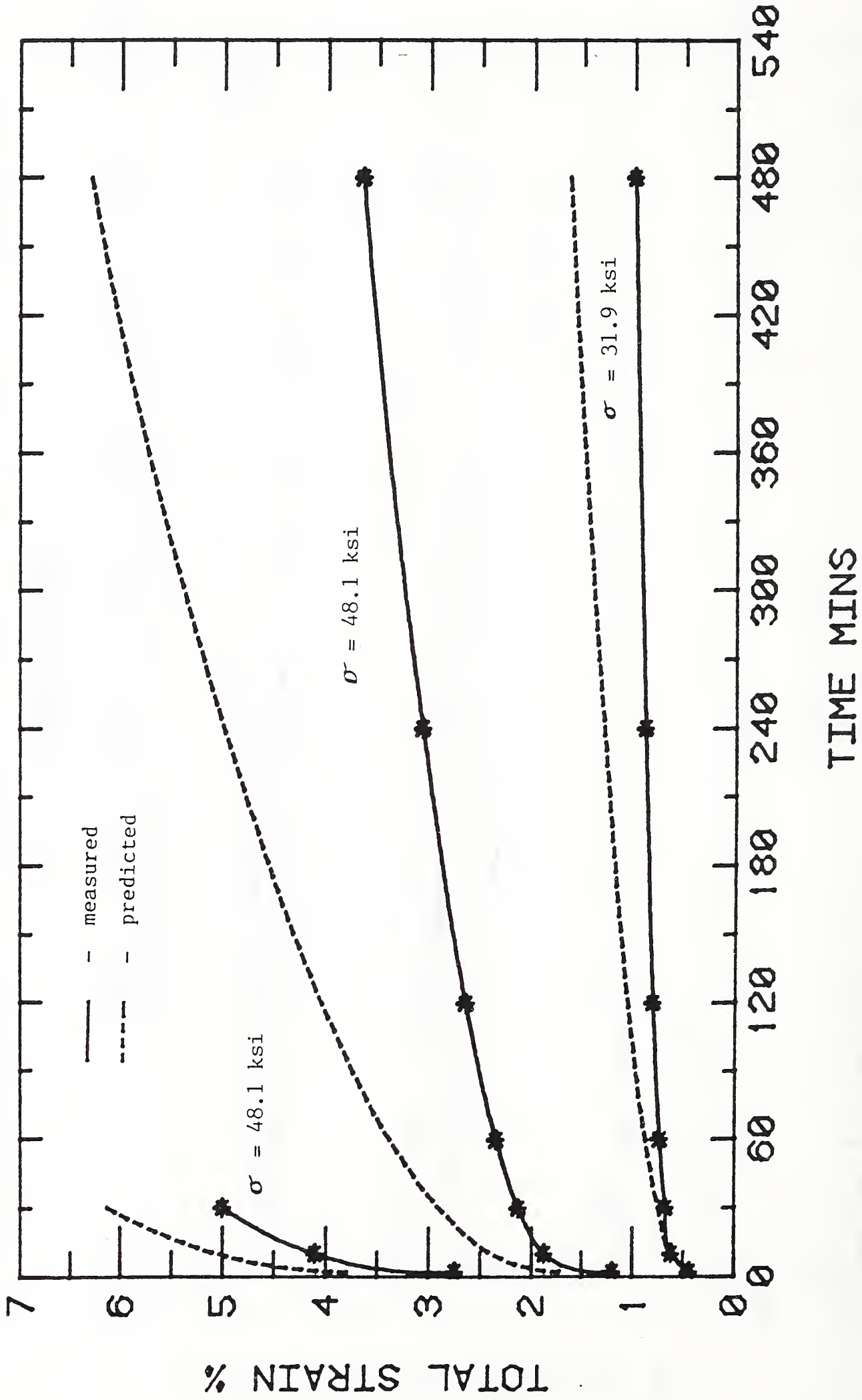


Figure 13c. Correlation of measured and calculated total strain at 450°C.

AS A149 STEEL - TOTAL STRAIN VS TIME AT 500 DEG C

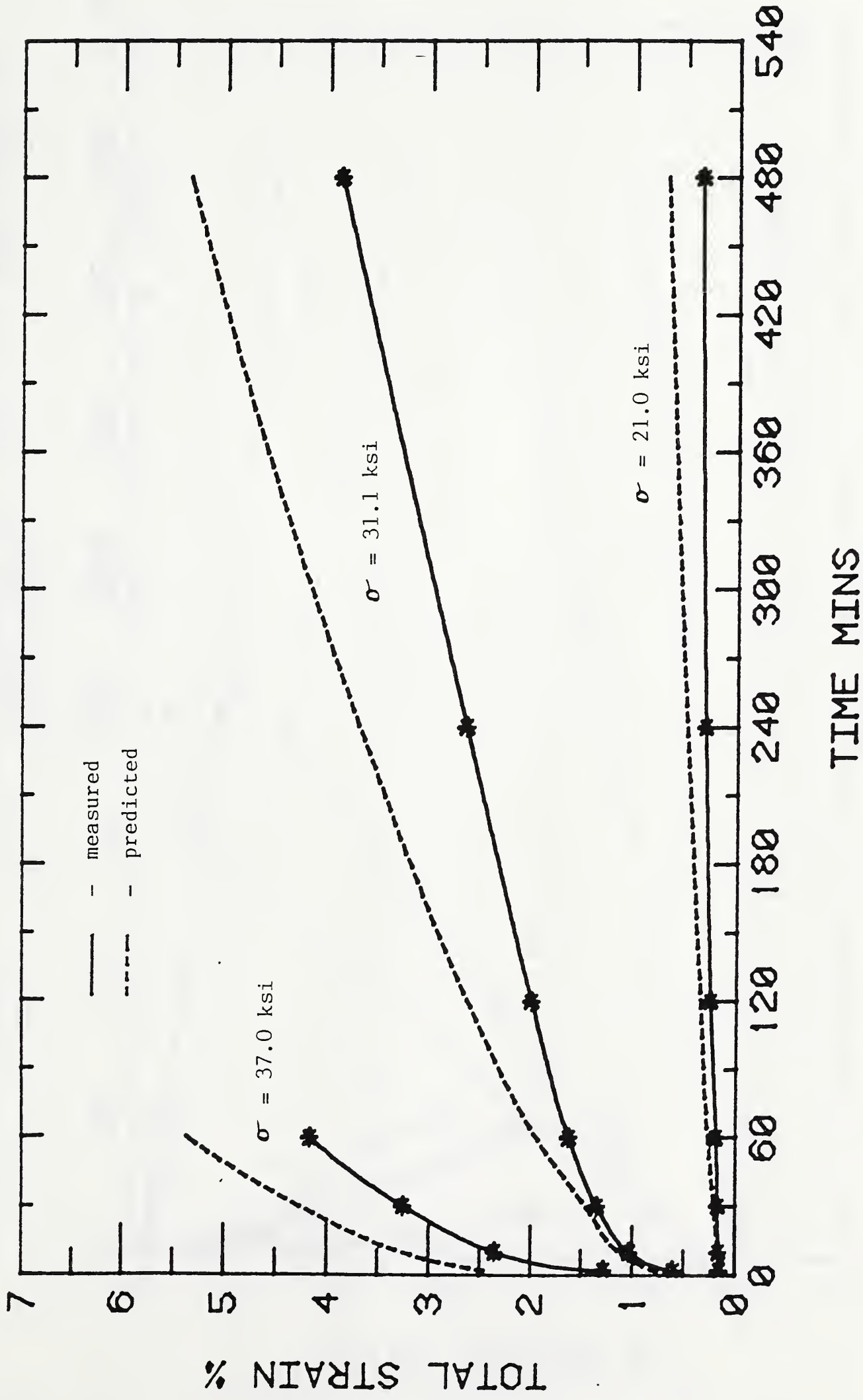


Figure 13d. Correlation of measured and calculated total strain at 500°C.

AS A149 STEEL - TOTAL STRAIN VS TIME AT 550 DEG C

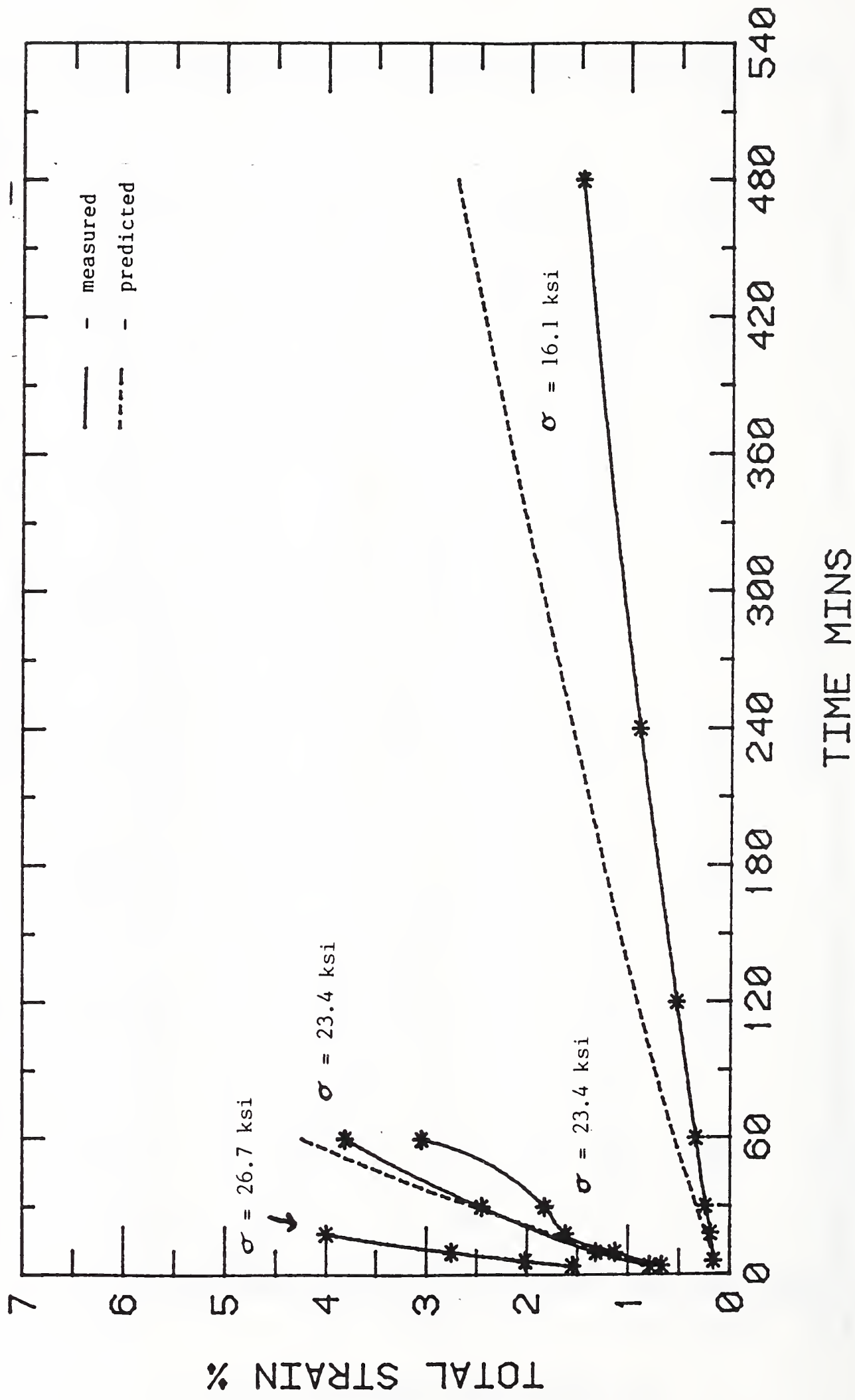


Figure 13e. Correlation of measured and calculated total strain at 550°C.

AS A149 STEEL - TOTAL STRAIN VS TIME AT 600 DEG C

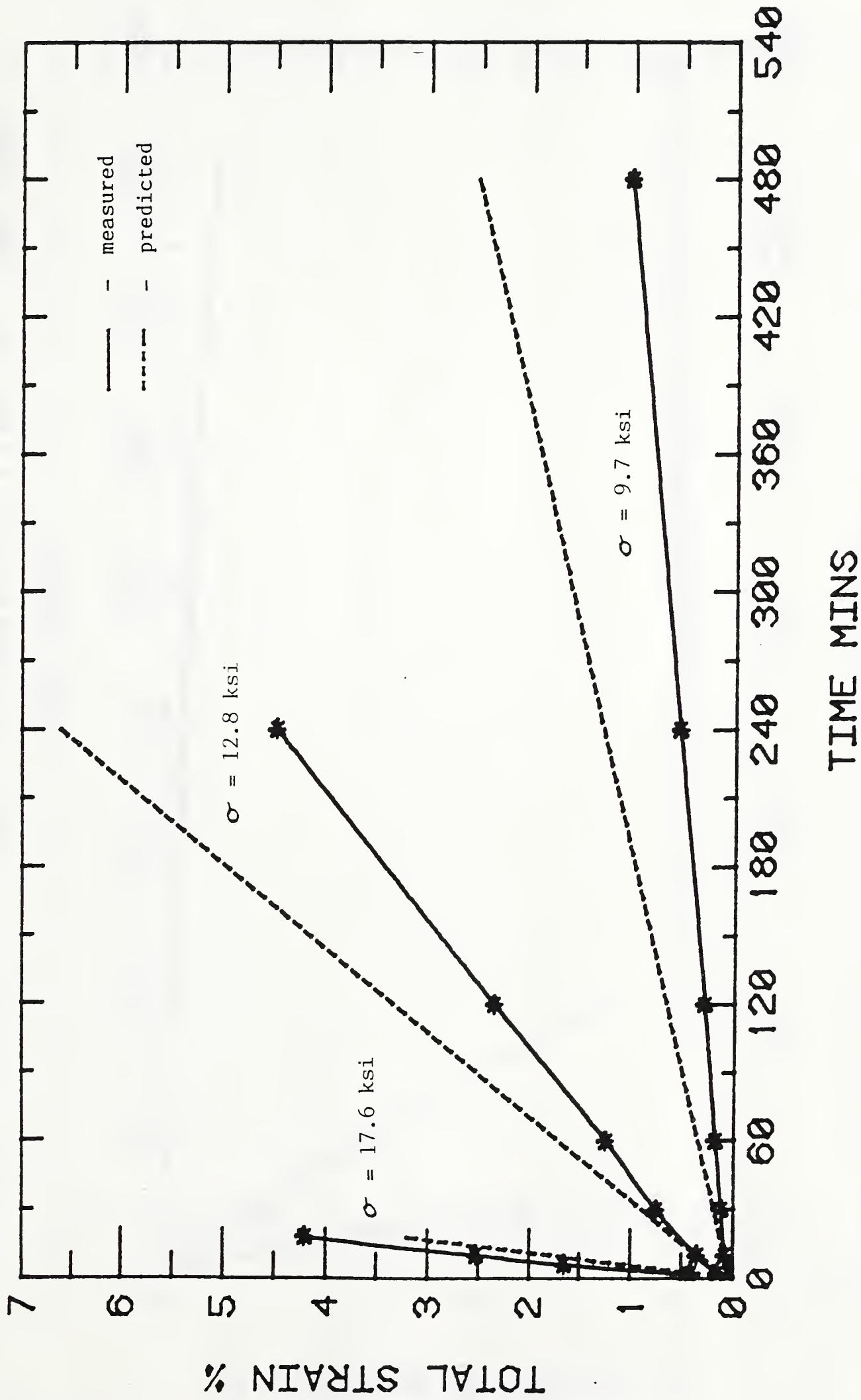


Figure 13f. Correlation of measured and calculated total strain at 600°C.

AS A149 STEEL - TOTAL STRAIN VS TIME AT 650 DEG C

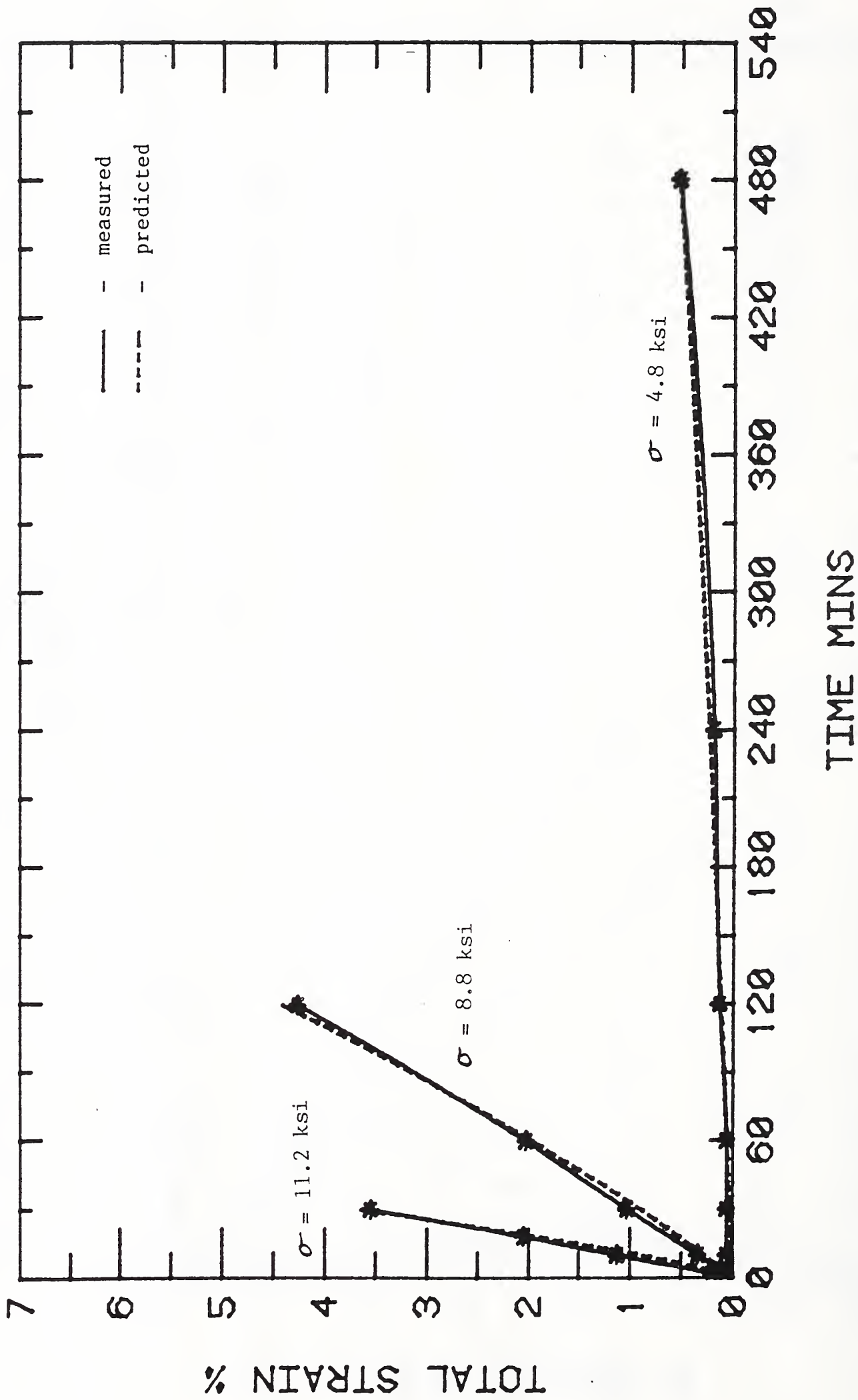


Figure 13g. Correlation of measured and calculated total strain at 650°C.

SS41 STEEL - CREEP STRAIN VS TIME AT 350 DEG C

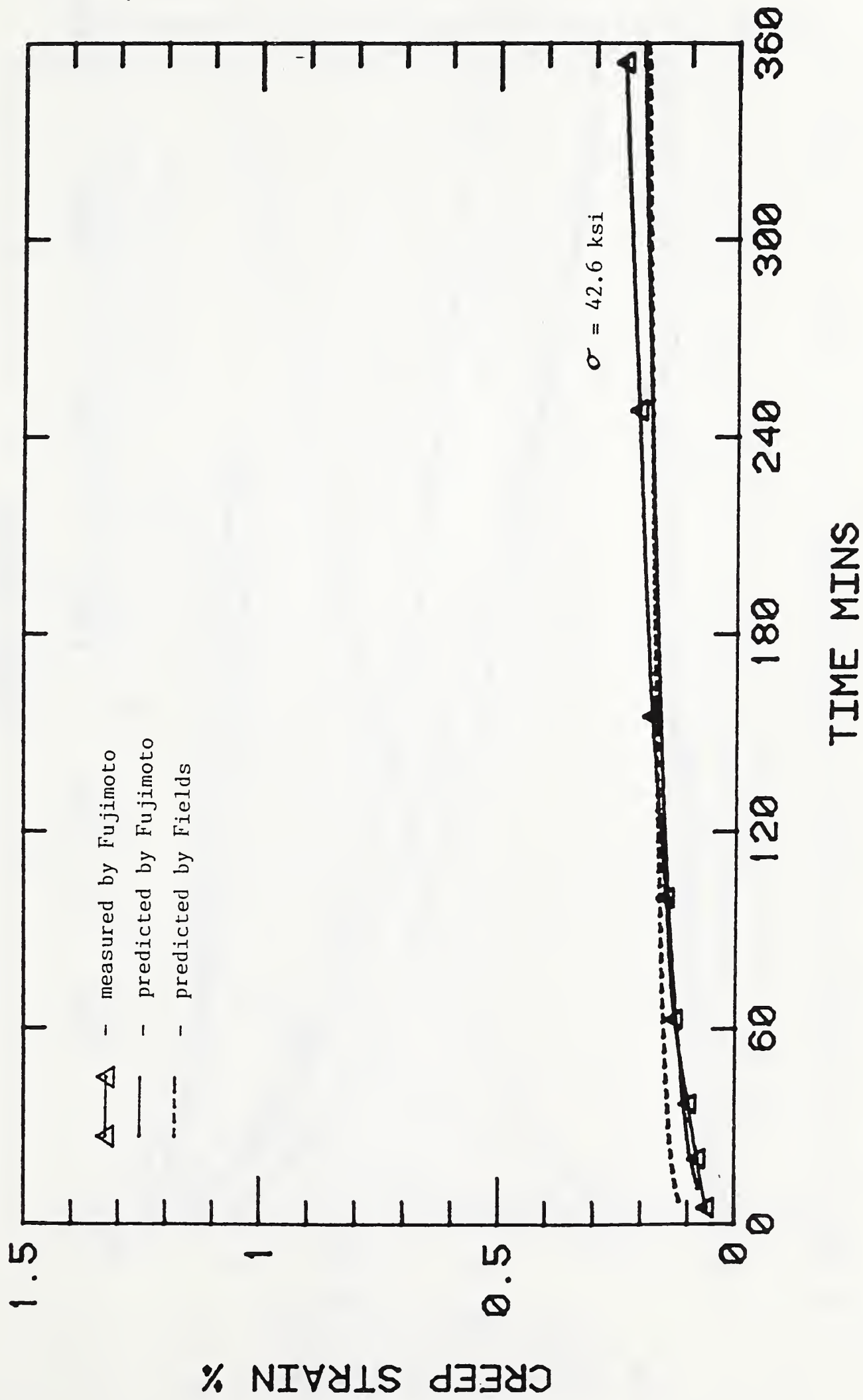


Figure 14a. SS41 Steel - Correlation of measured and calculated creep strain at 350°C.

SS41 STEEL - CREEP STRAIN VS TIME AT 450 DEG C

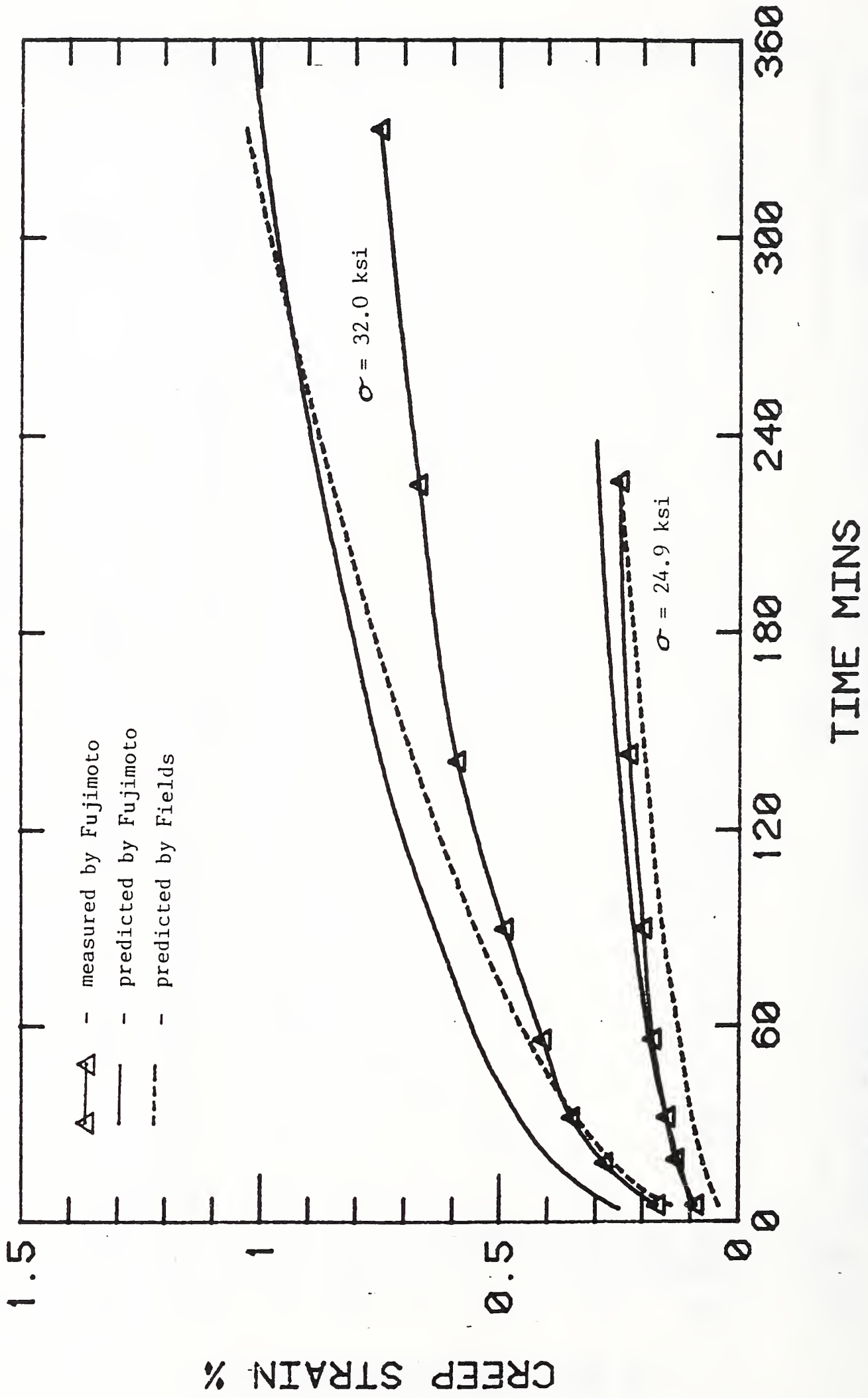


Figure 14b. SS41 Steel - Correlation of measured and calculated creep strain at 450°C.

SS41 STEEL - CREEP STRAIN VS TIME AT 550 DEG C

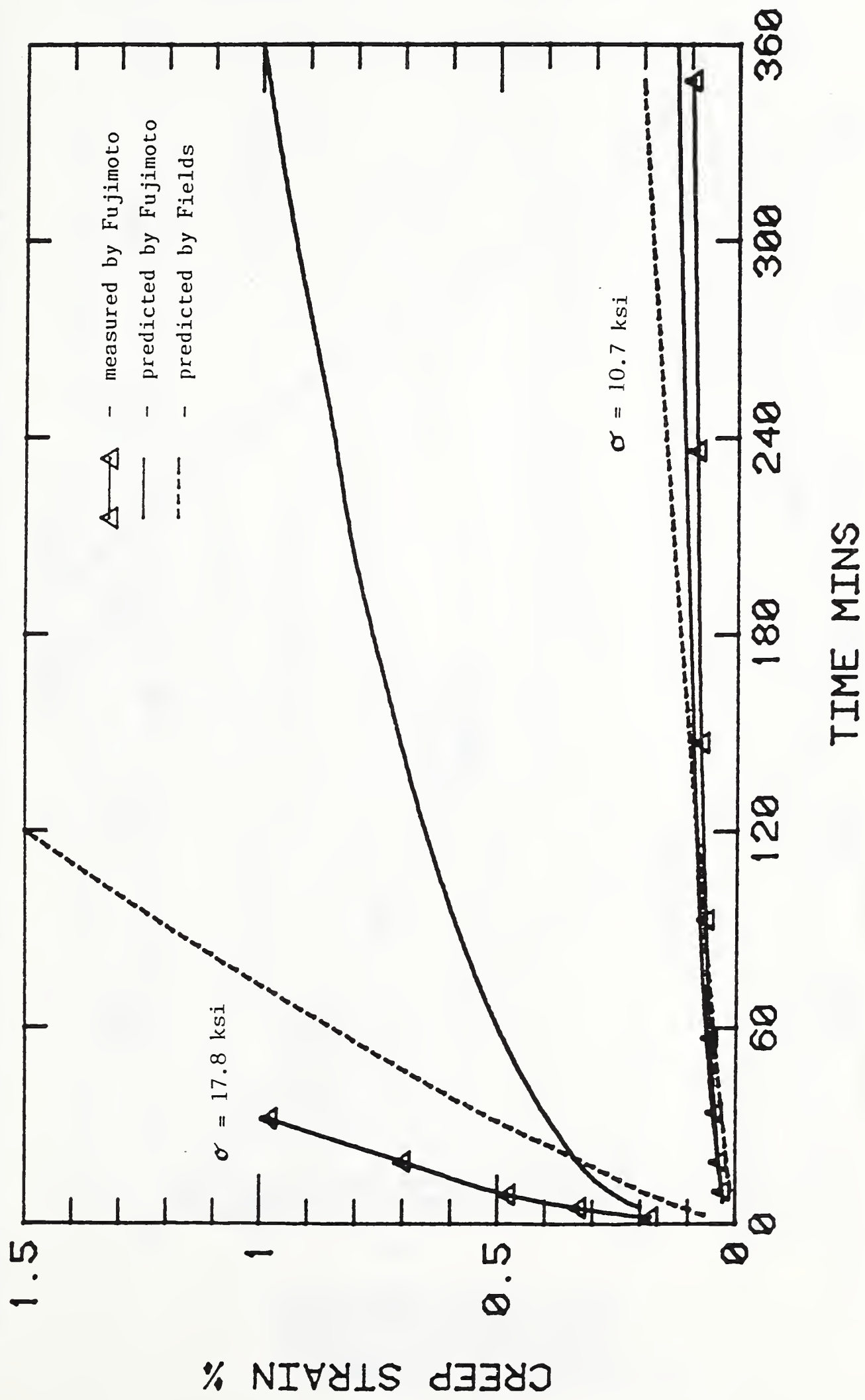


Figure 14c. SS41 Steel - Correlation of measured and calculated creep strain at 550°C.

SS41 STEEL - CREEP STRAIN VS TIME AT 600 DEG C

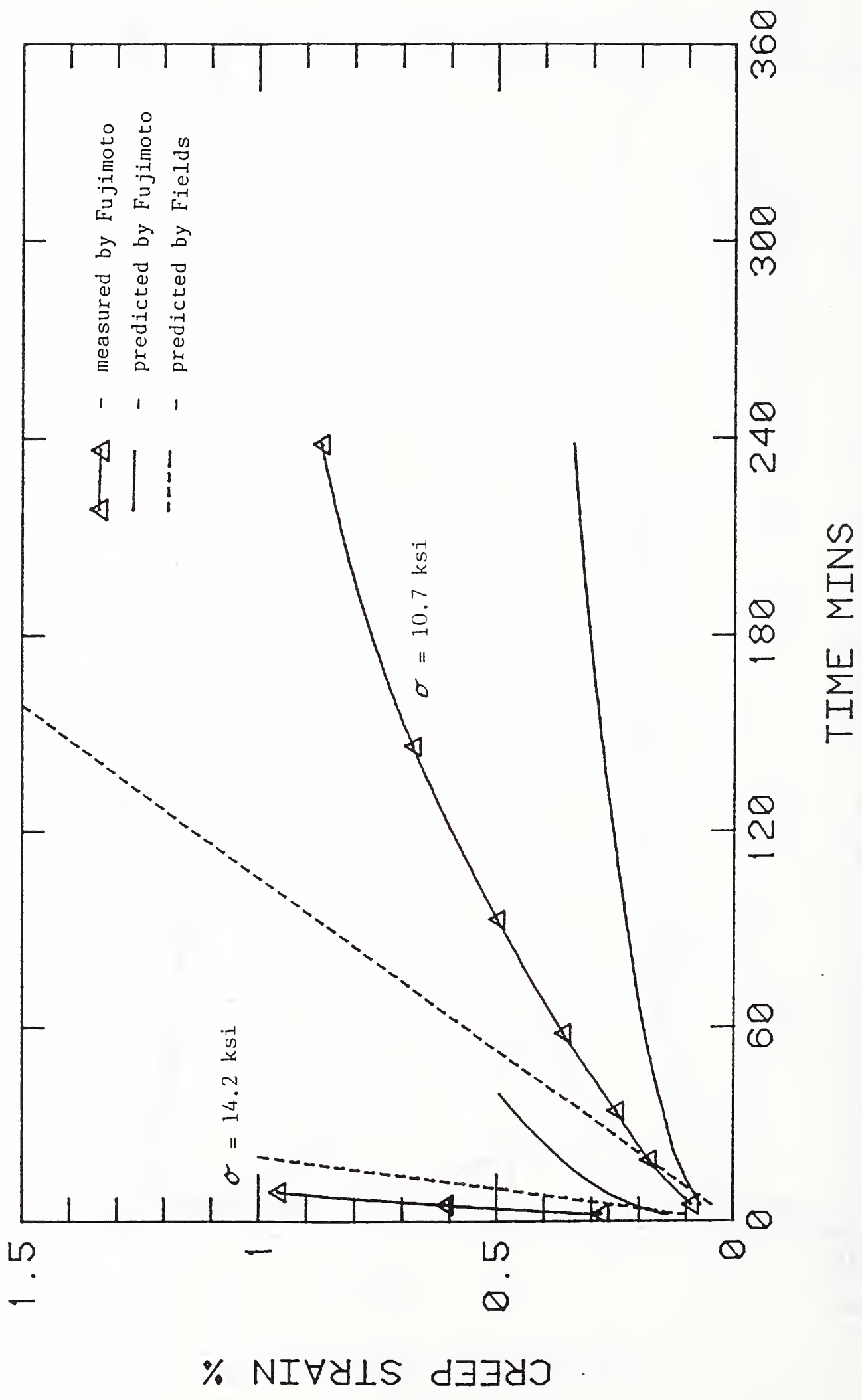


Figure 14d. SS41 Steel - Correlation of measured and calculated creep strain at 600°C.

A36 STEEL

DEFORMATION MODES FOR 2 MIN. AT TEMPERATURE

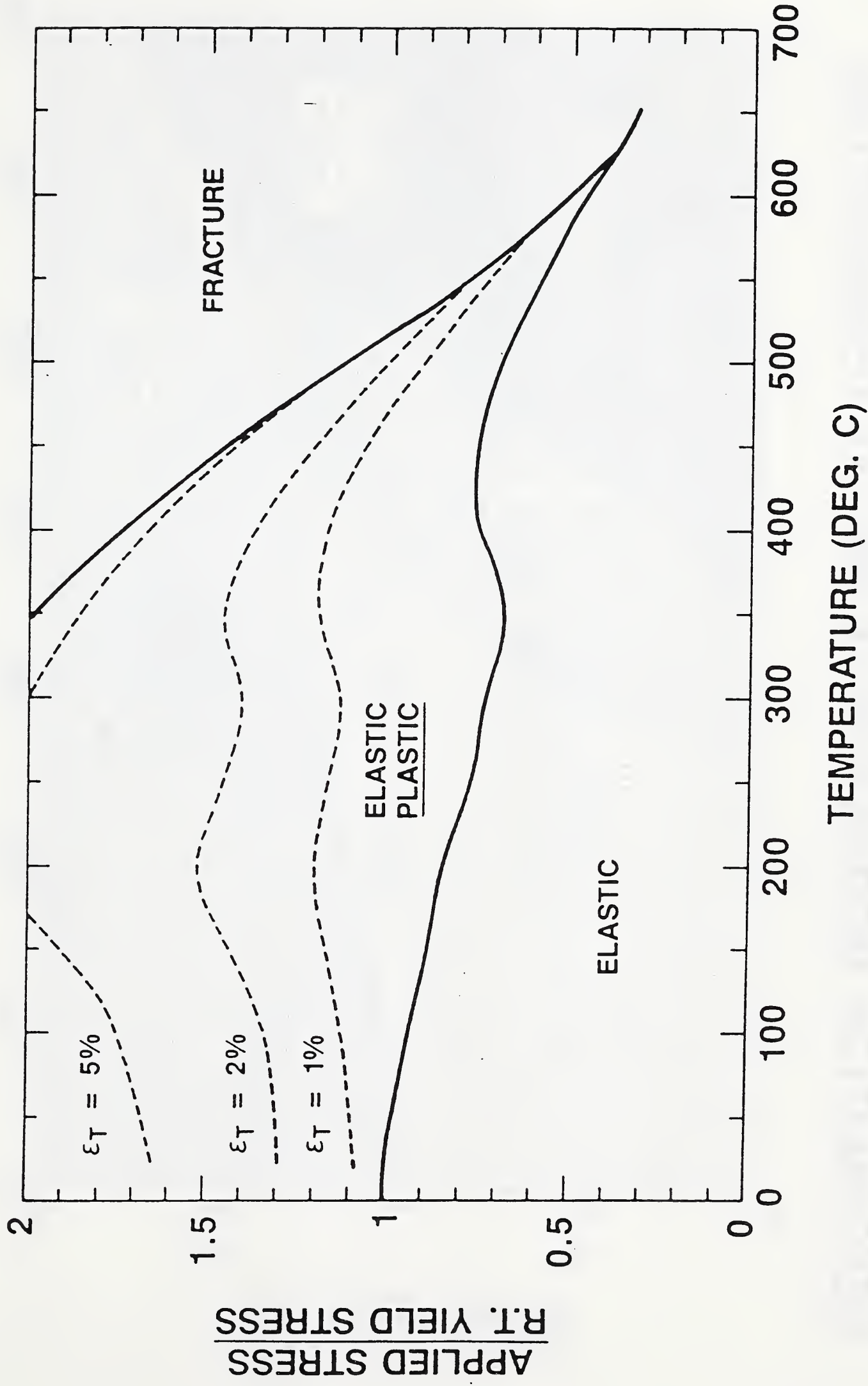


Figure 15. Deformation modes for 2 minutes at temperature.

A36 STEEL

DEFORMATION MODES FOR 15 MIN. AT TEMPERATURE

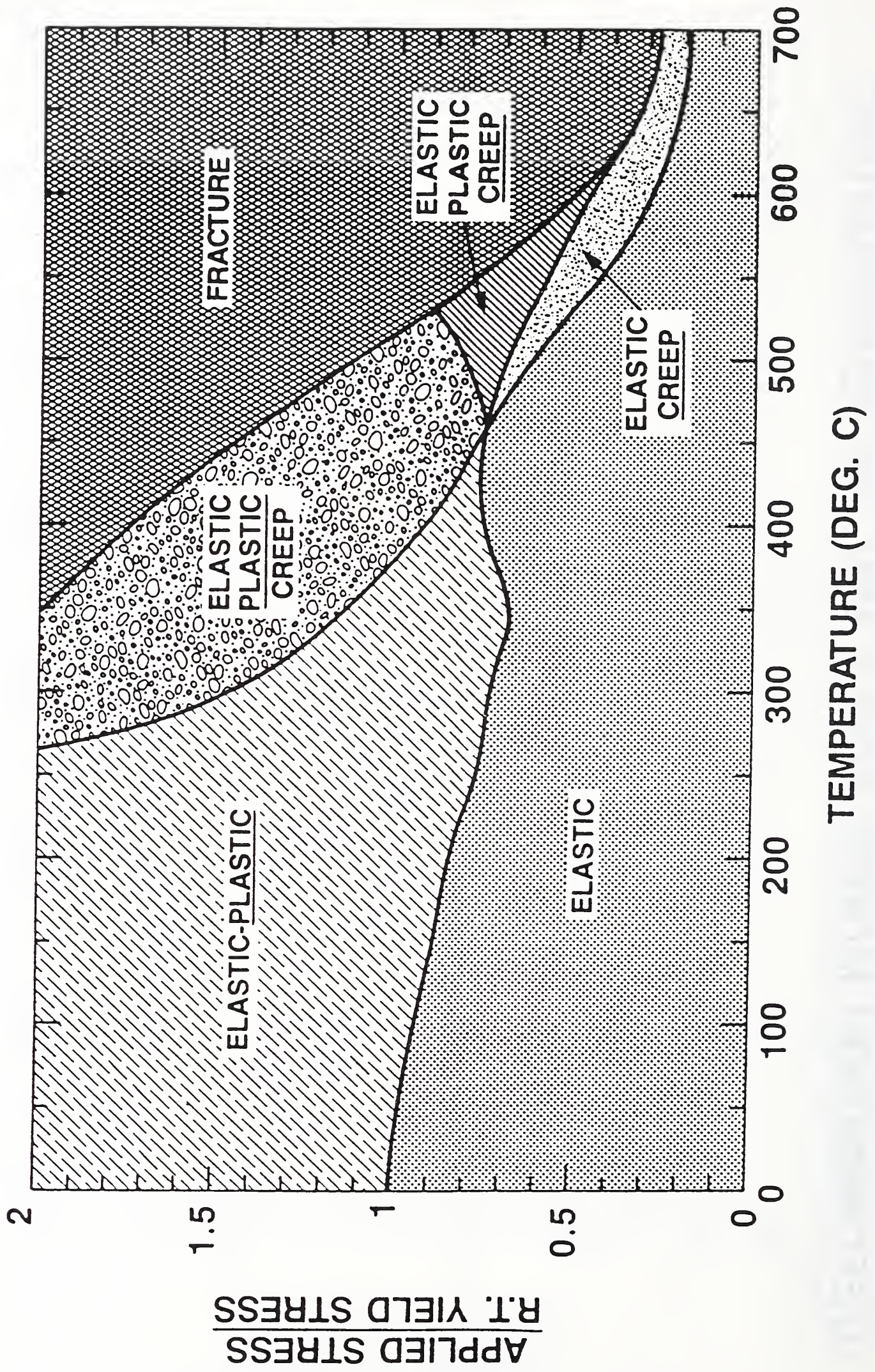


Figure 16a. Deformation modes for 15 minutes at temperature.

A36 STEEL

DEFORMATION MODES FOR 15 MIN. AT TEMPERATURE

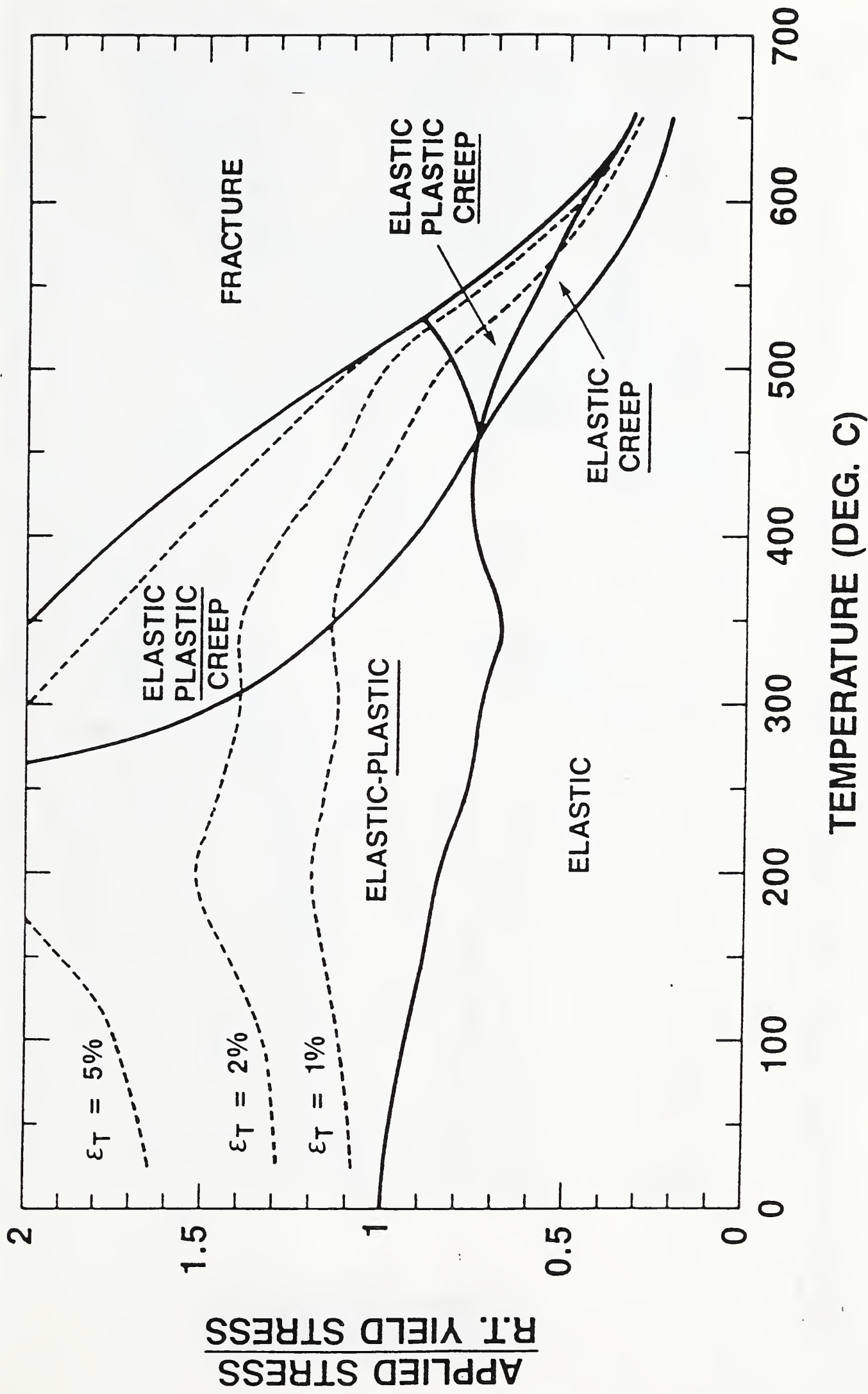
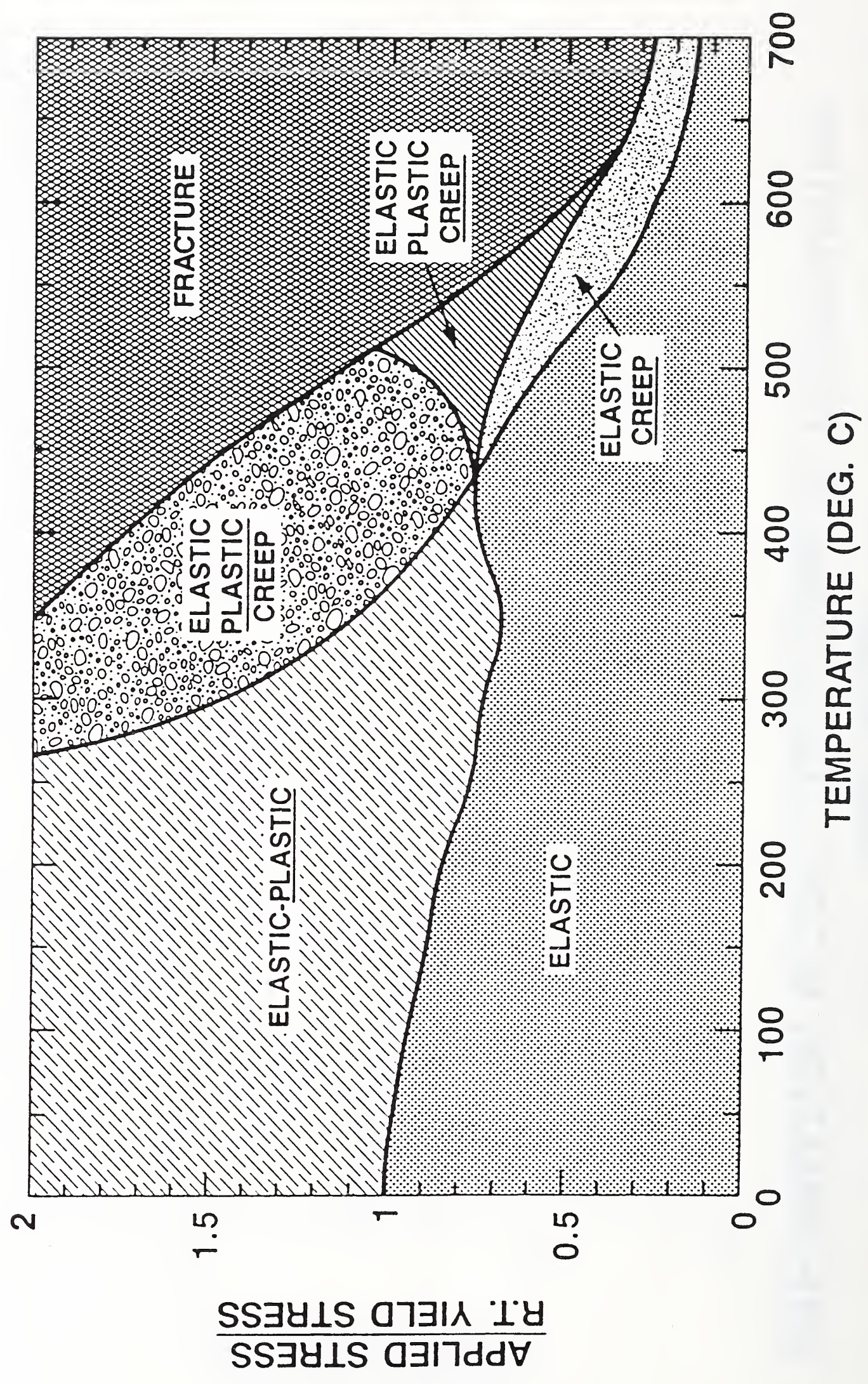


Figure 16b. Deformation modes for 15 minutes at temperature.

A36 STEEL DEFORMATION MODES FOR 30 MIN. AT TEMPERATURE



A36 STEEL

DEFORMATION MODES FOR 30 MIN. AT TEMPERATURE

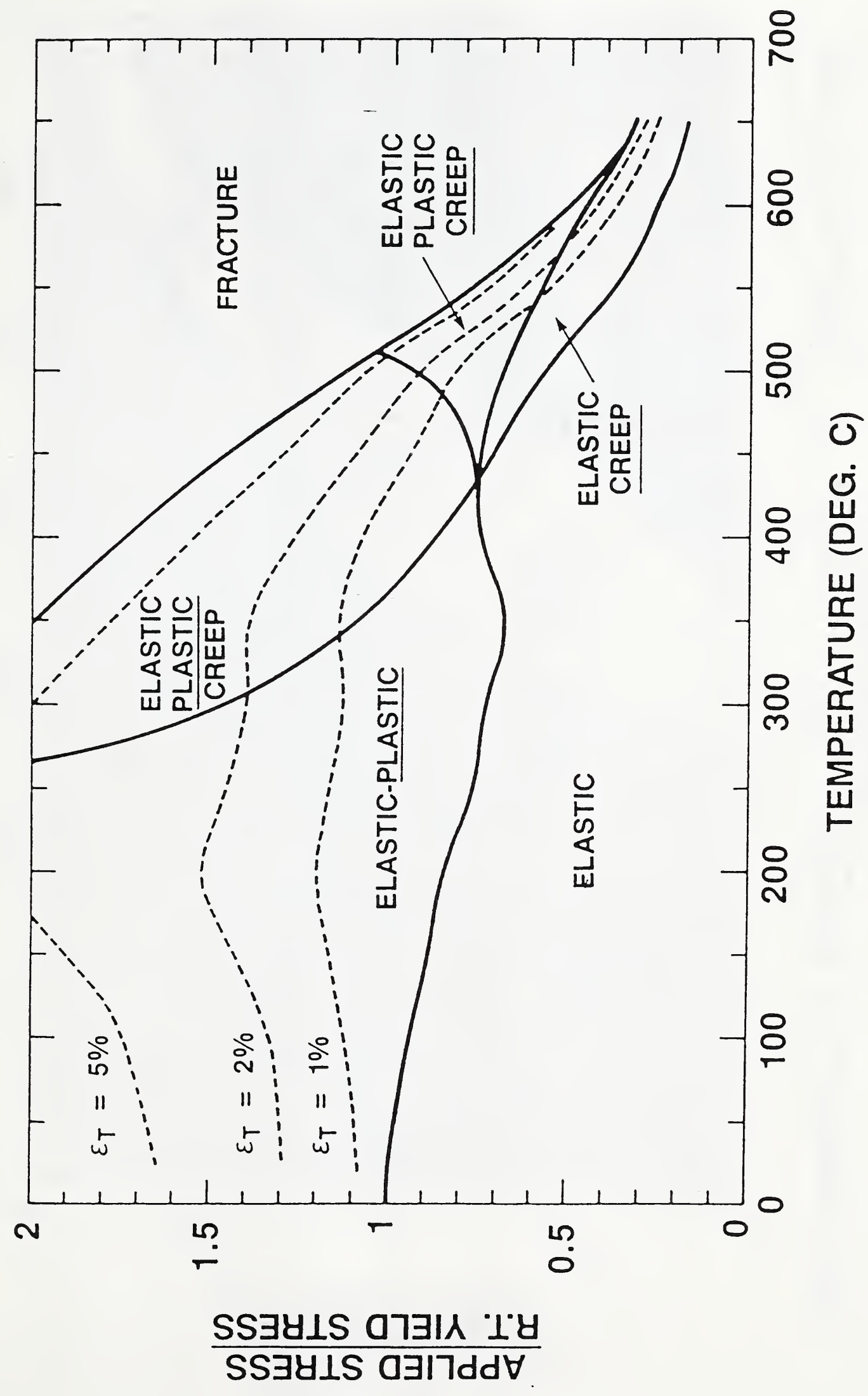


Figure 17b. Deformation modes for 30 minutes at temperature.

A36 STEEL DEFORMATION MODES FOR 1 HOUR AT TEMPERATURE

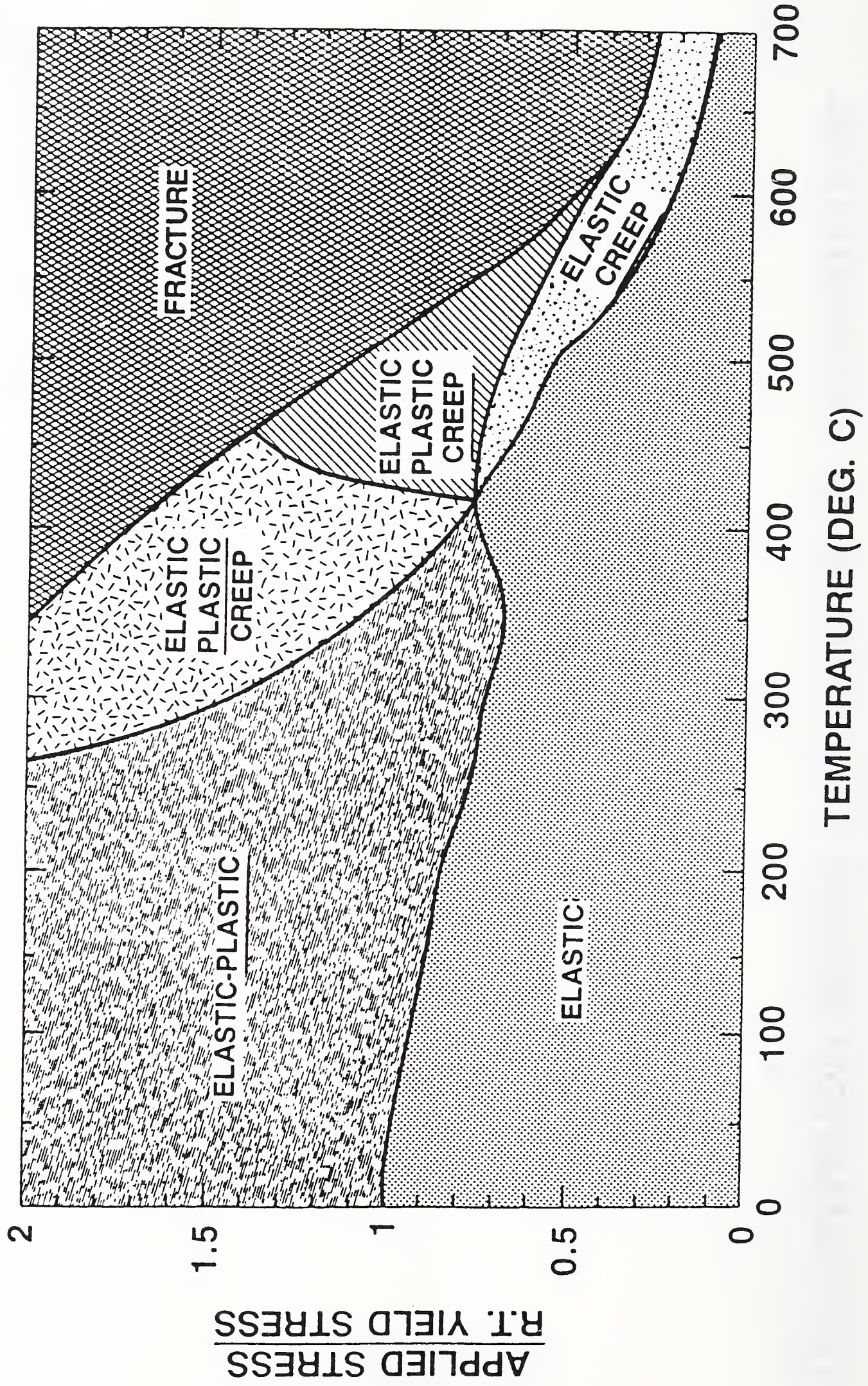


Figure 18a. Deformation modes for 1 hour at temperature.

A36 STEEL

DEFORMATION MODES FOR 1 HOUR AT TEMPERATURE

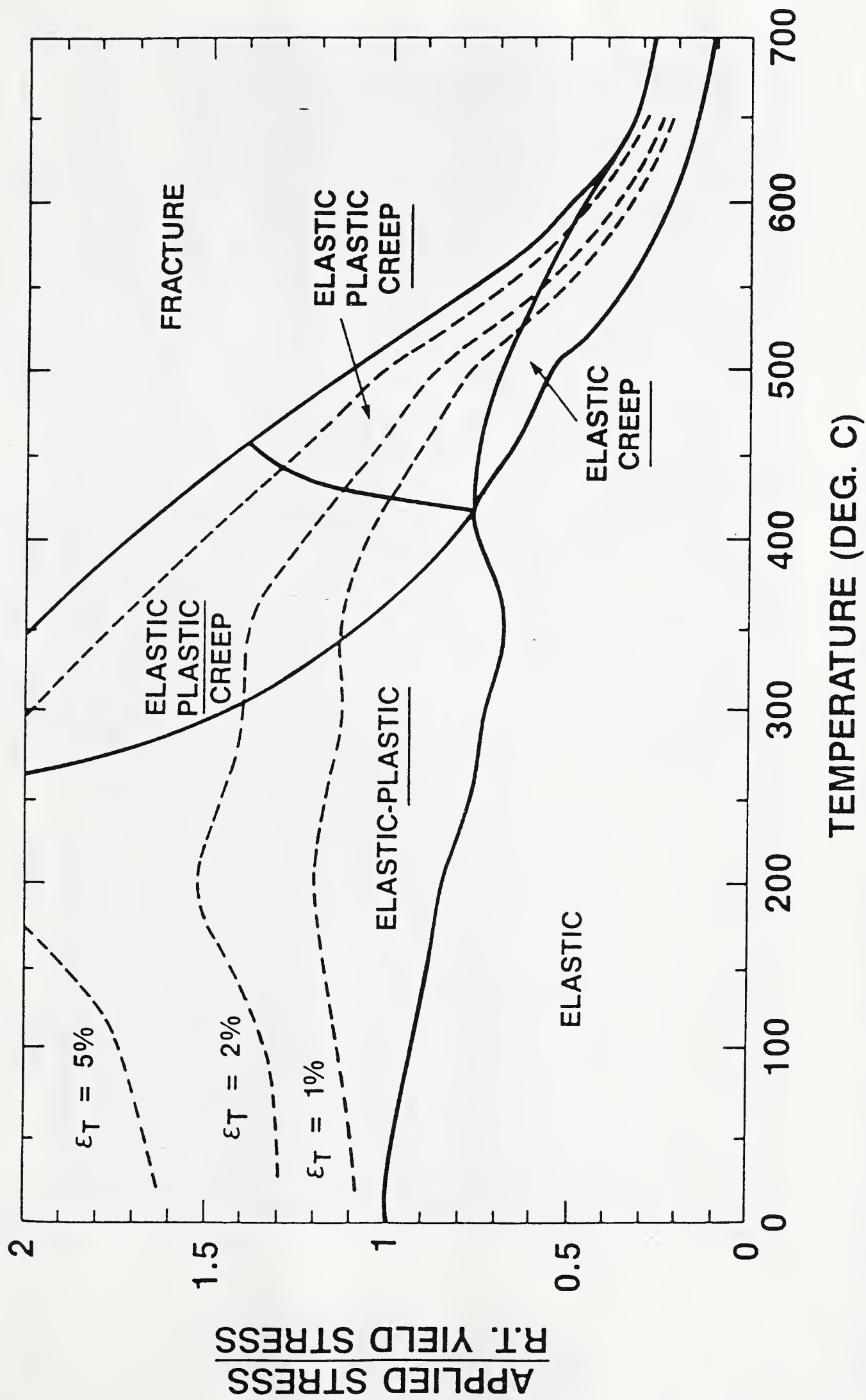


Figure 18b. Deformation modes for 1 hour at temperature.

A36 STEEL DEFORMATION MODES FOR 4 HOURS AT TEMPERATURE

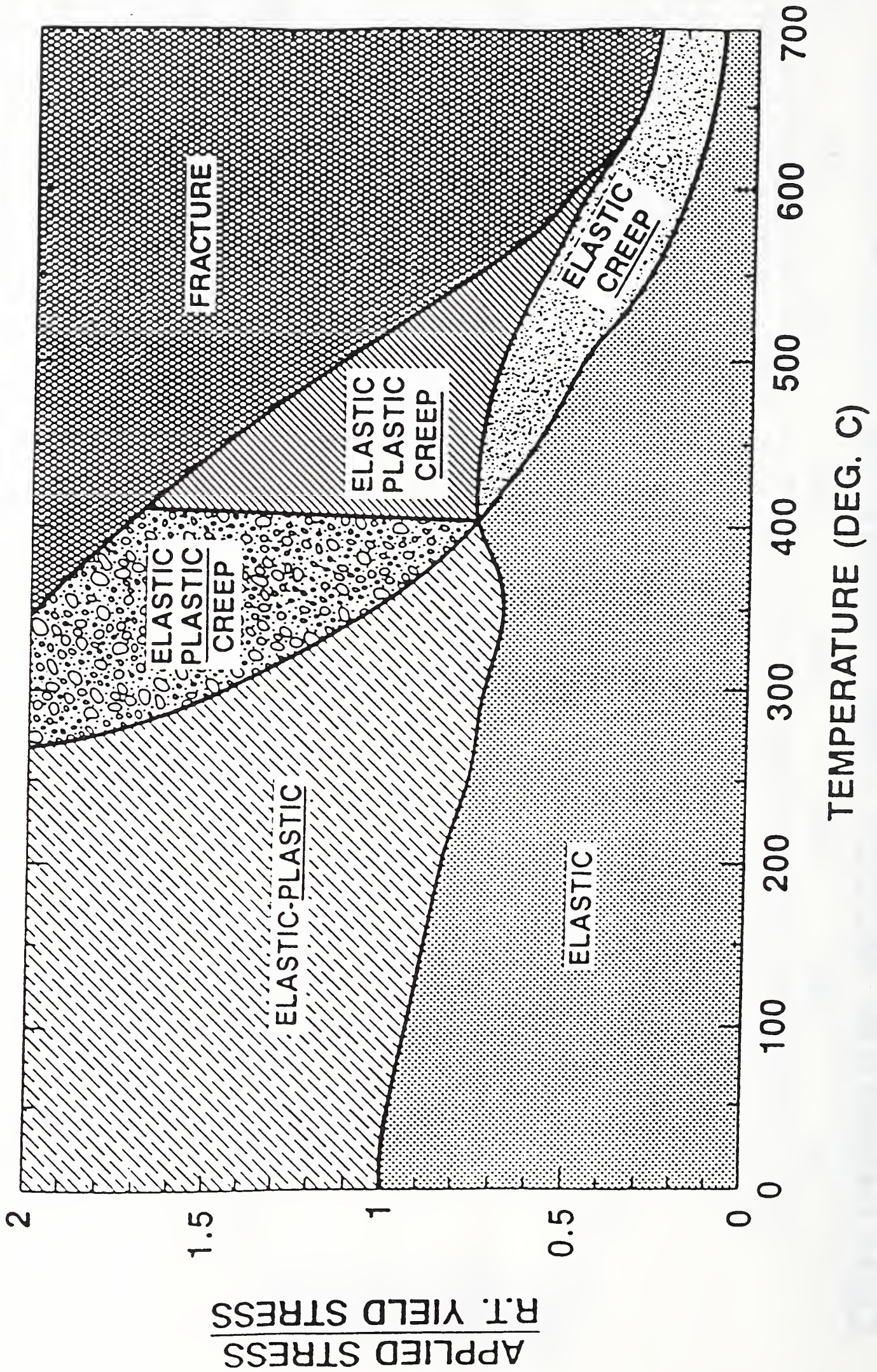


Figure 19a. Deformation modes for 4 hours at temperature.

A36 STEEL

DEFORMATION MODES FOR 4 HOURS AT TEMPERATURE

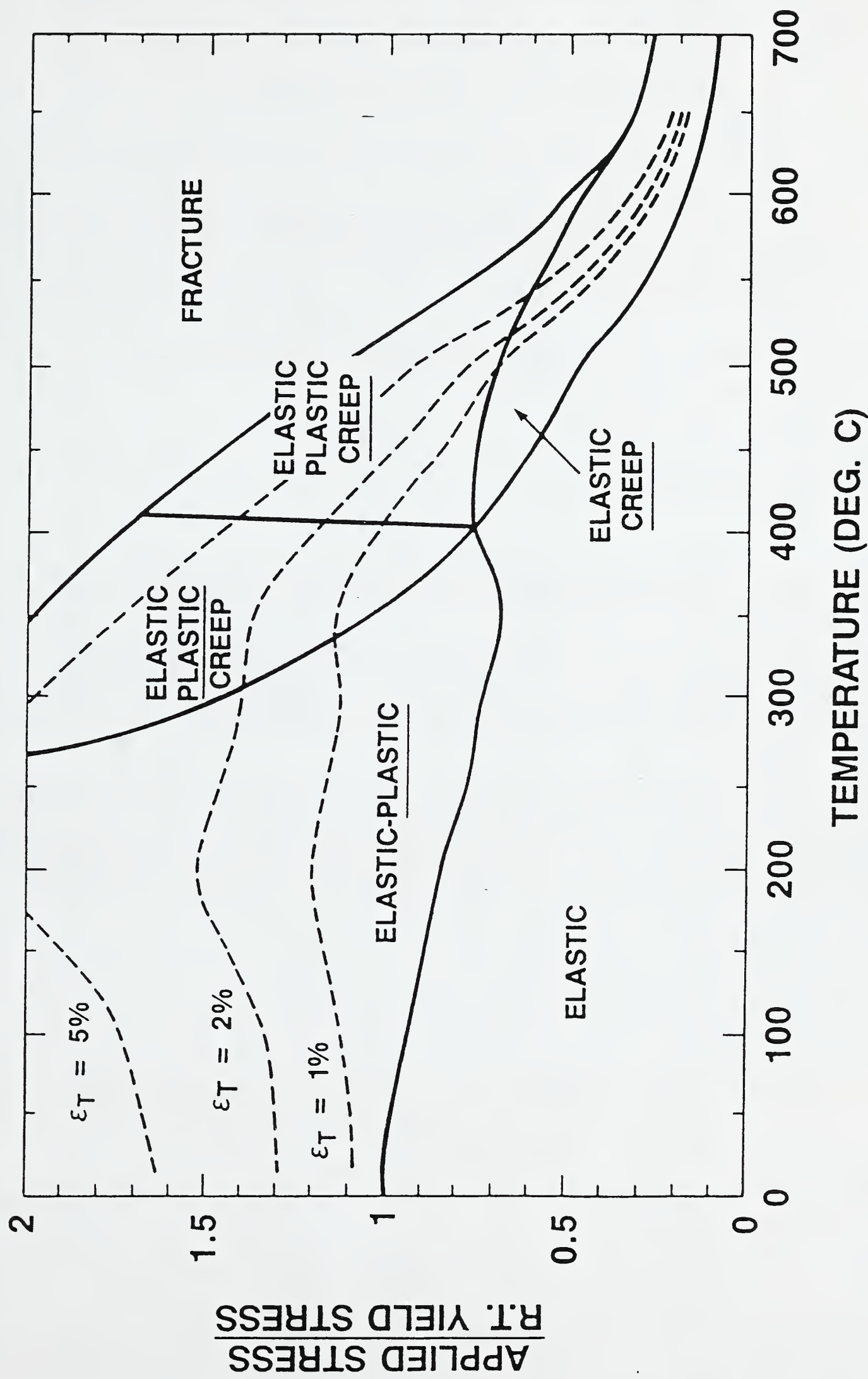


Figure 19b. Deformation modes for 4 hours at temperature.

U.S. DEPT. OF COMM. BIBLIOGRAPHIC DATA SHEET <i>(See instructions)</i>	1. PUBLICATION OR REPORT NO. NISTIR 88-3899	2. Performing Organ. Report No.	3. Publication Date MARCH 1989
4. TITLE AND SUBTITLE Elevated Temperature Deformation of Structural Steel			
5. AUTHOR(S) B.A. Fields and R.J. Fields			
6. PERFORMING ORGANIZATION <i>(If joint or other than NBS, see instructions)</i> National Institute of Standards and Technology NATIONAL BUREAU OF STANDARDS DEPARTMENT OF COMMERCE WASHINGTON, D.C. 20234			7. Contract/Grant No. 8. Type of Report & Period Covered
9. SPONSORING ORGANIZATION NAME AND COMPLETE ADDRESS <i>(Street, City, State, ZIP)</i> American Iron and Steel Institute 1133 15th Street, N.W. Washington, DC			
10. SUPPLEMENTARY NOTES <input type="checkbox"/> Document describes a computer program; SF-185, FIPS Software Summary, is attached.			
11. ABSTRACT <i>(A 200-word or less factual summary of most significant information. If document includes a significant bibliography or literature survey, mention it here)</i> The results of tensile and creep tests on steels close to the American specification for ASTM A36 have been used to formulate an equation from which elastic, plastic, creep and total strains can be calculated. Correlations between measured and predicted strains for Australian AS A149 and Japanese SS41 steels, both close to the A36 specification, are shown and good agreement is found. The above mentioned equation is also used to construct deformation mechanism (i.e., elastic, plastic, or creep) maps for times of 2 minutes to 4 hours at temperature. From these maps the deformation mechanisms operating at a given temperature and stress can be seen. The dominant mechanism for each set of conditions is given. In addition the maps show contours of total strain values 1, 2, and 5%.			
12. KEY WORDS <i>(Six to twelve entries; alphabetical order; capitalize only proper names; and separate key words by semicolons)</i> A.S.T.M. A-36 steel; creep deformation; elastic deformation; fire resistance; plastic deformation, structural steel.			
13. AVAILABILITY <input checked="" type="checkbox"/> Unlimited <input type="checkbox"/> For Official Distribution. Do Not Release to NTIS <input type="checkbox"/> Order From Superintendent of Documents, U.S. Government Printing Office, Washington, D.C. 20402. <input checked="" type="checkbox"/> Order From National Technical Information Service (NTIS), Springfield, VA. 22161			14. NO. OF PRINTED PAGES 120 15. Price \$19.95

NISTIR 88-3899
Jun 13, 2016

